PHYSICOCHEMICAL AND GEOTECHNICAL EVALUATION OF LIME TREATED SOILS IN NEW AND EXISTING INDUSTRIAL APPLICATIONS

A Dissertation

by

NARAIN HARIHARAN

Submitted to the Office of Graduate and Professional Studies of
Texas A&M University
in partial fulfillment of the requirements for the degree of

DOCTOR OF PHILOSOPHY

Chair of Committee,	Dallas N. Little
Committee Members,	David H. Allen
	Robert L. Lytton
	Youjun Deng
Head of Department,	Robin Autenrieth

May 2020

Major Subject: Civil Engineering

ABSTRACT

Lime products (quicklime, hydrated lime and quick or hydrated lime slurry) have been widely studied and effectively used for chemical stabilization of expansive subgrade soils beneath roadways. However, several unanswered questions remain regarding the long-term durability of lime treatment and the nature of chemical interactions between lime and the soil minerals in new and less common industrial applications. The emphasis of this work is to evaluate the use of lime products for two such applications; the treatment and management of the Canadian oil sands fluid fine tailings (FFTs) having solids concentrations by mass of about 30%, and the treatment of soils used in the construction of hydraulic structures in permanent contact with water. In addition, modifications are proposed to two existing methods used for characterizing the volumetric stability of expansive soils to account for the changes in material properties due to lime treatment and ultimately improve the design of roadways built on expansive soils.

First, a physicochemical and geotechnical evaluation is performed on hydrated lime slurry treated FFTs after dewatering them using a decanter centrifuge or a benchtop pressure filter to obtain a solids fraction comprising of 55% to 70% solids by mass. The results demonstrate three unique benefits of lime over other calcium-based coagulants and polymeric flocculants; the ability to increase pH and enhance clay capture within the solids and clarify the release water, the ability to deplete carbonate phases up to a pH of 11.5, and the ability to produce a material with undrained shear strengths in excess of

100 kPa within 28 days suitable for reclamation. A numerical model is developed using the experimental results to predict the liquidity index and shear strength of lime treated FFT solids over the first 180 days.

Next, a case study is conducted to evaluate the durability of nearly 50-year-old lime treated sections at the Friant-Kern canal in a similar manner to the oil sands application but considering the impact of leaching and carbonation due to environmental factors. The results indicate minimal leaching of lime over time and demonstrate the benefits of lime towards increasing strength of the soils through pozzolanic reactions, reducing soil erosion and mitigating expansion by improving drainage characteristics due to textural modification of the clays to lean silts.

Finally, two modifications to existing methods are proposed to understand the true impact of lime treatment on reducing the vertical movement in roadways due to expansive soils; the first using the soil water characteristic curve to define the initial moisture state of soils in the Tex-124-E method, and the second using the packing arrangement of soil particles to define a shift factor to relate the suction compressibility index of reconstituted and intact soils.

DEDICATION

To my entire family who I love so dearly and who are an immeasurable source of strength, support and happiness in my life.

ACKNOWLEDGEMENTS

I would like to thank my advisor, Dr. Dallas Little for his guidance and support throughout the course of my Ph.D. program. Aside from serving as my graduate advisor during my MS and Ph.D. programs, he has been a friend, professional mentor and a constant source of inspiration. I look forward to collaborating with Dr. Little for many years to come.

Thanks to my committee members, Dr. David Allen, Dr. Robert Lytton and Dr. Youjun Deng for the many insightful discussions I have had with each of them on their respective areas of expertise. Every minute I spent with them was an enriching experience and brought to light their depth of knowledge and dedicated contributions to the academic society.

I am extremely grateful for the opportunity to get to know and work with Mike Tate and Nikolas Romaniuk from Graymont. I have enjoyed the numerous interactions we have had about lime, the oil sands and other topics. I look forward to working closely with them on many more projects when I join Graymont after my graduation. Thanks also to Jesse Fox and Jared Leikam from Graymont for their help and contributions during my summer internship.

I was lucky to have shared office space with my colleague and friend, Pavan Akula, who I admire for his dedication and passion for research. Special mention and thanks to my Texas A&M friends Abdullah, Atish, Bidemi, Fawaz, Jason, Javier, Jun,

Lorena, Sajib and Saureen for their help and support at various times. Thanks also to all my other friends and colleagues at Texas A&M.

Words are not enough to express thanks to my parents, in-laws and cousins for their support and love without any expectations. My life is not complete without you all.

Finally, and most importantly, thanks and love to my wife and best friend, Aishwarya. I am lucky and blessed to have you as my life partner and owe the happiness and success in my life entirely to you. Loads of love to our kids, Avyukth and Advik for making us smile multiple times every day and for helping us realize the true meaning of life.

Thank you all!

CONTRIBUTORS AND FUNDING SOURCES

Contributors

This work was supervised by a dissertation committee comprising of Professor Little (advisor) and Professor Lytton of the Department of Civil Engineering, Professor Allen of the Department of Ocean Engineering and Professor Deng of the department of Soil and Crop Sciences at Texas A&M University.

The samples collected and the analysis performed in Chapter 5 were conducted in part by Pavan Akula of the Department of Civil Engineering. The contents related to this work have been accepted for publication in the Journal of Transportation Research Record. The data in Table 3-1, Table 4-1 and the part of the data used for development of numerical models in Chapter 4 were provided by Graymont.

All other work conducted for the dissertation was completed by the student independently.

Funding Sources

The work performed in parts of Chapters 1 and 2 relevant to the use of lime in the oil sands tailings management and in Chapters 3 and 4 were funded by Graymont. The work performed in parts of Chapters 1 and 2 relevant to the use of lime in hydraulic structures and in Chapter 5 of this dissertation was funded by Lhoist.

TABLE OF CONTENTS

Page

LIST OF FIGURES

Page

LIST OF TABLES

Page

1. INTRODUCTION*

1.1. Role of Lime in Chemical Stabilization of Subgrade Soils

Lime (calcium oxide or calcium hydroxide) is a versatile material and has been successfully used in infrastructure construction worldwide and in soil treatment applications including pavement base and subgrades, airports and rail-road beds etc. for thousands of years [1]. Lime has especially been effective in providing a workable soil platform in construction operations through its ability to alter the physical properties of clays and specifically reduce the plasticity index and expansion index. Furthermore, lime treatment can increase the pH of soils to as high as 12.45 due to the release of hydroxyl ions to solubilize and interact with the silicates and aluminates released from the clay minerals to result in long-term strength building pozzolanic reactions [1].

Chemical stabilization of subgrade soils typically accomplishes one or a combination of three tasks: achieve threshold strength and/or stiffness, moderate or eliminate volumetric instability, or provide both strength and volumetric stability. The choice of stabilizer, among other factors depends on the plasticity of the soil at the location in consideration. For several years, lime has been most widely used for treating subgrade soils having a plasticity index (PI) >25 to improve resilient modulus and other strength gain properties. Studies have shown that the strength of most fine-grained soils improves significantly with lime stabilization due to the cation exchange reactions that

* Section 1.5 of this chapter has been accepted for publication in the Journal of Transportation Research Record

occur in the lime-soil system followed by flocculation-agglomeration and pozzolanic reactions [2]. Further, lime stabilization has been reasonably effective in controlling the swell-shrink potential of highly plastic clays [2].However, lime stabilization of the subgrade has some inherent downsides such as inducing reflection cracking on the surface layers and being responsible for the formation of deleterious minerals such as ettringite in sulfate rich soils [3].

The use of calcium hydroxide to modify the surface of fine clays to improve strength, increase particle size and reduce moisture content is well established in soil treatment applications. Treatment with lime can either modify or stabilize the soil.

Calcium ions released from the hydrated lime migrate to the surface of the clay particles and displace univalent cations through cation exchange caused by concentration and valence effects. This exchange facilitates the release of water from the clays, increases particle size and reduces the plasticity index of the soil. Benefits from this process can be seen within a few hours to overnight. Certain researchers [4] argue that pozzolanic reactions dominate the modification and stabilization reactions from the outset and that cation exchange has considerably lesser impact.

As calcium hydroxide increases pH above 10.5, alumina and silica from the clay become soluble and react with calcium cations to form cementitious products. The calcium silicate and calcium aluminate hydrates formed result in a more permanent modification compared to cation exchange. When lime is added to a reactive soil, it has been proven by extensive laboratory and field testing that plasticity index decreases,

water release occurs, resilient modulus increases and compressive strength exceeding 1400 kPa can be obtained [5].

1.2. Scope of the Dissertation

The motivation for conducting the research is to explore the uses of lime and lime products in new and less common industrial applications using the background knowledge gained through the use of lime products for chemical stabilization of subgrade soils.

The two major applications for lime that are investigated in this research are the vast sources of oil sands in Alberta, Canada and the soils used to construct hydraulic embankments, which are in permanent contact with water. The potential role for lime in the treatment of tailings generated from the oil sands extraction is evaluated from a physicochemical and geotechnical standpoint. The role of lime in hydraulic structures will be evaluated using a case study aimed at analyzing the long-term durability of lime treatment. In addition, the dissertation introduces some important method improvements for the characterizing the volumetric stability of lime treated expansive subgrade soils. The link between the uses of lime to coagulate and modify the oil sands clays and embankment durability is practical and not abstract. If the oil sands clays are to be considered for use as a construction material, embankments are a logical target and their durability will be a prime focus.

1.3. Organization of the Dissertation

This dissertation is organized into seven chapters. Chapter 1 begins with a background of the role of lime in chemically stabilizing subgrade soils followed by

defining the scope of research performed in this dissertation. The rest of this chapter will provide a general introduction regarding the oil sands tailings and the role of chemical additives in their management followed by the problem statement concerning the role of lime in hydraulic structures. The final topic presented in this chapter will introduce the topic of volumetric stability of lime treated expansive soils.

Chapter 2 presents a review of existing literature on each of the topics. The literature review on oil sands includes a discussion on the tailings dewatering techniques, mineralogy of oil sand tailings, the role of lime and other calcium-based coagulants in the treatment of oil sand tailings and the geotechnical properties of oil sand tailings deposits. The literature review of hydraulic structures includes a review of the historical use of lime in hydraulic structures in the United States and the history of the use of lime at the Friant-Kern Canal (FKC). The final component of this chapter presents the limitations of existing methods to characterize the volume change properties of expansive soils.

Chapter 3 discusses the physicochemical properties of lime treated FFTs dewatered using the centrifuge technology and includes the experimental design and methods followed. The physicochemical characterization of the lime treated tailings includes analysis of the pH, cation exchange capacity (CEC) and Methylene blue index (MBI) of the FFT solids. The focus of this chapter is to understand the chemical reactions taking place due to interaction of lime with the soil minerals using analytical tools such as X-ray diffraction analysis (XRD), Fourier transformed infrared (FTIR) spectroscopy and scanning electron microscope (SEM) image analysis.

Chapter 4 discusses the geotechnical properties of lime treated FFTs dewatered using the pressure filtration technology and includes the experimental design and methods followed. This chapter focusses on the impact of lime on influencing the long-term geotechnical properties namely Atterberg limits, clay content and undrained shear strength of the dewatered FFT solids and compares the performance of lime against that of a polymer and a combination of alum and polymer. The final section of this chapter presents a numerical model to predict the liquidity index of lime treated FFTs and provides examples of potential applications of the model.

Chapter 5 presents a case study evaluating the durability of lime treatment at the FKC nearly 50 years after initial treatment. The chapter presents details regarding the field sample exploration, chemical and engineering experimental methods along with the results obtained. The influence of lime on matric suction in the embankment soils is demonstrated through an analysis using the Hydrus-2D software.

Chapter 6 presents the proposed method improvements to the Tex-124-E method to predict the potential vertical rise (PVR) caused by expansive soils. The chapter also presents a model to determine the suction compressibility index of in-situ soils using experimental data obtained after reconstituting the field samples. The method improvements proposed in this chapter are focused towards improving the characterization of the volumetric stability of lime treated expansive subgrade soils. As with the link between the durability assessment of lime stabilization in hydraulic embankments, Chapter 6 and the use of lime for stabilizing the oil sands clays are also linked. In this case it relates to assessing the volumetric stability of the lime treated end

product from the oil sands application if the material is considered for use towards constructing a stabilized pavement subgrade.

Chapter 7 summarizes the work performed in this dissertation and highlights the contributions made within each of the applications investigated. The chapter also provides recommendations for further work on the topics studied.

1.4. Oil Sands Tailings Background

The Athabasca region of northern Alberta, Canada, is home to huge deposits of oil sands, approximately 300 billion barrels of recoverable bitumen. A map of the oil sands deposits locations in Alberta is shown in Figure 1.1 [6].

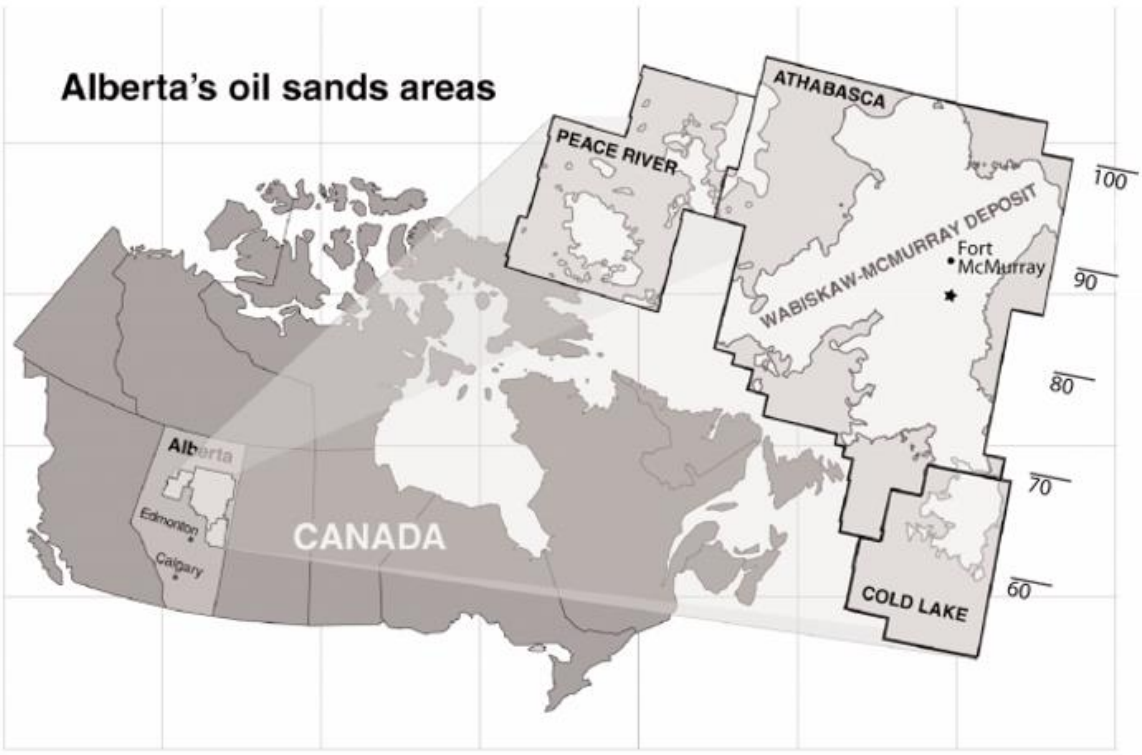

Figure 1.1 A map of the oil sands deposit locations in Alberta (reprinted from [6])

The average oil sands feedstock consists of between 8% and 12% bitumen; between 80% and 86% sand, silts and clays; and 3% to 6% water. Bitumen is extracted at the rate of about 1.3 million barrels per day from the surface minable oil sands using the Clark Hot Water Extraction (CHWE) process. The extraction process has been used since 1967 and uses NaOH as a dispersive agent. NaOH improves liberation of bitumen from oil sands by increasing pH, activating natural surfactants in the bitumen, and decreasing viscosity. The extraction plant discharges a tailings stream composed of water, solids (sand, slit and clay) and residual bitumen in a wide range of compositions, which are discharged into tailing ponds [7].Tailings generated from the extraction of bitumen from oil sands represent one of the largest inventories of fluid fine tailings (FFT) in the world, now exceeding 1.2 billion cubic meters, and represent an increasing environmental risk to the Athabasca region and economic risk for the operators [8].

A majority of the sand fraction in the oil sands tailings settle out to the bottom due to their higher density and are mostly deposited as sand beaches. The dispersed clays are deposited in ponds and form a stable suspension referred to as fluid fine tailings (FFTs) and mature fine tailings (MFTs) and are comprised of about 30% solids concentrations by mass [9]. The FFTs and MFTs are dominated by particles smaller than 45 microns with 40-60% smaller than 2 microns (clay particle size). The remaining solids is a mix of coarser sand and silt fractions and 1 to 3% residual bitumen. MFT have very high moisture contents, their compressibility is non-linear and very high, and they are highly thixotropic and have a very low hydraulic conductivity.

1.4.1. Role of Chemical Additives in Oil Sands Tailings Treatment

The oil sands FFTs inventories generated are mostly contained by large dams. The large quantities of fluid tailings stored in dams pose serious liability concerns for both operators and the investors [10].Furthermore, recent failure of containment facilities in Brumadinho, Mt Polley, and Fundão highlight the liability to the environment, human health and safety posed by FFTs [11, 12]. These recent failures have resulted in an increasing push by critics and regulators to move to dry-stackable tailings, away from traditional fluid tailings containment strategies.

Chemical process additives, such as coagulants and polymeric flocculants that can improve water release and filtration rates are hence critical for the viability of high-performance dewatering techniques such as pressure filtration and in general to the management of oil sands FFT. Particularly, achieving a dry stackable material suitable for landform development requires the use of effective chemical additives, which can reduce the activity of the clays present in the FFT and contribute to strength gain. Further, for the reclaimed material to be geo-mechanically stable and self-supporting, there is a growing need for coagulants such as lime that are capable of not only reducing the clay activity but can also permanently modify the clays present in FFT. This is possible by texturally transforming them to larger aggregate fractions and/or by partially dissolving them at pH above 12.0 to form pozzolanic reaction products such as calcium silicate hydrates (C-S-H) and calcium aluminate hydrates (C-A-H).

1.5. Role of Lime in Hydraulic Structures: Problem Statement

The use of lime in stabilizing hydraulic levees and embankments is relatively less popular compared to the use of lime in pavement subgrade stabilization. This is mainly because lime competes with other conventional and temporary repair techniques such as dewatering, importing replacement materials from local borrow pits, flattening the slopes [13] and less commonly adopting electrochemical methods to stabilize the soils [14]. In addition, questions arise concerning the sustainability of lime treatment due to the high pH levels and potential for leaching. However, the McGee Creek dam and the FKC serve as some precedents for the successful use of lime for hydraulic purposes to mainly control erosion related issues resulting from dispersive soils [15]. Although lime has been used in the treatment of some major hydraulic structures in the U.S. and in most cases produced satisfactory results, documentation regarding the mechanisms contributing to the long-term durability of lime treatment for soils in constant or intermittent, long-duration contact with water has been limited.

For owners and administrations in charge of maintenance, safety and working issues of hydraulic structures, the durability of constituting materials is of significant concern. Durability of a structure is defined by its capability to retain the required properties in order to maintain the designed functions. Durability of materials on the other hand can be defined by the resilience of its properties with time, while facing a series of stresses both mechanical and environmental. A major component of distress impacting the FKC soils are linked to contact of the soils with water, which can lead to risk of lime leaching, erosion, decrease of strength and ultimately compromise the long-

term durability of the lime treated soils and stability of the canal as a whole. Moreover, climate significantly impacts the long-term aging related performance of the lime treated soils in FKC. The FKC region has experienced several freeze-thaw and flood-drought cycles since 1970 as shown in Figure 1.2 [16].

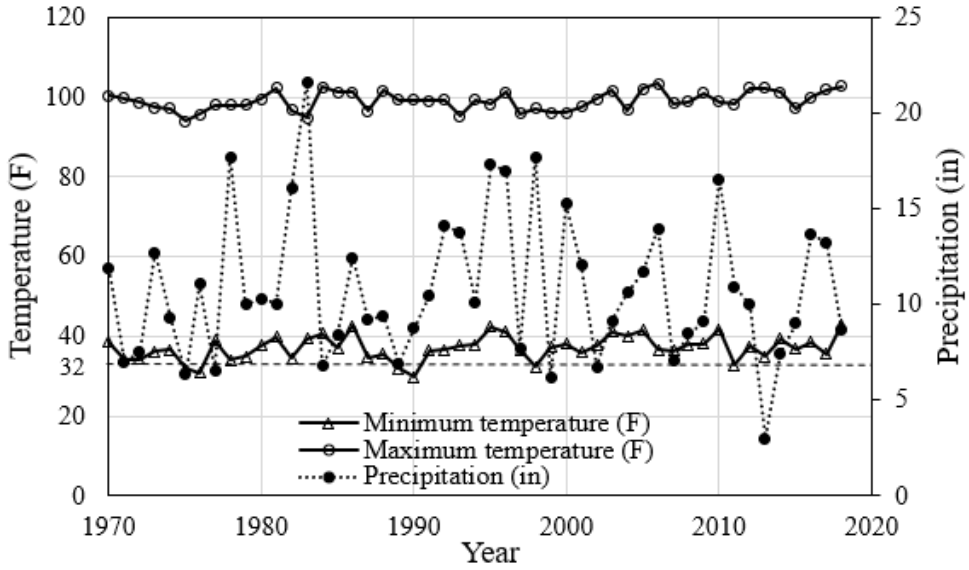

Figure 1.2 Average annual climatic data for FKC (1970-2019) (adapted from [16])

Most of the follow up performance evaluations in such projects are limited to reporting mechanical properties focusing mainly on strength of the soils immediately or soon after lime treatment. To my knowledge there is no open literature, even from pavement durability studies, that evaluates the mineralogical evolution of lime treated soils concurrently with changes in engineering properties over a performance period of nearly five decades, as that of the FKC.

1.5.1. Motivation and Objectives of FKC Case Study

The case study performed as part of this dissertation is aimed at assessing the long-term behavior of lime-treated materials in the specific context of hydraulic canals such as the FKC with continuous water flow so as to unearth the technical locks linked to lack of knowledge and feedback about their long-term behavior. In addition, the motivation for conducting such as case study is to contribute to the literature regarding the engineering, mineralogical and geochemical changes that can be expected in lime treated soils over a long period.

The case study was designed to perform a field evaluation of the long-term durability of lime treatment at the FKC from an engineering as well as mineralogical standpoint. While it is possible to simulate the effects of aging due to climatic factors and water contact in a lab, the motivation behind conducting a field study was to evaluate the durability of pozzolanic reactions taking place in the soil-lime system considering the impact of leaching and carbonation. C-S-H is the primary pozzolanic product that holds the soil matrix together contributing to the strength and durability of lime treated soils [17]. C-S-H is highly disordered with a gel like structure and is expect to form when lime initiates a geochemical reaction in clay rich soils at a pH of 12.4 [1]. The formation of C-S-H and other phases contributing to the durability of lime treatment were investigated using analytical methods.

1.6. Volumetric Stability of Lime Treated Expansive Soils: Background

Engineering problems due to expansive soils have been reported in many countries all around the world and result in millions of dollars' loss due to their severe

damages on pavement systems. There is an abundance of expansive soils throughout Central United States from Texas to Montana mainly because of the deposition of clay minerals (smectite) along the Central sea bed because of reaction between the volcanic emissions from the Pacific with the sea water dating back to several million years. Soils which contain smectite minerals such as montmorillonite are capable of absorbing a considerable amount of water and expanding. The more water they absorb the more their volume increases. Expansive soils also shrink when they dry out leading to the development of cracks and fissures which promotes water penetration to deeper layers. The vertical movement resulting from alternations of swell-shrink cycles leads to significant structural damage especially in lightweight structures such as sidewalks, driveways and foundations.

Lime has been the preferred chemical stabilizer to lower the plasticity of expansive soils, increase strength and to reduce the impact of vertical movement caused during climatic cycles. The role of lime in chemically stabilizing subgrade soils is well-established and was discussed in the opening section of this chapter. Existing methods to predict vertical movement do not consider the impact of chemical stabilization on the material properties of the soils.

To determine the real impact of lime on reducing the swell-shrink potential of the in-place subgrade clays, method improvements are proposed in this dissertation to two of the existing methods to predict vertical movement namely the Tex-124-E method [18] and the modified suction-based method [19]. The recommended improvement to the Tex-124-E method focuses on incorporating the soil-water characteristic curves (SWCC)

of the lime stabilized soils to determine the initial moisture state of the soil as either 'dry', 'average' or 'wet' with respect to equilibrium suction instead of using the Atterberg limits. The recommended improvement to the suction method involves using the packing theory of soils and aggregates to arrive at a shift fact between laboratory and field values of the suction compressibility index, γ_h.

2. LITERATURE REVIEW*

2.1. Oil Sands Tailings

This section presents the literature review pertinent to the dewatering techniques used in oil sands, the differences between coagulation and flocculation, the common soil minerals present in the oil sands, the role of calcium-based coagulants and polymeric flocculants in oil sands tailings management and the strength requirements for reclamation of oil sands.

2.1.1. Oil Sands Dewatering Techniques

Current commercial dewatering techniques that can directly transform oil sands fluid fine tailings into materials suitable for upland development such as filter presses are either economically or operationally infeasible given the throughputs and the requirement to produce materials having shear strengths above 20 kPa which typically require dewatering of the FFT above 70% solids content by mass [20].

Commercial centrifuge operation at Canadian Natural Resources Limited (CNRL) and Syncrude can only reliable produce caked between 45% to 55% solids content, though Syncrude has combined this technique with overburden mixing to achieve higher solids contents. Other dewatering strategies, such as Suncor's Tailings Reduction Operation (TRO), CNRL's enhanced Non-Segregating Tailings (NST), and Imperial Oil's thickened tailings, all require significant amounts of time for the tailings

* Section 2.2 of this chapter has been accepted for publication in the Journal of Transportation Research Record

to dry or consolidate and in many cases these strategies underperform their predicted drying or consolidation rates. The reliance these methods have on drying and consolidation introduce an element of risk, as drying is extremely sensitive to variations in weather and consolidation and thus may never achieve their designed solids content.

High performance dewatering of fine tailings is necessary to achieve stackable tailings comprising of at least 70% solids by mass, where the optimal dewatering process is dependent on the tailings mineral properties and climate of the operations. In dry climates, with easily dewatered tailings, thickeners can be used effectively with atmospheric drying to achieve a dry stackable product; however, many operations have tailings which contain troublesome clay minerals or are in climates where atmospheric drying is not possible[21].

Filtration, while costlier, is one of the few dewatering techniques capable of providing a dry-stackable product [22]. There are many types of filtration, but pressure filtration is increasingly being adopted as vendors produce larger and larger pressure filtration devices that can tolerate higher pressures [23]. The greatest downside to pressure filtration is large upfront capital cost; however, these costs can be offset by water recovery in dry regions and lower cost of tailings containment. The economics of pressure filtration are largely driven by the cycle time of the process. Process additive chemistries, such as coagulants and flocculants, that can improve water release and filtration rates are critical for the viability of pressure filtration processes.

2.1.2. Coagulation versus Flocculation

The use of coagulants and flocculants is a key component of most oil sands tailings treatment technologies. The fine FFT particles have proven difficult to consolidate and achieve the desired high solids contents for reclamation. Kasperski indicates that electrostatic, steric, Van der Waals and hydration forces influence the ability of fine particles to consolidate [24]. Coagulants and flocculants can influence these forces by modifying the surface of the clay particles and/or binding them together to form large particles that settle and dewater more easily. However, coagulants and flocculants function using very different mechanisms [25].

Coagulants primarily act by destabilizing the electrostatic repulsion of suspended solids through cation exchange or chemical reaction. This neutralization of charge combined with bridging mediated by multivalent cations helps link individual particles together, which increases the average particle size. High shear mixing can be used to ensure that inorganic coagulants are well dispersed in FFT and able to diffuse to the clay-water interfaces. Previous FFT studies have focused on investigating lime, gypsum, alum and carbon dioxide as coagulants [26].

Flocculation is commonly used to increase the settling rate of fine suspensions by using very large organic polymers to capture suspended solids and form large agglomerates called flocs. While the clay particles are chemically unchanged, being trapped in flocs increases their size and density which allows for rapid settling. The effectiveness of the polymer is dependent on a number of factors including its type (anionic, cationic or nonionic), molecular weight, degree of ionization, and mixing

procedure. Undermixing of polymers with FFT results in poor fines capture; however, overmixing or high shear conditions during slurry conveying will result in the breakdown of flocs. Some studies have investigated double polymer treatments using cationic then anionic polymers to enhance flocculation by bridging and charge neutralization [27].

2.1.3. Oil Sands Tailings Mineralogy

The mineralogical composition of the oil sands tailings is expected to play a vital role in determining the efficacy of various coagulants and flocculants. The surface properties of the minerals such as cation exchange capacity (CEC) is vastly dependent on the mineralogy of the tailings.

Oil sands tailings minerals consists of sands, clays, amorphous oxides, and some heavy metals. The sand fraction in the oil sands is composed of 97.5-99% SiO_2, 0.5-0.9% Al_2O_3, and 0.1-0.9% Fe [28]. The fines fraction in oil sands is defined as particles having a mean diameter less than 44 micron while clays are defined by a mean diameter less than 2 micron[29]. The predominant clay minerals present in the oil sands are kaolinite and illite with minor amounts of chlorites, montmorillonite and mixed-layer clay minerals [30].

2.1.4. Role of Calcium Based Coagulants in Oil Sands Tailings Management

The use of calcium based inorganic coagulants, such as lime and gypsum have played an important role in the technologies proposed for treatment of the oil sand tailings. Calcium is a divalent cation that has a demonstrated performance record in the modification and stabilization of fine clay soils [1]. The interaction of calcium (Ca^{2+})

with the fines fraction in oil sands has been investigated in the NST and MFT processes [31] with a primary focus on cation exchange reactions with clays.

Lime provides calcium in solution that can balance the negative surface charges of colloids and destabilize the inter-colloidal electrostatic repulsions to promote coagulation. In the case of fine inorganic particles, such as phyllosilicate clay minerals, cation exchange is a critical process whereby the bivalent calcium cation can replace a monovalent sodium cation on the mineral surface. The bivalent nature of the calcium cation promotes cationic bridging of the clay particles to form larger agglomerates [1, 32, 33]. Several factors related to solution chemistry including pH, alkalinity, ionic strength and concentration of other cations can influence the effectiveness of the cation exchange [34]. Cation exchange reactions modifies the water film thickness of clay mineral surfaces. In aqueous solutions, water is coordinated with different cations in solution; therefore, a sodium or calcium ion bound to the clay surface will carry water with it. Sodium tends to form thick water films while calcium cations form much thinner water films. This mechanism can considerably reduce the volume of water in slurries rich in clay minerals with high surface areas, such as FFT. These reactions proceed only after lime has consumed and precipitated all bicarbonate as calcium carbonate [35].

Unlike some acidic coagulants like alum, hydrated lime can also destabilize and permanently modify colloidal particles by chemically reacting with them and improve strength through pozzolanic reactions. It is well established in soil stabilization applications that at a pH of 12.4, phyllosilicates dissolve into their aluminate and silicate constituents which can react with soluble calcium and water to form pozzolanic products

such as calcium aluminate hydrates (C-A-H) and calcium silicate hydrates (C-S-H) [1, 36-38]. Unlike cation exchange which occurs quickly and is generally limited by diffusion, the pozzolanic reactions occur over several months and depend on temperature, soil chemistry and soil mineralogy [39, 40]. Under favorable conditions, the pozzolanic reactions promote remineralization which is characterized by formation of new mineral phases with significantly stronger and more resilient bonds.

Water chemistry also plays an important role in determining the effectiveness of coagulants. The primary difference between lime and other calcium-based coagulants such as gypsum and calcium chloride is that lime increases the pH while the rest of the coagulants, including non-calcium based coagulants such as alum, sulfuric acid and carbon dioxide are acidic in nature. A major downside of using gypsum, for instance, is that it increases Ca^{2+} and Mg^{2+} concentrations in the recycled release water and potentially causes H_2S emission by anaerobic reduction of SO_4^{2-} with the residual bitumen in the tailings. In comparison, lime has been tested to dewater effectively without increasing the concentration of Ca^{2+}, Mg^{2+} or SO_4^{2-} in recycle waters [35]. However, it is the high levels of accumulated sodium ions resulting from caustic sodium hydroxide that is thought to most adversely impact not just the process water chemistry but also the efficacy of coagulant aids including lime.

While there are obvious advantages of using lime as a coagulant in the treatment of fluid tailings, there exists gaps in knowledge regarding the chemical reactions occurring between lime and the oil sands minerals which must be addressed in order to achieve a geotechnically stable reclaimed material.

2.1.5. Use of Polymeric Flocculants for Dewatering of Oil Sands Tailings

Although there are obvious applications of using inorganic coagulants to modify the clays and build strength, there exist some concerns regarding the water chemistries of the release water. The use of organic polymeric flocculants has the potential to eliminate the salinity concern [41]. The major issue with polymers is their high sensitivity to shear forces. Polymeric flocculants breakdown due to shearing during the transport of FFTs thereby reversing their agglomeration properties. The use of polymer-treated MFT in pressure filtration to dewater oil sands tailings is currently being explored. The University of Alberta has researched the combination of anionic and either cationic or nonionic polymers to improve the dewatering of MFT [42]. Shear forces, polymer charge, polymer molecular weight and the presence of bitumen were factors that influenced dewatering. The use of anionic and cationic polymers was also investigated by Ledcor [43]. Their research indicated that both polymers were needed to prevent excessive filter cloth cleaning and that inline mixing could be used.

In summary polymeric flocculants are effective in reducing the initial volume of the tailings due to faster initial water release compared to the inorganic coagulants but they neither chemically modify the clays present in the FFT nor contribute to strength improvement with time and are susceptible to breakdown during shear.

2.1.6. Strength Requirements of Reclaimed Oil Sands Tailings

The geotechnical properties of the oil sands tailings are heavily influenced by the mineralogy of the fine clays present in the system. It is the fraction less than 2 micron that is considered to be extremely problematic to long-term geomechanical stability of

FFTs [44, 45]. To obtain a reclaimed material that is self-supporting and geomechanically stable, it is not merely sufficient to dewater the tailings to achieve an initial solids concentration in excess of 70% by mass but also to reduce the plasticity of the clays and chemically transform them into silts-like material. The Atterberg limits and the liquidity index are commonly used to define the fluidity, plasticity and brittleness of the material over a range of water contents. The undrained shear strength of the tailings has been related to the liquidity index by Beier [46]. The fact that many engineering properties such as hydraulic conductivity, permeability and shear strength can be correlated with the liquidity index makes it a popular index property to represent the physical state of the tailings[21].

Shear strength is arguably the most important engineering property that determines the ultimate fate of the reclaimed oil sands tailings. A thick layer of tailings deposit is often prone to failing by shear when subjected to a localized or non-uniform vertical load. The mechanical stresses acting on the tailings and the drainage conditions are two critical factors that are likely to impact the shear strength of dry stack tailings [21]. Since there are significant amounts of water still trapped in the soil matrix even at nearly 70% solids concentration, undrained conditions are expected to dominate since the rate of shear would exceed the rate at which water can dissipate the soil matrix. Due to the above reasons, the shear strength of the tailings deposits determine to what extent they can be accessed for capping or surface applications and whether they are viable to support steep slopes in the topography created as part of surface reclamation.

The strength requirement for various oil sands reclamation technologies was proposed initially by BGC Engineering [47] and recently updated by McKenna [20]. The nomogram developed by McKenna [20] detailing the strength requirement for various reclamation strategies is presented in Figure 2.1.

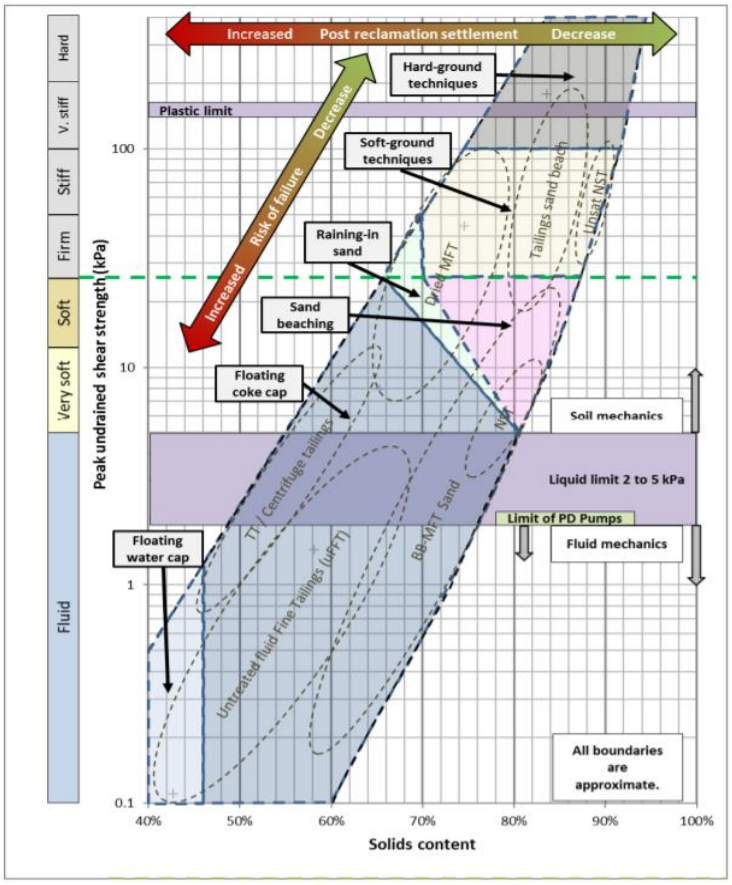

Figure 2.1 Strength requirement nomogram for various oil sands reclamation options (reprinted from [20])

The following strength guidelines pertaining to oil sands tailings are important to take note of from Figure 2.1:

1. The undrained shear strength of the tailings at liquid limit ranges between 2 and 5 kPa and the strength of untreated FFTs ranges between 0.1 to 4 kPa implying that FFTs have a liquidity index greater than 1 before treatment.
2. The undrained shear strength at plastic limit is about 80 to 100 times the strength at liquid limit implying that an increase in plastic limit is critical to achieving the desired strength at a lower solids content.
3. A minimum undrained shear strength of 20 kPa is required to deploy soft ground reclamation techniques and use the material in development of uplands supporting steep slopes in topography in excess of 1 in 6.
4. An undrained shear strength in excess of 100 kPa is required to consider using the reclaimed material as sublayer material for applications such as roadways either as is or after significant further soil stabilization.

The Alberta Energy Regulator (AER) in its initial Directive 74 [48] required the oil sands operators to achieve tailings with a minimum undrained shear strength of 5 kPa within one year of placement in a dedicated disposal area (DDA). AER abandoned Directive 74 and issued Directive 85 [49] which requires the operators to identify environment friendly and holistic approaches to produce reclaim-ready materials from the tailings without mentioning any specific strength requirements. The coagulants currently used in the management of oil sands tailings including gypsum and alum and the polymeric flocculants have not been able to meet the Directive 85 requirement. Lime

is expected to offer the unique ability to provide continual strength increase by increasing the pH and either suppressing the activity of the clays to increase their plastic limit or by dissolving them to form pozzolanic products thereby possesses the potential to produce a reclaimable end product from the tailings.

2.2. Construction and Repair of Hydraulic Structures

This section provides an overview of the existing literature on the history of the use of lime for the construction and repair of hydraulic structures in the United States. The existing literature regarding the use of lime at the FKC are also presented.

2.2.1. History of the Use of Lime in Hydraulic Structures

Table 2.1 summarizes the history of some of the hydraulic structures in the United States where lime has been used. The use of lime at the FKC will be discussed separately.

Table 2.1 History of the Use of Lime in Hydraulic Structures in the United States

Site	Location	Type of Construction	Age	Soil Type/ PI	Lime Content/ Type of Lime	Role of Lime	Reference
US SCS Mississippi dams (18 sites)	Mississippi	Repair	47	9-25	3%, Hydrated	Control dispersive soils	Perry, 1977[50]
West Memphis	Arkansas	Repair	46	Gumbo clays	5%, Hydrated	Mitigation of shrinkage cracks due to expansive clays	Gutschick, 1979[51]
Bog Hole Waterfall	Arizona	New	44	37-54	8.75%, Lime Kiln Dust (70% CaO)	Control soil erosion	Gutschick, 1979[51]
US SCS TN Dam 2	Tennessee	New	42	Unknown	2%, Unknown	Increase strength and protect against earthquakes	Gutschick, 1979[51]
Los Esteros Dam - Santa Rosa	New Mexico	New	41	Unknown	4%, Hydrated	Control dispersive soils	McDaniel and Decker, 1979[52]
McGee Creek Dam	Colorado	New	33	Unknown	Unknown	Control dispersion, improve workability and strength of clays	Torres, 2011[53]

2.2.2. History of the Use of Lime in FKC

The FKC was constructed in the 1940's and is located in California. The irrigation canal was designed to operate at a peak water flow rate of 4000 ft^3/sec and has a total span of 152 miles extending from the Friant Dam on the southeast of Fresno to the Kern River near Bakersville (Figure 2.2). About one-third (54 miles) of the FKC was built using expansive clays belonging to the Porterville formation and lined with either earth or concrete [14]. The earth-lined sections were built on a 2:1 side slope while the concrete-lined sections of the canal were built flatter with a 3:2 side slope. Onset of failures and maintenance issues due to shrinkage cracks, sliding and sloughing of the slopes were reported in both sections within two to three years after construction of the canal [54]. The problems were further compounded due to the dispersive nature of the soils which lead to erosion in many parts of the FKC.

Figure 2.2 Location of the Friant-Kern canal (reprinted from [55])

In the early 1970's, the Bureau of Reclamation (USBR) employed the use of lime to treat the native clays along the banks of the canal as part of a major effort to control further deterioration and to restore the damaged sections of the FKC. This operation was mostly carried out in the winter months and involved removing and replacing the original lining with a compacted soil-lime mixture prepared using 3.0 to 4.0% quicklime (CaO). Current engineering practice for determining the lime content required for soil stabilization do not directly consider the potential for lime leaching and are essentially based on finding the optimum lime content in order to achieve the target properties such as compressive strength and plasticity reduction [1]. The lime content used at FKC was chosen based on plasticity and swell measurements [14]. Two additional lime treatment projects were undertaken by the USBR in the mid 1970's to restore damaged earth-lined sections and in the mid 1980's in response to failure of portions of the concrete-lined sections that were left untreated during the initial operation.

The performance of the lime treated sections of the FKC have been monitored periodically since construction [13, 51, 54, 56]. Gutschick [51] reported that no known slips or slides occurred in the lime treated sections and that the strength of the treated soils continued to increase with time even after sustained exposure to water flow. Fleming [56] testified that the use of lime was both beneficial to repair slough slides and considerably more economical compared to the traditional repair method of flattening the slopes. More recently, Herrier [54] stated that the FKC served as a standout example for the successful application of lime in hydraulic structures based on feedback from the Friant Water Authority (FWA) regarding its remarkable maintenance history, essentially

non-existent, of the lime treated sections since rehabilitation in the 1970's. However, the durability of the lime treated soils at the FKC had neither been qualitatively or quantitatively evaluated until this study. A review of the average annual historical climate data for Fresno obtained from the National Oceanic and Atmospheric Administration (NOAA) database indicated sustained periods of heavy rainfall, two to three freeze-thaw cycles and some extended periods of drying thereby generating curiosity regarding the long-term durability of lime treated canal slopes.

2.3. Volumetric Stability of Expansive Subgrade Soils

The literature review of this section focusses on the important limitations in the existing approaches to predict vertical movement (swell and shrink) caused when expansive soils are exposed to frequent climatic cycles.

2.3.1. Limitations of Existing Methods to Characterize Movement in Expansive Soils

The Tex-124-E method [18] is widely used to predict the PVR due to expansive soils and in-turn determine the thickness of the chemically stabilized subgrade layer. The Tex-124-E method however has been criticized by Lytton as an overly conservative approach [19] that does not factor the changes in material properties of the soils due to chemical stabilization. The method relies on the Atterberg limits to determine the moisture state of the soils instead of factoring the changes in pore size distribution and drainage properties of the soils after chemical stabilization with lime. Moreover, the method assumes that soil at all depths up to 15 feet below the surface has access to

capillary water and does not apply a shift factor to correlate the behavior of properties obtained on reconstituted soils to their in-situ properties.

Lytton proposed a more fundamental suction-based method to generate a suction profile with depth [19] based on the constitutive equations developed by Mitchell [57] relating matric suction to the diffusivity and frequency of climatic cycles. Lytton's method then relies on the suction compressibility index, γ_h of the soils to predict volume change. While the suction-based method yields more accurate results compared to the Tex-124-E method [58], it does not account for the changes to γ_h as a result of modifying the in-situ soil fabric during experiments thereby resulting in over predicting vertical movement.

3. PHYSICOCHEMICAL EVALUATION OF LIME TREATED FLUID FINE TAILINGS DEWATERED USING A DECANTER CENTRIFUGE

3.1. Basic Characterization of the Source FFT

The FFT source was analyzed for initial solids content (SC), pH, bitumen content, methylene blue index (MBI), critical cations in the pore water such as calcium, magnesium and sodium, and sodium absorption ratio (SAR). The SAR measures the Na^+ relative to the square root of the sum of the square of the Ca^{2+} and Mg^{2+}. Table 3.1 provides a summary of the basic characterization properties of FFT G. A chemical and mineralogical (physicochemical) evaluation was performed on FFT G after dewatering using a decanter centrifuge.

Table 3.1 Summary of Basic Characterization Properties of FFT G

FFT ID	SC, %	Dean-Stark Analysis (%)			MBI, meq/100g	pH	Na^+, mg/L	Ca^{2+}, mg/L	Mg^{2+}, mg/L	SAR
		Bitumen	Minerals	Water						
G	25.9	1.2	24.7	74.1	8.6	8.6	306	16	6.1	17

3.2. Dewatering of FFT Using Decanter Centrifuge

Decanter centrifuges are currently used by Syncrude and Albian Sands as commercial methods to reduce FFT volumes by separating the FFT into a thickened centrifuge cake and a centrate. The ‘Sharpless P-660 Solid-Liquid Centrifuge’ equipment at the Process Engineering Research and Development Center at Texas A&M

University was used for performing dewatering experiments on FFT G. The bowl speed of the centrifuge was set at 2800 rpm which was equivalent of gravitational force or G-force of 2000 g. The FFT feed rate ranged between 10 and 20 liters per minute. A constant scroll differential speed of 55 Hz was used eliminate the influence of residence time on dewatering of the FFT. A 5% by mass hydrated lime slurry was freshly prepared in a mixing container to treat the FFT feed. The lime slurry was added directly to the FFT and pumped immediately to the centrifuge for separation. The operating parameters were chosen based on the results from preliminary smaller scale tests performed using a benchtop centrifuge and previous field trials with lime conducted at Canmet. The test setup and FFT mixing chamber are shown in Figure 3.1. The solids fraction obtained after centrifugation are referred to as centrifuge cake samples.

Figure 3.1 Pilot scale horizontal decanter centrifuge test study for dewatering FFTs

3.3. Selection of Lime Dosage

The initial lime dosages used to treat the FFTs were selected to achieve target pH levels of 11.5, 12.4 and 12.45. The pH target of 11.5 was chosen as it represented a dosage of lime adequate to deplete the carbonates and bicarbonates present in the FFTs [59] and subsequently release Ca^{2+} ions to participate in cation exchange reactions with the clays and promote coagulation. A pH target of 12.4 is widely regarded as the optimum lime dosage in soil stabilization applications for promoting the onset of strength building long-term pozzolanic reactions and stabilizing the clays [1]. A pH of 12.45 represents an overdose of lime with the intent to understand the impact of excess soluble Ca^{2+} ions can have on the physicochemical properties of the FFTs. The initial pH targets of 11.5, 12.4 and 12.45 were achieved using hydrated lime slurry dosages of 1500 ppm, 4000 ppm and 7000 ppm by mass of the FFT. The solids concentrations by mass of the untreated centrifuge cake and centrifuge cakes obtained after lime treatment ranged between 50% and 60%.

3.4. Experimental Test Program

This section presents the experimental test program to evaluate the physicochemical properties of lime treated FFT cakes obtained after the centrifugation process over the first 60 days after treatment. X-ray Diffraction (XRD) data together with the cation exchange capacity (CEC) and pH were used for qualitative assessment of the chemical reactions taking place in the lime treated FFTs and defining the mechanism and conditions required for the onset of pozzolanic reactions. Scanning electron microscopy (SEM) and Fourier Transform Infrared (FTIR) spectroscopy data were used

to support the XRD findings and justify selective chemical reactions taking place between lime and the soil minerals. The methylene blue index (MBI) data was used to assess the impact of lime dosage on the clay capture with time in the FFT cakes. The experimental test program followed is presented in Table 3.2.

Table 3.2 Experimental Program for Physicochemical Evaluation of Lime Treated FFTs

Test	Fraction	Day 0	Day 1	Day 7	Day 28	Day 60
pH	FFT, Cake	X			X	X
CEC	Cake	X		X		
MBI	Cake	X			X	
XRD	FFT, Cake		X		X	
SEM	Cake					X
FTIR	Cake	X				

3.5. Discussion of Experimental Test Methods and Results

3.5.1. pH of Lime Treated FFT Cakes

The pH of the untreated and lime treated FFT cakes were recorded immediately after the centrifuge experiment (Day 0) and subsequently on Day 28 and Day 60. The samples were stored in closed containers for the entire duration of the experimental study except while taking pH measurements. The pH data recorded at the various lime dosages and time periods described is presented in Figure 3.2.

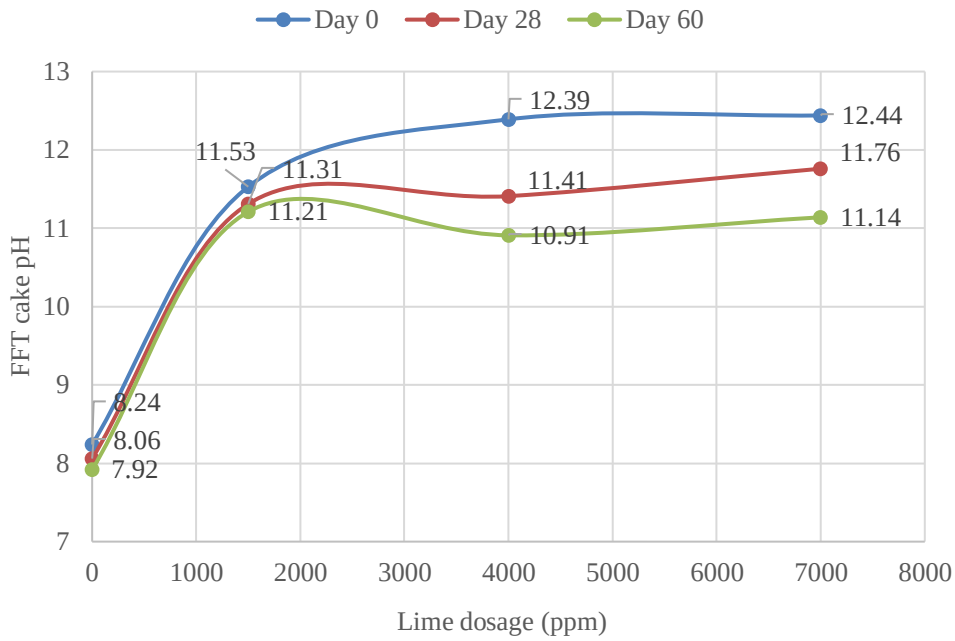

Figure 3.2 pH of the centrifuge cakes as a function of lime dosage and time

The initial pH of the untreated FFT was 8.24 and there was minimal drop in pH after 60 days likely due to exposure to the atmospheric CO_2 during test measurements. The target initial pH levels used to treat the FFT were retained in the cake fraction of the samples obtained after centrifugation. The reduction in pH with time in the lime treated cakes however is a consequence of carbonation during testing and due to chemical reactions taking place between lime and the soil minerals leading to dissolution and precipitation of new mineral phases. The chemical reactions likely to take place in the lime treated FFTs will be discussed later in this chapter.

3.5.2. CEC of Lime Treated FFT Cakes

3.5.2.1. Objectives and Experimental Test Method

The CEC of the untreated and lime treated FFT and cakes obtained after centrifugation were measured on Day 1 and Day 60 to understand the immediate and long-term impacts of lime on influencing cation exchange reactions with clay minerals.

The CEC of the extracted FFT cakes was determined by measuring the concentration of extracted sodium ions using ammonium acetate (1N, pH 7.0) after saturating the exchange sites of the inherent clays using sodium acetate (1N, pH 8.2).

3.5.2.2. Impact of Lime Treatment on CEC of FFT Cakes

The Day 1 and Day 60 CEC results obtained for various FFT cakes at the various lime dosages are presented in Figure 3.3. The values shown represent the average CEC measurements recorded on two samples.

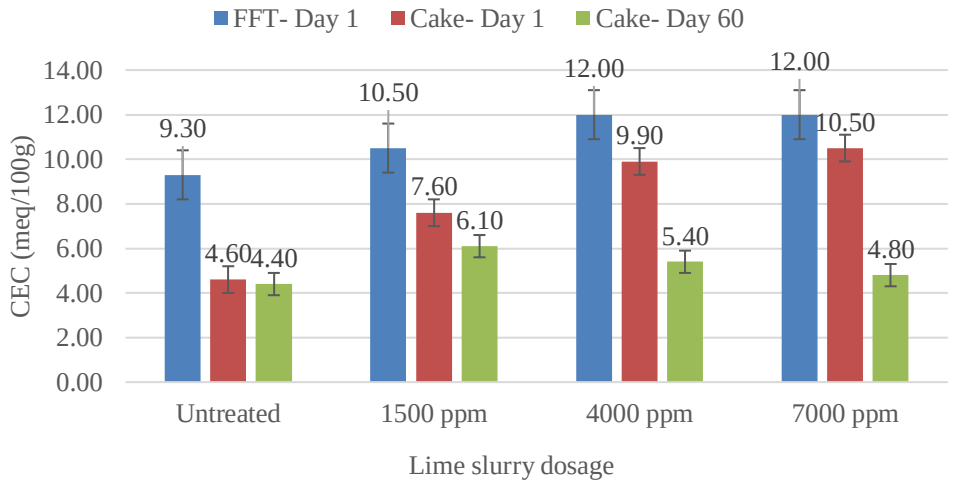

Figure 3.3 Comparison of CEC of FFT and cake as a function of lime dosage and time

The CEC values recorded range between 4 meq/100g and 12 meq/100g regardless of the fraction tested and lime treatment dosage. The CEC ranges for the common clay minerals present in oil sands are provided in Table 3.3, which is reprinted from Boxill [60]. The CEC values indicate that the predominant clay minerals present in FFT G are kaolinite followed by illite and possibly some mixed layer minerals. The actual mineralogical composition of the FFT was verified using X-ray diffraction (XRD) analysis and is presented in the later sections of this chapter.

Table 3.3 CEC Range of Common Clay Minerals Present in Oil Sands (Reprinted from [60])

Clay Mineral Type	Relative Plasticity	Activity	CEC (meq. /100g)
Kaolinite	Low	0.5	3-15
Illite	Low	0.5-1.0	10-40
Mixed layer (Kaolinite-Smectite, Illite-Smectite)	Medium-High	1.0-7.0	3-100
Chlorite	Low	0.5-1.0	10-40
Smectite	High	1.0-7.0	85-150
Vermiculite	Medium	1.0-7.0	100-150
Reference mineral: Montmorillonite	High	1.0-7.0	80-150

Since the primary objective was to gain some basic insight on the impact of lime addition on cation exchange properties of the clay minerals, the focus is on analyzing the trends of the CEC values with time and lime dosage and not on the absolute CEC values. Towards this end, the following observations and inferences are important based on the data obtained in Figure 3.3:

1. The initial (Day 1) CEC of lime treated FFTs are higher compared to the untreated FFTs likely due to the clays and residual organics becoming more reactive due to the increase in pH levels.
2. The ratio of the respective Day 1 CEC values of the cakes to FFT are 0.49 in the untreated sample and range between 0.72 and 0.87 for increasing dosage of lime indicating that more clays are captured in the cake fraction as the pH and lime dosage increases.
3. The CEC values of the untreated cake remain unchanged with time however there is a 20% to 55% reduction in CEC from over 60 days in the lime treated cakes with the maximum reduction at 7000 ppm dosage. This trend implies that the activity of the clay minerals is lowered with time as a result of direct chemical interactions with lime.

In summary, the CEC measurements provide a preliminary indication that the calcium released from lime is capable of exchanging with the sodium ions and other monovalent cations occupying the inner layer of clay minerals; the effectiveness of which is likely to be dictated by the relative concentration levels of the exchanging cations.

3.5.3. XRD Analysis of Lime Treated FFTs and FFT Cakes

3.5.3.1. Objectives

A series of XRD analysis was performed to understand the mineralogical changes taking place in FFT samples after separation of the solids through the decanter centrifuge. Understanding the impact of lime treatment on modifying the chemistry of the clays was the primary focus of the XRD analysis. The XRD experimental analysis was designed to only provide a qualitative understanding of the chemical reactions taking place with time in the FFTs after treatment with lime and other coagulants.

3.5.3.2. Experimental Setup

The soil minerals present in the FFTs were determined using a Bruker D-8 X-ray diffractometer using CuKα radiation powered to 40 kV at 40 mA. The samples were scanned from 2 to 70 degrees (2θ) for 60 min at 0.02 degrees/sec.

The focus of the XRD analysis of FFTs after treatment with lime was to evaluate the impact of lime dosage and the impact of time on the mineralogy of the FFTs. Toward that end, XRD patterns of the untreated FFT, untreated FFT cake obtained after centrifugation of the untreated FFT, FFT cake treated with 4000 ppm lime slurry and FFT cake treated with 7000 ppm lime slurry were recorded on the treatment day and after aging for 28 days in a closed container to negate the impact of carbonation. The XRD patterns were recorded after air-drying freshly obtained pastes from each of the samples at the respective times. The air-dry pastes were pulverized into powder form and placed on the XRD sample holder. The samples were leveled to ensure that the electron beam-sample interaction height remains nearly the same for all measurements to

assist with a relative comparison of the mineral peak intensities as a function of lime addition and sample aging. All the samples were analyzed as bulk samples without performing size fractionation to separate the clays from the sands and silts. It is important to note that 4000 ppm represents the optimum dosage of lime slurry required to elevate the pH of the FFTs to 12.4 while the dosage of 7000 ppm represents an over dose of lime to increase the pH above 12.4 and provide an excess supply of calcium ions for long-term reactions with the soil minerals.

3.5.3.3. Mineralogical Transformations in Aging Lime Slurry

Lime was added to the FFTs in the form of a 5% hydrated lime slurry to the FFTs in all the XRD experiments. Hence a logical first step was to evaluate the impact of aging on the mineralogy of the lime slurry used. Figure 3.4 shows the XRD patterns of fresh and 1-hour air-dry lime slurry.

The freshly prepared lime slurry is composed purely of portlandite or hydrated lime. On the other hand, there is significant amount of calcite in addition to portlandite in the lime slurry after 1 hour of air drying.

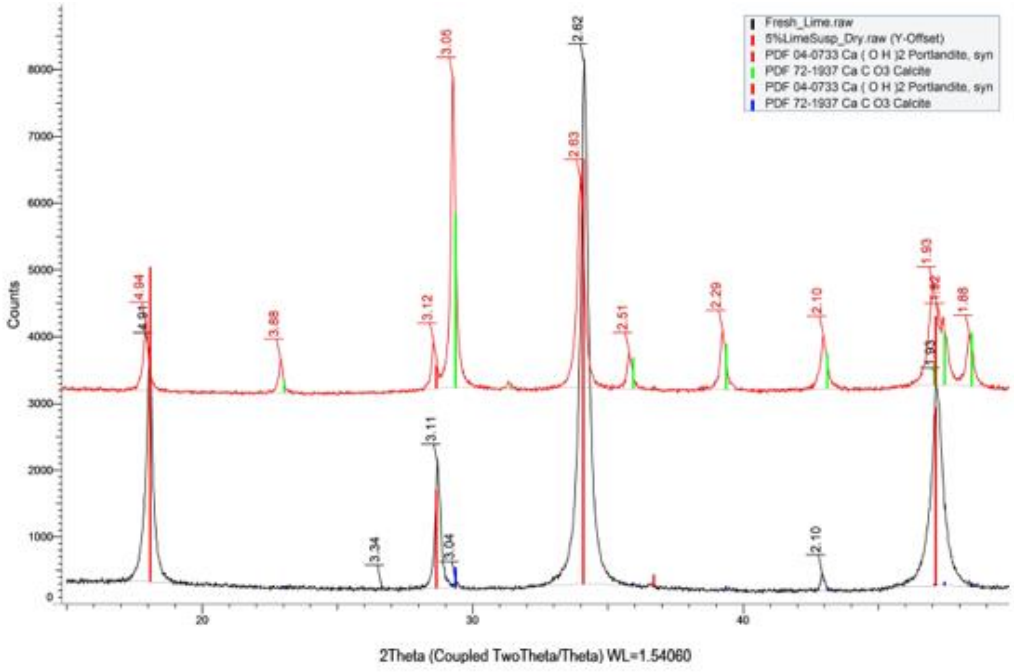

Figure 3.4 Comparison of XRD patterns of fresh and 1-hour air-dry lime slurry

The XRD patterns in Figure 3.4 clearly illustrate the transformation of portlandite or hydrated lime into calcite due to atmospheric carbonation per the following reaction.

$$Ca(OH)_2 + CO_2(atm) \rightarrow CaCO_3 + H_2O \quad (3.1)$$

The take-away from this exercise is that it is extremely important to limit the exposure of lime slurry to open air to 5 minutes or lesser prior to mixing with the FFTs. This would allow the $Ca(OH)_2$ to form calcite by reacting with the sodium-bound carbonates and bicarbonates present in the FFT according to equation 3.2 and equation 3.3 and subsequently increase the pH of the FFTs due to dissolution of the remaining $Ca(OH)_2$ according to equation 3.4.

$$Ca(OH)_2 + 2NaHCO_3 \rightarrow CaCO_3 + Na_2CO_3 + 2H_2O \quad (3.2)$$

$$Ca(OH)_2 + Na_2CO_3 \rightarrow CaCO_3 + 2NaOH \quad (3.3)$$

$$Ca(OH)_2 \rightarrow Ca^{2+} + 2OH^- \quad (3.4)$$

The formation of calcite due to carbonation prior to treatment of the FFTs would deplete the availability of Ca^{2+} ions for consuming the carbonates and bicarbonates, participating in cation exchange reactions with the FFT clays and for other direct chemical reactions with the soil minerals.

3.5.3.4. Immediate Impact of Lime Treatment and Dosage on FFTs

A comparison of the XRD patterns of the four samples obtained on the same day (Day 0) of treatment is presented in Figure 3.5.

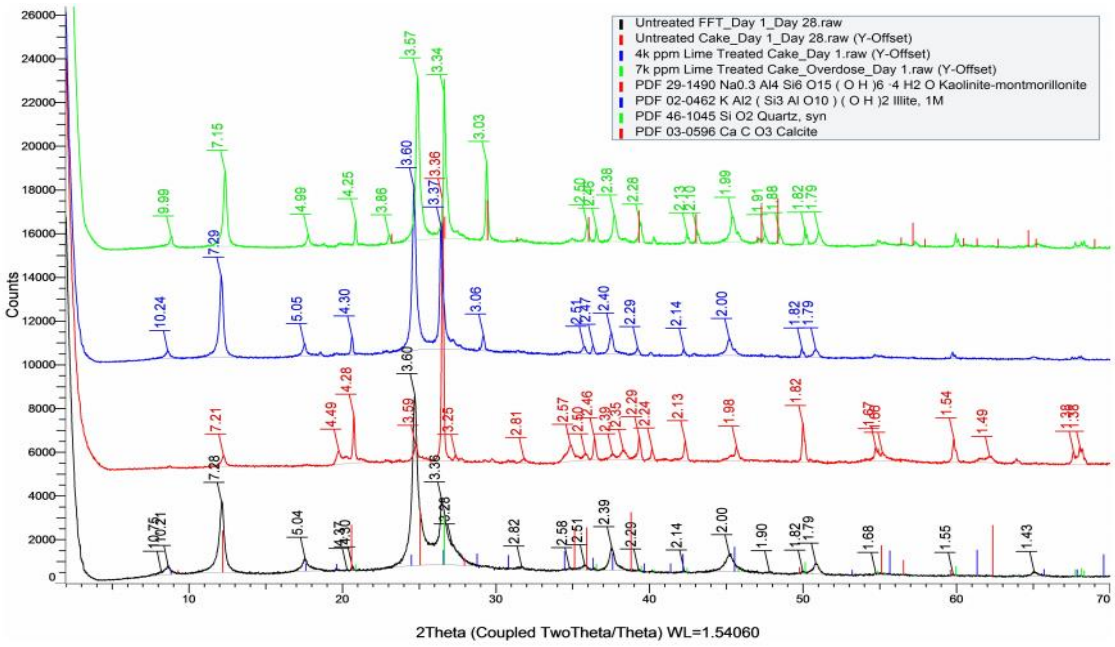

Figure 3.5 Comparison of the XRD patterns of untreated and lime treated FFT cakes with the untreated FFT – Day 0

As expected, the mineralogical composition of the FFT comprises quartz, kaolinite and mica mineral as identified and marked in the XRD pattern of the untreated FFT sample in Figure 3.5. The mica mineral present is expected to be illite given the dominance of illite in the oil sands. In Figure 3.5, the illite peak is identified by the 001-peak at a d-spacing of nearly 10 Å, the kaolinites are identified by the 7.2 Å 001-peak and quartz is identified by the peaks at 3.3 Å and 4.25 Å. The 002-peak of kaolinite is observed at a d-spacing of about 3.57 Å. When comparing the XRD patterns of the untreated and lime treated cake fractions with the untreated FFT, it is clear that there is improved clay capture in the cake fraction after lime addition due to the following observations:

1. The intensity of the 001-peaks of kaolinite and illite in the 4000 ppm and 7000 ppm lime treated cakes are similar to peaks observed in the untreated FFT.
2. The intensity of the 001-kaolinite peak is significantly reduced in the untreated cake sample compared to the untreated FFT accompanied by an increase in intensity of the 3.3 Å quartz peak and an absence of the illite peak in the untreated cake pattern.

The other interesting observation from Figure 3.5 is the formation of calcite in both the 4000 ppm and 7000 ppm lime treated cake samples identified by the peak at about 3.05 Å. The presence of calcite is expected to be due to both atmospheric carbonation and the consumption of both free and sodium-bound carbonates and bicarbonates in the FFT by the calcium from lime as previously discussed in equations 3.2 and 3.3. The combined impact of increasing supply calcium and increase in pH due

to lime addition on depleting the carbonates and bicarbonates is shown in Figure 3.6 [59].

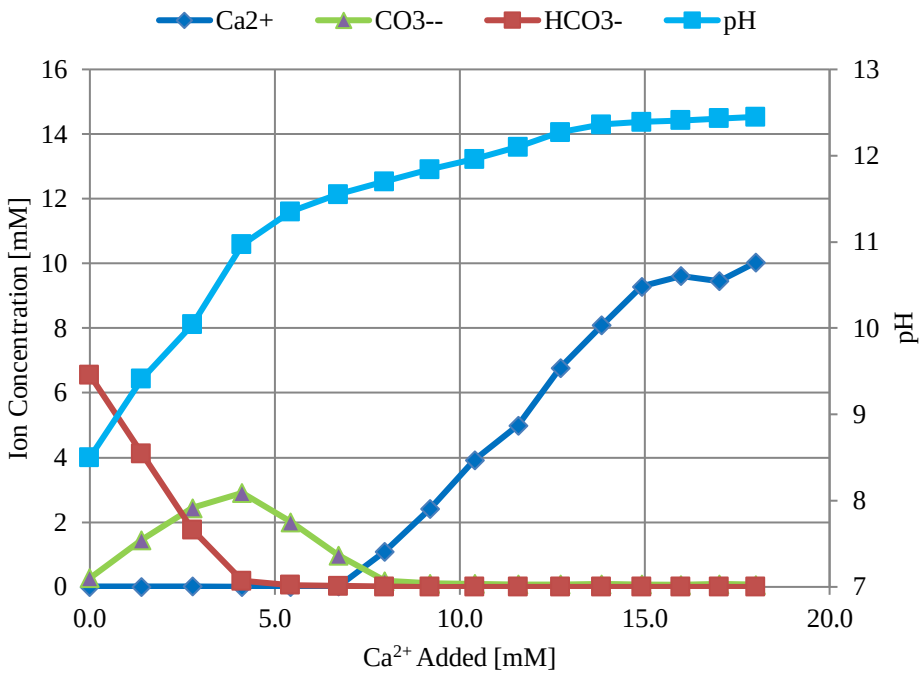

Figure 3.6 Titration of sodium bicarbonate with lime (reprinted from [59])

Figure 3.6 illustrates that the carbonates and bicarbonates precipitate out as calcite before soluble calcium is available for other chemical reactions with the soil minerals. Further, the intensity of the calcite in the lime overdose cake sample is higher compared to the calcite peak intensity in the 4000 ppm cake. This indicates that the excess lime supplied by the overdose samples continues to build up calcite in the FFT cakes even after the depletion of carbonate phases. The formation of calcite in the lime

treated samples is supported by spectroscopic data obtained using FTIR data and SEM images later in this chapter.

In summary, the XRD patterns in Figure 3.5 confirm that lime treatment enhances the capture of the clay fractions in the FFTs within the solids phase after centrifugation while only the quartz fraction is predominantly being captured in the solids phase of the untreated samples. Capturing the fine clays within the solids phase is a crucial first step in the treatment of FFTs as it clarifies the water and makes it suitable for recycling into the oil sands extraction process.

3.5.3.5. Impact of Lime Treatment and Dosage after 28 Days

A comparison of the XRD patterns of the 4000 ppm lime treated cake samples obtained on Day 0 and Day 28 is presented in Figure 3.7 along with the untreated FFT, untreated FFT cake.

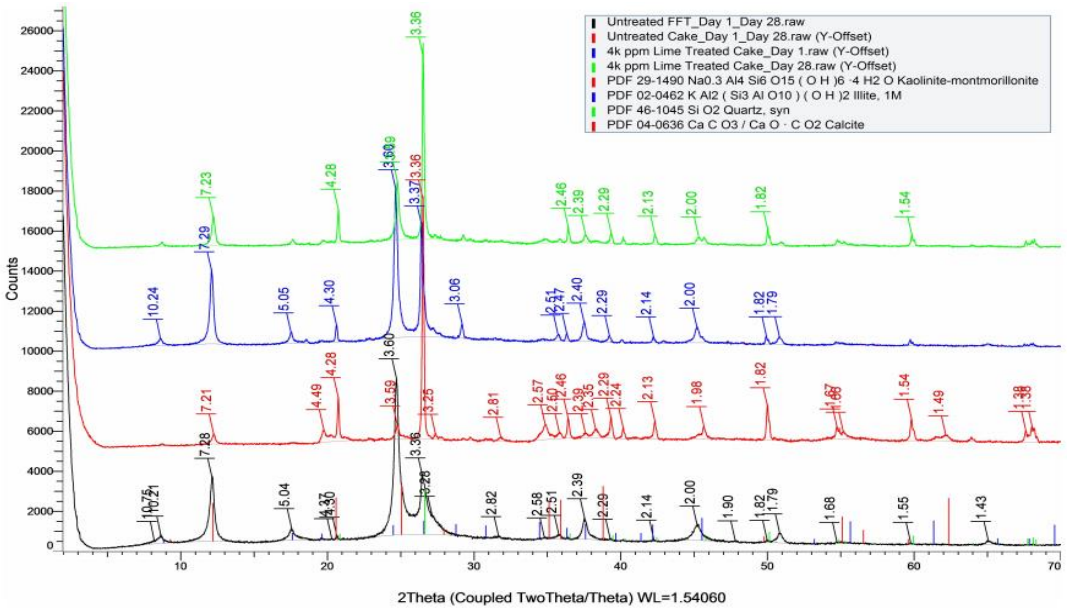

Figure 3.7 Comparison of XRD patterns of 4000 ppm lime treated cakes after Day 0 and Day 28 with the untreated samples.

The untreated FFT was resampled and analyzed to confirm that there are no changes in mineralogy with time due to the influence of external impurities during the experimental procedures. Based on the XRD patterns in Figure 3.7, the following observations can be made regarding the mineralogical changes in the FFT cakes:

1. The mineralogy of both the untreated FFT and cake samples remain unchanged as expected confirming that there are no changes in the chemistry of the minerals with time.
2. There is a reduction in the intensity of the 001 and 002 kaolinite peaks in the Day 28 lime treated cakes compared to the Day 0 lime treated cake.
3. There is a reduction in the intensity of the calcite peak in the lime treated sample after Day 28.

The changes observed in the XRD patterns of the lime treated samples taken on Day 0 and Day 28 help provide a preliminary understanding of the possible chemical interactions between lime and the clays present in the FFTs, in particular kaolinite.

First, there is a reversal in the trend in the intensities of the 002-kaolinite peak at 3.60 Å and the 3.3 Å quartz peak in the Day 28 when compared to the XRD patterns of both the untreated parent FFT and the Day 0 lime treated cake indicating that lime was effective in coagulating the FFT resulting in increased particle size of minerals and textural modification of the clays to a lower plasticity silty fraction.

The XRD observations regarding the impact of lime on enhancing initial clay capture in the cakes and subsequently coagulating the clays over the first 28 days are supported by MBI measurements shown in Table 3.4 determined following the method outlined by Kaminsky [61]. The clay contents in Table 3.4 were calculated using equation 3.5 proposed by Kaminsky [61].

$$\%\ Clay\ Content = \frac{MBI\left(\frac{meq}{100g}\right)+0.04}{0.14} \tag{3.5}$$

Table 3.4 Comparison of Day 0 and Day 28 MBI before and after Lime Treatment

Sample Description	**Day 0**		**Day 28**	
	MBI (meq/100g)	**% Clay Content**	**MBI (meq/100g)**	**% Clay Content**
0ppm cake	3.51	25.35	3.45	24.92
4000 ppm lime cake	7.40	53.14	4.28	30.85
7000 ppm lime cake	7.10	51.10	3.90	28.14

Next, the interaction of the calcium ions released from lime directly with the soil minerals is not fully understood based on the XRD patterns. However, the silicates and aluminates present in the clay minerals illite and kaolinite tend to dissolve at pH above 10.5 as shown in Figure 3.8 leading to the possibility of forming pozzolanic reaction products over time such as calcium silicate hydrate (CaH_2SiO_4 or C-S-H) and calcium aluminate hydrate ($CaAl_2O_4 \cdot H_2O$ or C-A-H) through reactions similar to those presented in equations 3.6 and 3.7.

$$Ca^{2+} + SiO_2 + 2H_2O \rightarrow CaH_2SiO_4 + 2H^+ \quad (3.6)$$

$$Ca^{2+} + Al_2O_3 + 2H_2O \rightarrow CaAl_2O_4.H_2O + 2H^+ \quad (3.7)$$

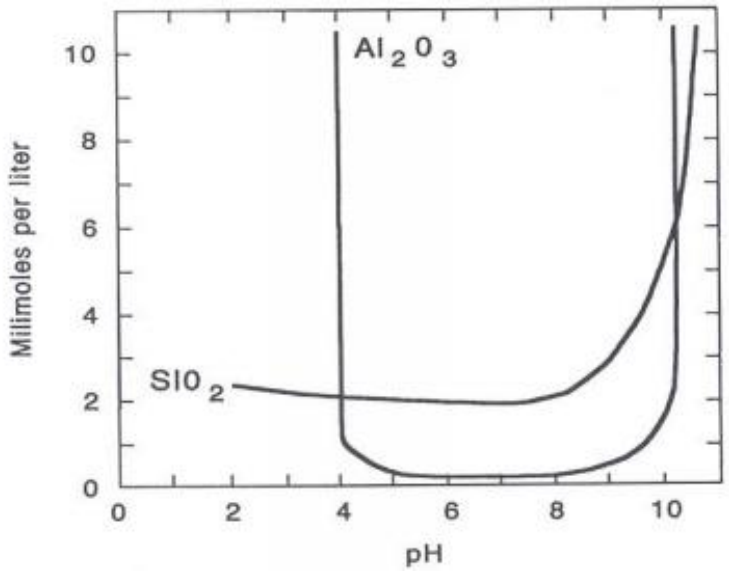

Figure 3.8 Solubility of aluminum oxide and silicon dioxide as a function of pH (reprinted from [62])

Per the reaction in equation 3.5, calcium cations from lime ($Ca(OH)_2$) react with silicic acid ($Si(OH)_4$) functional groups of the clays (*e.g.*, kaolinite ($Al_2Si_2O_5(OH)_4$) or illite ($K, H_3O)(Al,Mg,Fe)_2(Si,Al)_4O_{10}[(OH)_2,(H_2O)]$) to produce calcium silicate hydrates ($C\text{-}A\text{-}H_2SiO_4 \cdot 2H_2O$). Per the reaction in equation 3.6, the calcium cations react with aluminate ($Al(OH)_4$) functional groups of the clays to produce calcium aluminum hydrates ($C\text{-}A\text{-}H_2SiO_4 \cdot 2H_2O$). Both the above reactions are expected to occur in an environment having a pH of above 12.0 based on the solubility trends of alumina and silica ions shown in Figure 3.8. A drop in pH is expected as a consequence of the formation of C-S-H and C-A-H due to the consumption of hydroxyl ions in equation 3.6 and 3.7.

The pozzolanic reaction products described are poorly crystalline and mostly exists in an amorphous state thereby making them difficult to detect using XRD analysis. The pozzolans exhibit properties associated with a strong cementation matrix therefore resulting in substantially increasing the long-term shear strength of the FFTs. Given that the solubility of the clay minerals is the driving force for the pozzolanic reactions to occur, such reactions do not occur when the tailings are treated with acidic coagulants such as gypsum, alum or calcium chloride. Some evidence of the formation of interstratified gel-like strands of calcium silicates and calcium aluminates in lime treated FFT cakes was observed through scanning electron microscope (SEM) image of the lime treated cakes as seen in the red-circled portion of Figure 3.9 and accompanying elemental composition analysis recorded 60 days after treatment.

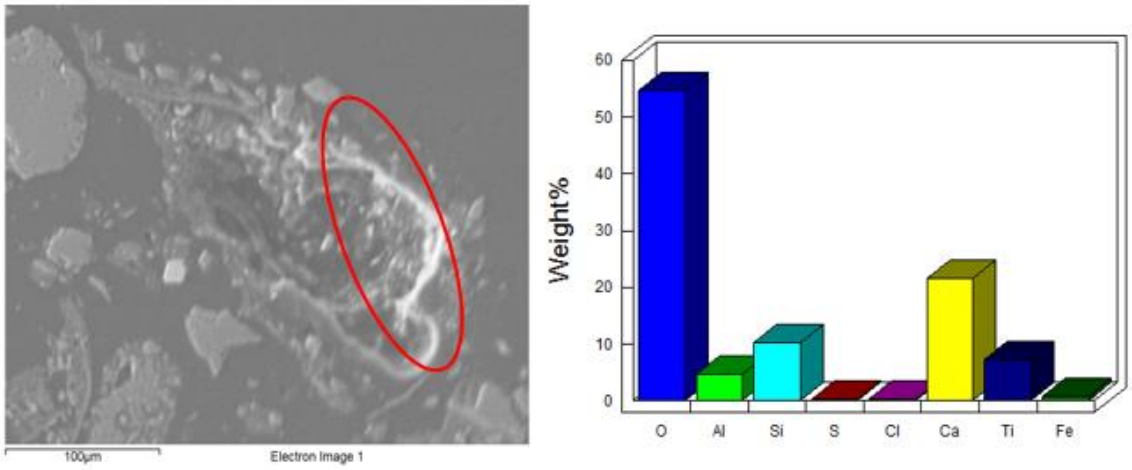

Figure 3.9 SEM image and elemental composition analysis of the 4000 ppm lime treated cake on Day 60

The other chemical reaction that could modify the clays and contribute to long-term strength gain in lime treated FFT cakes is due to the interaction of free calcium ions released either from lime or calcite dissolution with the kaolinites. In this reaction, the calcium ions from lime could replace the H^+ ions present in the silol group of the kaolinite edges at high pH and cement the kaolinite by forming a calcium kaolinite compound through the reactions shown in equation 3.8 and equation 3.9.

$$Ca(OH)_2 + Kaolinite_{edge} - SiOH \rightarrow Kaolinite_{edge} - Si - O - CaOH + H_2O \quad (3.8)$$

$$Kaolinite_{edge} - SiO - CaOH + Kaolinite_{edge} - SiOH \rightarrow (Kaolinite - SiO)_2Ca + H_2O \quad (3.9)$$

Such interaction of the calcium ions with the silol groups in kaolinite is also expected to contribute to a drop in pH after the precipitation of new phases due to the consumption of hydroxyl ions similar to the trend observed as a consequence of pozzolanic reactions.

3.5.4. FTIR Spectroscopy Analysis of Lime Treated Cakes

3.5.4.1. Objectives and Experimental Setup

The purpose of obtaining FTIR spectra on lime treated FFT cakes was to support the findings of the XRD analysis relating to the formation of calcite due to immediate chemical reactivity with the bicarbonates and carbonates in the FFTs as explained through equations 3.2 and 3.3 and to illustrate the excellent initial clay capture after lime treatment. Both these observations were recorded through the Day 0 XRD analysis of the samples in Figure 3.5.

FTIR spectra was recorded on the untreated FFT, 4000 ppm lime treated cake and 7000 ppm lime treated cake samples using the Attenuated total reflection (ATR) method in the Thermo Nicolet 380 FTIR spectrometer. The samples were tested in a wet state to minimize the impact of carbonation 6 hours after treatment.

3.5.4.2. Discussion of FTIR Spectra

Figure 3.10 shows a comparison of the FTIR spectra obtained for the three samples tested.

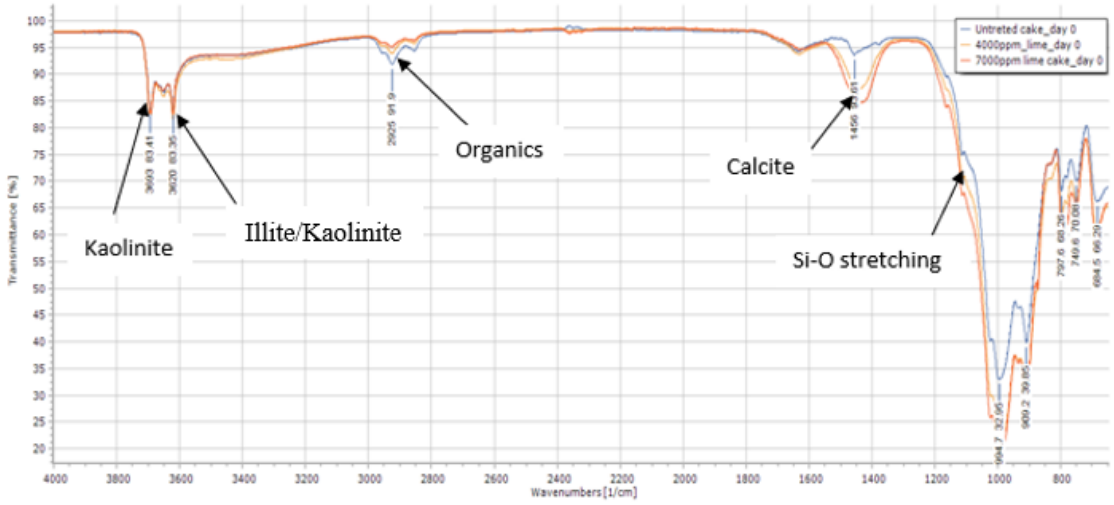

Figure 3.10 FTIR spectral bands of Day 0 untreated FFT and lime treated FFT cakes

The transmittance bands of interest in the FTIR pattern are those pertaining to calcite at a wave number of 1450 cm^{-1} [63] and the kaolinite and illite patterns at wave numbers 3693 cm^{-1} and 3620 cm^{-1} [64], respectively. The bands of kaolinite and illite in

all three samples match closely, which proves that most of these clays were captured within the solids fraction after lime treatment. The wider and deeper calcite band in the lime treated cakes implies that significantly higher quantities of carbonates were absorbed by the FFTs compared to the untreated FFT resulting in precipitation of calcite. The FTIR spectra hence validates the XRD findings in Figure 3.5 and provide important supporting evidence regarding initial mineralogy of the lime treated FFTs.

Further analysis is required to fully establish the changes in mineralogy of the clay minerals with time and understand the nature of the bonds involving silica and alumina using the FTIR technique.

3.5.5. SEM Analysis of Lime Treated Cakes

3.5.5.1. Objectives

The main goal of obtaining SEM images of the untreated and lime treated FFT cakes was to identify the formation of pozzolanic reaction products such as C-S-H and C-A-H in the lime treated samples. An example of the formation of C-S-H as a separate amorphous phase was captured using SEM and shown in Figure 3.9. This section focuses on identifying the phases of existence of calcite and C-S-H by mapping the elements detected through SEM images.

3.5.5.2. Experimental Setup and Sample Preparation

SEM images of untreated and 4000 ppm lime treated cakes were taken after aging for 60 days to study the durability of the products formed as a result of chemical reactions. The samples for SEM analysis were sampled separately from the initial centrifuge cakes, concealed and stored at room temperature. After 60 days, 0.5 gram of

material was sampled and polished thin film sections 2 inches long by 1-inch wide were prepared for SEM analysis. A polished thin section of the sample was used so that the interaction height between the electron beam and the sample surface is constant and uniform across the sectional area [65]. The SEM samples were prepared by National Petrographic Service, Inc.

3.5.5.3. Characterization of Calcite in the Lime Treated FFT Cakes

An SEM image of the 4000 ppm lime treated cake is shown in Figure 3.11 together with the elemental spectrum data of the location of a mineral and calcite deposits.

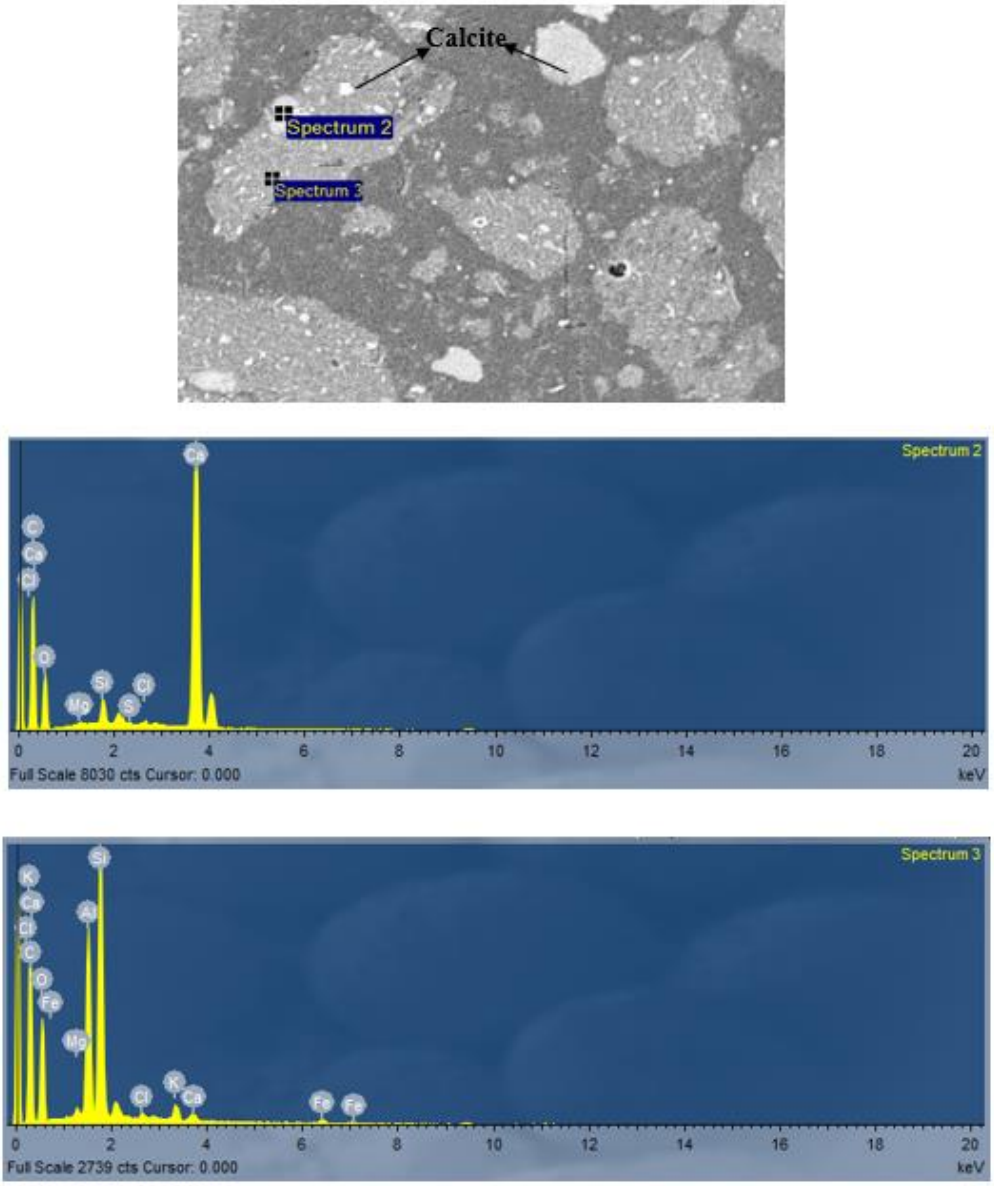

Figure 3.11 SEM image and spectral map of Day 60 lime treated FFT cake showing calcite deposits

The ratio of Si to Al in spectrum 3 is between 1 and 2 indicating that the mineral located is kaolinite having equal proportion of Si and Al composed of one tetrahedral layer and an octahedral layer. The excess Si intensity in spectrum 3 is likely due to the influence of some quartz particles (SiO_2) surrounding the kaolinite mineral.

Upon analyzing the SEM image and the accompanying elemental composition data in Figure 3.11, it is evident that the distinctly bright structures in the image correspond to calcite deposits in the lime treated FFT cake. Another important observation that can be made is that calcite forms both as a separate phase and is also deposited on several locations within the surface of the kaolinites.

3.5.5.4. Characterization of Calcium Phases in Lime Treated FFT Cakes Using Elemental Mapping

To understand if there are any other calcium deposits besides calcite existing either separately or coating the surface of minerals, the locations of $Ca, Al\ and\ Si$ peaks were individually mapped within the SEM images taken using the Day 60 untreated and lime treated samples and analyzed. The SEM images of the untreated cakes and lime treated cakes along with the phase maps are shown in Figure 3.12 and Figure 3.13 respectively.

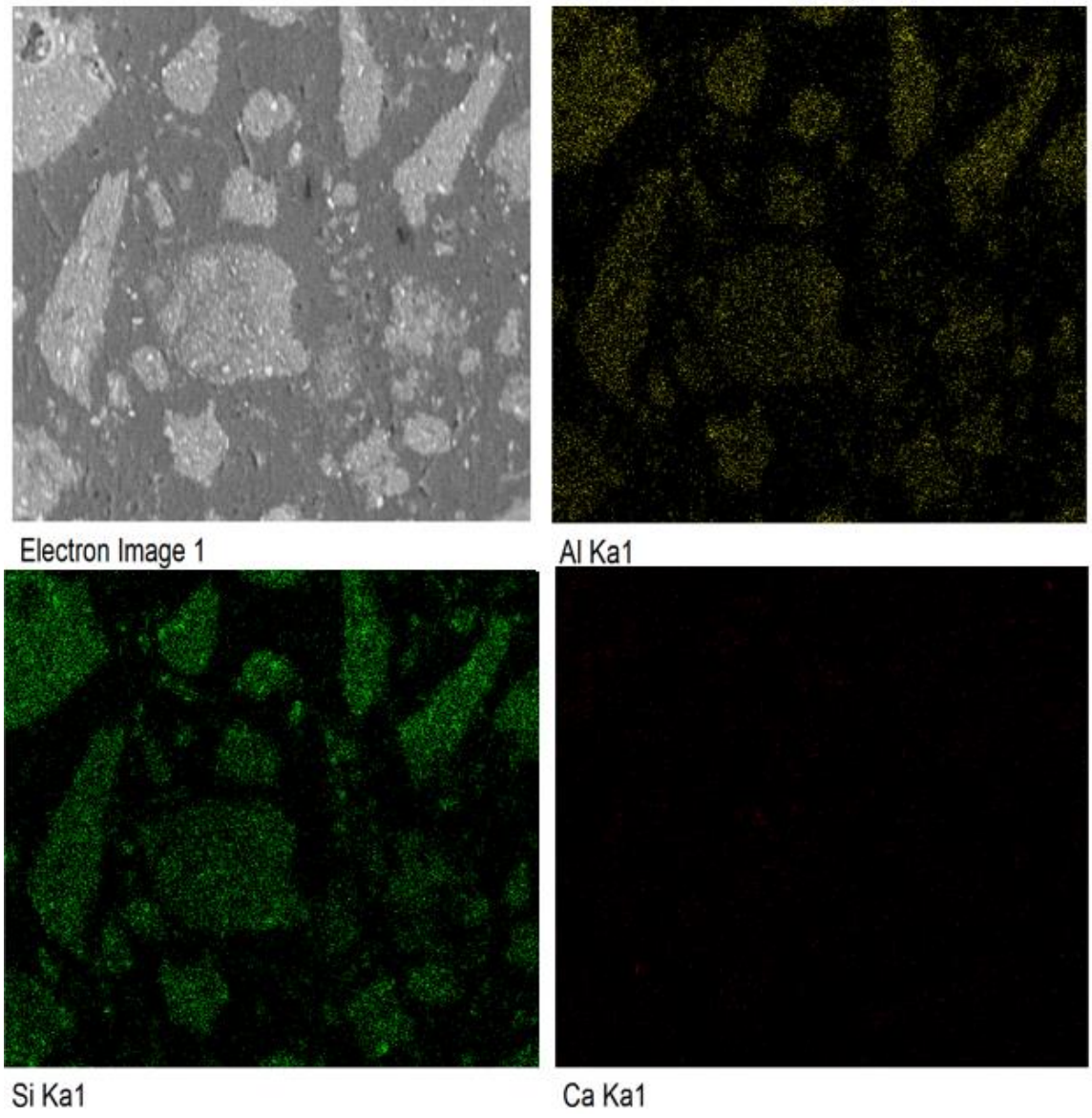

Figure 3.12 Elemental phase mapping within Day 60 SEM image of untreated FFT cake

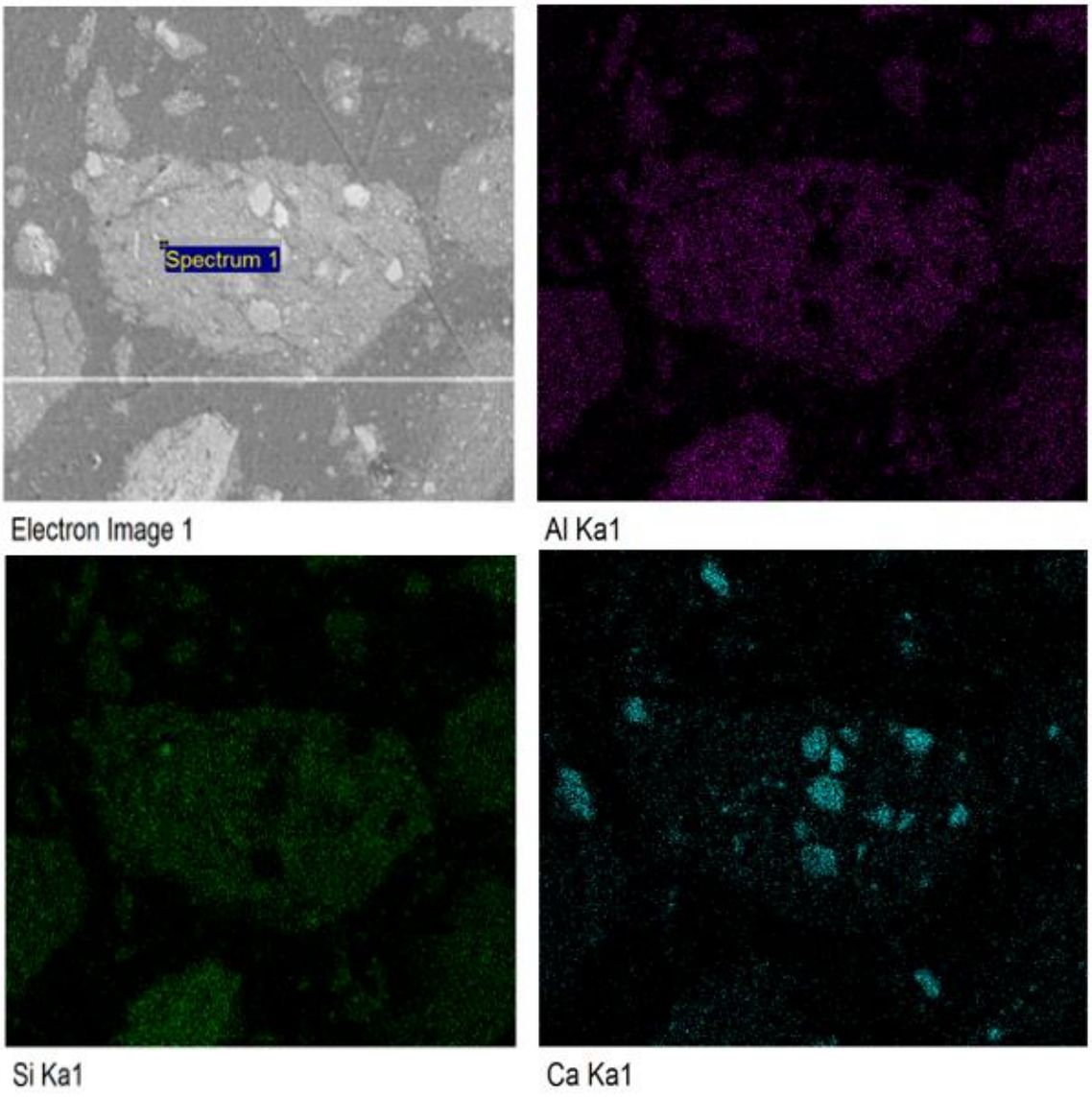

Figure 3.13 Elemental phase mapping within Day 60 SEM image of 4000 ppm lime treated FFT cake

The obvious and general observation that can be made comparing the elemental phase maps in Figure 3.12 and Figure 3.13 is that there significant amounts of calcium deposits in the lime treated cake while calcium is non-existent in the untreated FFT cake. Also, the calcium deposits in the lime treated sample existing as calcite are easily

distinguished by the well-defined bright spots within the Ca phase map. To further probe the fate of the remaining calcium deposits within the lime treated sample, a spectral map of all elements constituting a general location (spectrum 1) rich in $Ca, Al\ and\ Si$ was obtained and is shown in Figure 3.14.

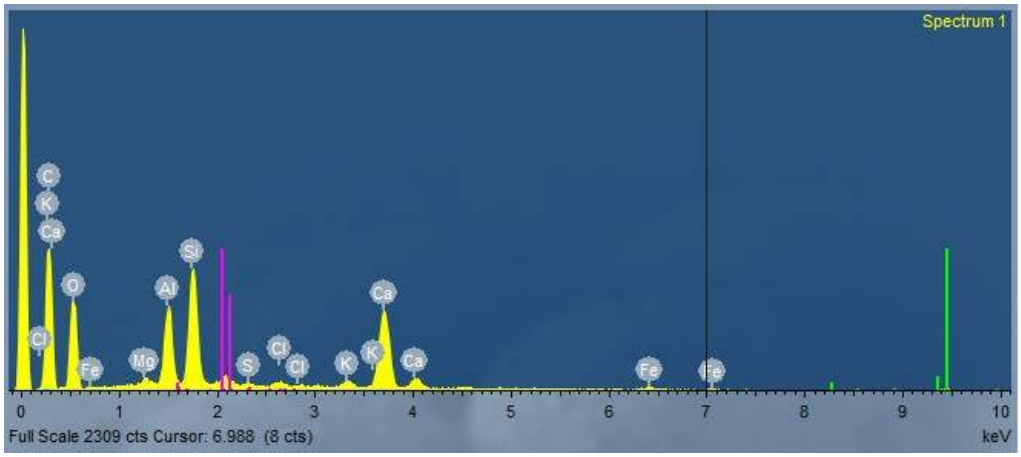

Figure 3.14 Spectral map of a location within the lime treated sample rich in Ca, Al and Si

The elemental composition observed in the spectral map in Figure 3.14 confirms the presence of $Ca, Al\ and\ Si$ and also confirms the dominance of Ca^{2+} ions coating the surface of minerals, kaolinite in the instance of spectrum 1. The data hence serves as an important reference to support the earlier proposed hypothesis that calcium could interact with the kaolinite forming a cementitious product through reactions such as or similar to those proposed in equation 3.8 and equation 3.9.

3.5.6. Comparing the Impact of Ca-based Coagulants on FFT Cake Mineralogy Using XRD

3.5.6.1. Objectives and Experimental Setup

The primary objective of this exercise was to compare the impact of the same supply of calcium ion concentration through lime and acidic calcium-based coagulants namely gypsum and calcium chloride. The XRD analysis was performed on 28-day aged FFT cake samples treated with approximately 1600 ppm calcium concentration supplied through either 3000 ppm lime slurry, 4500 ppm calcium chloride or 7000 ppm gypsum slurry. The FFT cake samples used for this analysis were obtained after dewatering the coagulant treated FFT using a benchtop centrifuge. The same sample preparation method described in the previous XRD analysis of the effects of lime dosage with time was adopted in this experiment. The pH of the lime, calcium chloride and gypsum treated cakes at the time of testing were recorded to be 12.1, 6.4 and 5.8 respectively.

3.5.6.2. Discussion of XRD Patterns

The XRD patterns of the lime, gypsum and calcium chloride treated cakes are shown in Figure 3.15 along with the XRD pattern of the parent FFT.

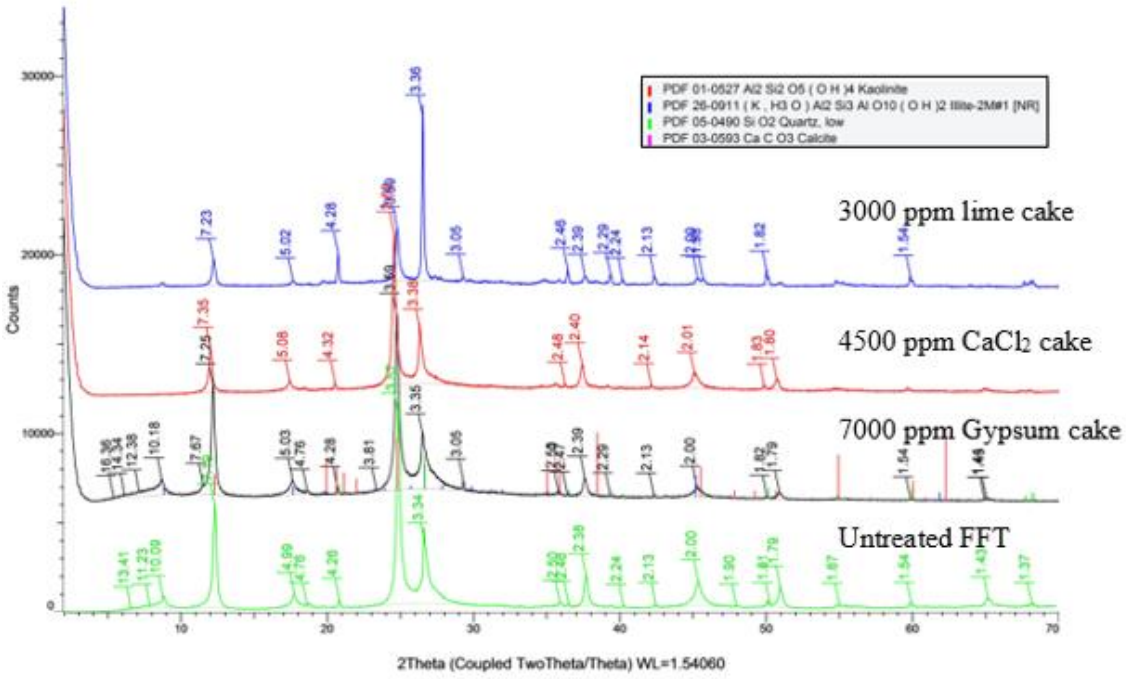

Figure 3.15 Comparison of XRD patterns obtained after FFT treatment with equivalent dosages of gypsum, lime and calcium chloride

The mineralogical composition of the parent untreated FFT was the same as that described in the previous XRD analysis. The mineralogy of the gypsum treated FFT cake remained largely unchanged except for precipitation of small amounts of calcite. The most important take aways from Figure 3.15 are the reduction in intensity of the 001 and 002 kaolinite peaks in the 3000 ppm lime treated FFT cake similar and consistent with the patterns observed in previous lime treated samples. Further the 3.3 Å quartz peak in the lime treated cake appears to be sharper compared to the other patterns which is an indication that lime improves the crystallinity of the quartz particles and assists their settling behavior. Another interesting aspect to note in the XRD patterns of the calcium chloride and lime treated cake samples is their effects on dissolution of illite and

possible some other interstratified clay minerals. This observation is inconclusive and could be the result of a sampling anomaly based on other XRD patterns recorded on bulk samples treated with calcium chloride and lime. Nevertheless, it is clear from Figure 3.8 that a pH above 10.5 is required to solubilize either kaolinite or illite and result in any mineralogical changes with time, a requirement that is uniquely met by lime and not by gypsum and calcium chloride.

3.6. Summary and Conclusions

A chemical and mineralogical (physicochemical) evaluation was performed to assess the interaction between lime and the soil minerals present in the oil sands FFTs. The analysis was conducted on the solid cake fraction obtained after dewatering the FFTs using a decanter centrifuge. The focus of the investigation was to understand the sequence of chemical reactions taking place in the lime treated FFTs together with the conditions required to facilitate the reactions using basic chemical properties namely pH, CEC and MBI and analytical methods namely XRD, SEM and FTIR. The performance of lime was also compared against an equivalent supply of calcium concentration through two other calcium-based coagulants namely gypsum and calcium chloride. The following remarks and conclusions were drawn based on the experimental data obtained:

1. Comparison of the initial (Day 0) CEC, MBI and XRD patterns of the untreated and lime treated FFT cakes indicates that the mineralogy of the source FFT was retained in the cake fraction after lime treatment while there was poor clay capture in the untreated cake.

2. The XRD patterns also illustrate the formation of calcite in the lime treated FFT cakes likely due to a combination of the depletion of carbonates and bicarbonates and carbonation of the excess unreacted lime. Calcite in the lime treated cakes existed both as a separate phase and was deposited on the surface of kaolinites as illustrated through the FTIR and SEM analysis.
3. The formation of calcite was accompanied by an intensity reduction in the kaolinite peak in the XRD patterns recorded 28 days after lime treatment. Further, elemental phase mapping of the SEM patterns showed the coexistence of $Ca, Al\ and\ Si$ on the surface of the kaolinites leading to the possibility of calcite cementing the kaolinite particles as explained by equations 3.8 and 3.9.
4. Lime increases the pH of the FFTs above 12.0 due to the release of hydroxyl ions thereby enhancing the solubility of the aluminates and silicates present in the clay minerals and leading to the formation of pozzolanic products such as C-S-H and C-A-H. The formation of pozzolanic products was illustrated using an SEM image. Gypsum and calcium chloride on the other hand decrease the pH of the FFTs.
5. The optimum lime dosage required for modification of clays through cation exchange reactions and for development of long-term strength through pozzolanic reactions is expected to not only depend on the pH but also the clay content in the source FFT characterized by the MBI.

In summary, this chapter demonstrates the likely impact of lime on modifying the chemical and mineralogical properties of the FFTs through the various chemical

reactions discussed and illustrated. It is also important to understand that interpretation of the results obtained from the analytical methods discussed in this chapter should consider the assumptions involved in sample preparation and testing conditions. The physical effects of lime addition including reduction in plasticity of the clays and improving the long-term shear strength will be discussed in the next chapter.

4. GEOTECHNICAL EVALUATION OF LIME TREATED FLUID FINE TAILINGS DEWATERED USING PRESSURE FILTRATION TECHNIQUE

4.1. Basic Characterization of the Source FFT

Basic characterization of the FFT source analyzed using the pressure filtration technique included the same set of experiments performed on FFT G as described in Chapter 3. Table 4.1 provides a summary of the basic characterization properties of FFT I. The physical and geotechnical properties of FFT I were investigated after dewatering using the pressure filtration technology.

Table 4.1 Summary of Basic Characterization Properties of FFT I

FFT ID	SC, %	Dean-Stark Analysis (%)			MBI, meq/100g	pH	Na^{+}, mg/L	Ca^{2+}, mg/L	Mg^{2+}, mg/L	SAR
		Bitumen	Minerals	Water						
I	29.9	1.5	28.4	70.1	12.2	8.9	297	58	24	9

4.2. Dewatering of FFT Using Benchtop Filtration

An ‘Outotec Labox 100’ pressure filter was used to achieve filter cakes of approximately 55%, 65% and 70% solids content by mass. The slurries were filtered at 6 bar using an air operated double diaphragm pump. After filtration ceased, the filter cake further dewatered with a membrane squeeze applied at 15 bar. The membrane squeeze was stopped once enough water was removed to produce a filter cake with the target gravimetric solids content. The membrane was then relieved and an air blow of

approximately 2 bar was applied for 2 min. The filter cake was then homogenized immediately and transferred into specimen jars and sealed for strength measurements and subsequent geotechnical evaluation. The pressure filtration test setup is shown in Figure 4.1.

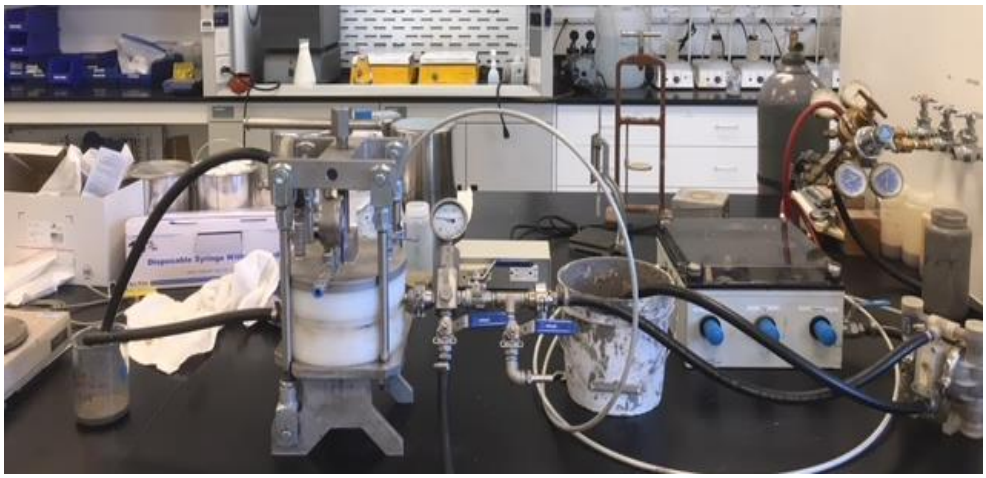

Figure 4.1 Pressure filtration test setup to dewater FFTs

The material obtained after the pressure filtration process is referred to interchangeably by one of the following terms in this Chapter: FFT cakes, filter cakes, filter pressure cakes or pressure filter cakes. An image of the FFT I sample before dewatering and a 70% solids lime treated pressure filter cake are shown in Figure 4.2.

Figure 4.2 A sample of FFT I (left) and a sample of a lime treated FFT cake (right)

4.3. Experimental Design

Experimental tests were designed to investigate the impact of various coagulant and flocculant treatments on FFT and cake fractions is presented. The FFT slurry was processed through the pressure filter without treatment, after treatment with a 5% lime slurry, a combination of alum slurry and A3338 polymeric flocculant and using A3338 separately. The tests were designed to focus on understanding the impact of lime treatment on the geotechnical properties of the pressure filter cakes over the first six months and compare the performance of lime with that of the polymeric flocculant separately and a combination of alum and polymer. Geotechnical evaluation of the FFT cakes included measuring the Atterberg limits,% clay fraction (finer than 2 micron) and undrained shear strength on Day 0, Day 1, Day 7 and Day 28 and undrained shear strength of the various pressure filter cake samples on Day 0, Day 1, Day 7, Day 28, Day

90 and Day 180. Undrained shear strength measurements included both peak and residual undrained shear strengths.

The data collected from the experimental test program was used as follows to assess the suitability of the lime treated FFT cakes for use as material for development of uplands:

1. The Atterberg limits namely liquid limit (LL) and plastic limit (PL) and the solids concentration of the cake samples were used to determine the liquidity index (LI) of the cakes and subsequently obtain a normalized liquidity index (LI') considering the change in colloidal clay activity with time.
2. The peak and remolded undrained shear strength data obtained together with the solids concentration data were compared against the target strength requirements for various oil sands tailings reclamation options provided in the nomogram (Figure 2.1) developed by McKenna [20] .
3. A multistep numerical model was developed to capture the effects of aging on LI' and strength of the lime treated cakes. The ultimate goal of this model was to predict the strength of lime treated FFT cakes over the first year for a given dosage using only the initial Atterberg limits, solids concentration of the untreated FFT and the pH of the lime treated samples.

4.4. Experimental Methods

4.4.1. Coagulant and Flocculant Treatments

The calcium-based coagulants used during various phases of this study are alum and hydrated lime. Hydrated lime was prepared as a 5% mixture in distilled water by

mass. The hydrated lime generates a lime slurry that must be re-suspended before addition. Alum was prepared as a 1% mixture in distilled water by mass. The hydrated lime used was high calcium from Graymont's Indian Creek quarry. The flocculant used in the study are partially hydrolyzed polyacrylamide (HPAM) anionic polymer flocculant namely A3338 and was produced by SNF.

After basic characterization of the FFT samples, the FFTs were treated with the hydrated lime slurry at an optimum dosage to achieve a pH target of 12.4 and another to achieve a pH target well in excess of 12.4 to investigate the effects of a calcium overdose on the FFT properties. The optimum dosage of alum slurry was selected by pH titration to lower the FFT pH to 7.0. A 1500 ppm dosage on a total dry solids mass of FFT of the polymeric flocculant A3338 was used to be consistent with the flocculant dosage used in oil sands tailings dewatering applications.

In summary, the FFT samples were treated using (a) 0 ppm coagulant or flocculant (*i.e.*, a control), (b) 4000 ppm (*e.g.*, ppm on a wet weight basis) hydrated lime slurry, (c) 10000 ppm hydrated lime slurry, (d) 1500 ppm A3338 polymer (*i.e.*, an anionic polyacrylamide polymer) on a dry solids basis, and (e) a combination of 700 ppm alum (ppm on a wet weight basis) and 1500 ppm A3338 polymer on a dry solids basis.

4.4.2. Measurement of Clay Content

The clay content in the FFT cakes were measured using the Cilas 1190 laser diffraction particle size analyzer after diluting 1 gram of the pressure filter cake samples with 500 mL of deionized water. Residual bitumen was removed from the FFT cake

samples before taking the measurements. The step-wise procedure to remove the residual bitumen is as follows:

1. Weigh out a desired amount of FFT
2. Bring FFT to an elevated temperature of about 50-80 ̊C on a hot plate. A beaker with excess volume is required to keep the reaction contained
3. Slowly add 10% hydrogen peroxide while stirring depending on the amount of FFT.
4. As the hydrogen peroxide starts to react with the organics present in the FFT and vigorous bubbling occurs, remove the FFT from the hot plate and wait until the reaction has subsided. Weigh and mix more of the hot FFT if required to stop the bubbling process.
5. Reweigh the beaker containing the FFT and bring it to the original mass to maintain integrity of sample.

4.4.3. Measurement of Liquid Limit of FFT Cakes

The liquid limit (LL) is defined as the gravimetric water content below which a material changes from the liquid to the plastic state. The LL of the FFT cakes were measured using the Humboldt H-5237 drop cone penetrometer in accordance with the ISO 17892-12 [66] procedure. The typical liquid limit consistency of FFT cakes is shown in Figure 4.3.

Figure 4.3 Consistency of a typical FFT cake sample at liquid limit

In this method the water content of the soil sample is increased progressively from a drier to a wetter state followed by recording the corresponding penetration depth of a 60°cone with a mass of 60-gram that is allowed to free fall for 5 seconds. The test is repeated to obtain a minimum of three penetration depths between 7 mm and 15 mm including a minimum of one penetration depth between 7 mm and 10 mm and one between 10 mm and 15 mm. The liquid limit is then reported as the gravimetric water content at which the 60°/60-gram cone penetrates the soil to a depth of 10 mm.

4.4.4. Measurement of Plastic Limit of FFT Cakes

The plastic limit (PL) is defined as the gravimetric water content below which a material changes from a plastic state to a semisolid state. Another interpreted definition of the plastic limit is the gravimetric water content of the soil at which its liquidity index

is zero. The PL of the filter press cakes was measured following the standard ASTM D4318 [67] procedure.

The drop cone penetrometer is not commonly used to determine PL. A new method has been proposed for specifically determining the plastic limit of filtered or centrifuged oil sands tailing cakes based on an assumed correlation of the material's shear strength at its liquid limit and plastic limit. The method proposed is included in Appendix A. A typical setup of the PL measurements using the drop cone penetrometer is shown in Figure 4.4 along with an image of an FFT cake sample near its PL.

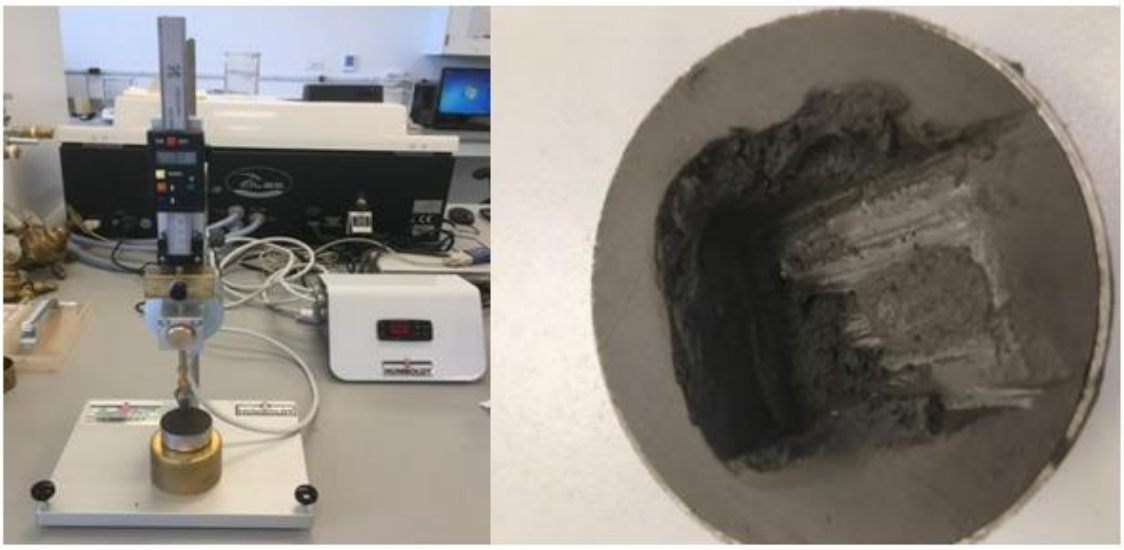

Figure 4.4 Plastic limit measurement setup using drop cone penetrometer

In this method the water content of the oil sands tailings cake is adjusted from its initial state by either drying in a convection oven at 43°C (110°F) in most cases or by wetting using water to achieve a penetration depth of approximately 5.45 mm using a

30° apex angle cone with a mass of 400-gram that is allowed to free fall for 5 sec. The test is repeated to obtain a minimum of three penetration depths between 4 mm and 7 mm including a minimum of one penetration depth above and below 5.45 mm. The plastic limit is then reported as the gravimetric water content at which the 30°/400-gram cone penetrates the cake to a depth of 5.45 mm.

4.4.5. Measurement of Peak and Residual Undrained Shear Strength of FFT Cakes

The undrained shear strength of the FFT cakes was measured using the Brookfield RST-SST Rheometer. The undrained peak shear strength of the cake samples corresponds to the maximum shear stress recorded during the test. The undrained residual or remolded shear strength of the cake samples corresponds to the shear stress retained by the samples post failure by shear. The average undrained peak or remolded shear strength corresponds to the arithmetic mean value of a minimum of three data points obtained during every undrained shear strength measurement to ensure repeatability of test results.

The test method in the RST rheometer was designed to measure the shear stress (Γ) of the FFT cake samples in a 4-ounce container by deforming them at a constant shear rate of 0.1 rpm for 15 minutes using a vane measuring system. The peak shear stress (Γ_{max}) was recorded as the maximum value of shear stress observed during the test while residual shear stress ($\Gamma_{residual}$) was recorded as the recovered portion of shear stress after shear failure. A typical shear stress patterns recorded as a function of time for a lime treated FFT cake is shown in Figure 4.5.

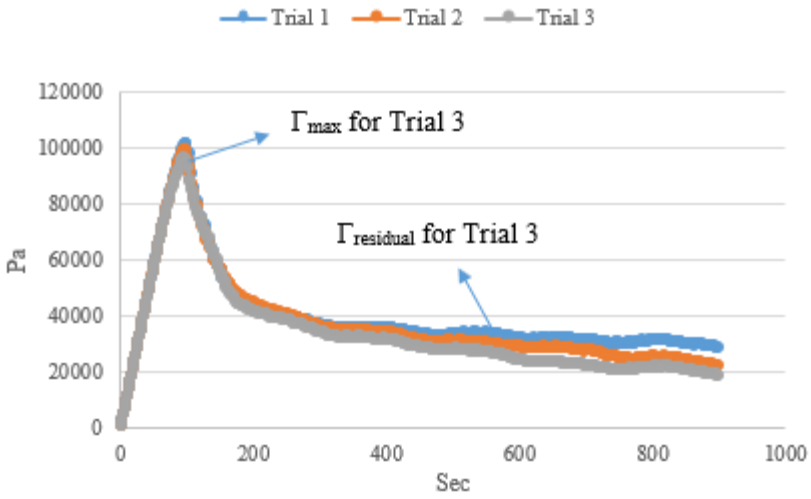

Figure 4.5 A typical shear stress pattern for FFT cakes

The pressure filter cakes produced were carefully placed into 8 mm diameter jars in two lifts to minimize the effect of air voids and then levelled to obtain a smooth surface. The VT-20-10 (20 mm height and 10 mm diameter) vane spindle was used for measuring undrained shear strengths less than 10 kPa and the VT-10-5 (10 mm height and 5 mm diameter) vane spindle was used for cakes with higher undrained shear strengths.

4.5. Results and Discussion

This section presents the experimental results obtained following the experimental program proposed to evaluate the geotechnical properties of the pressure filter cakes.

4.5.1. Atterberg Limits of FFT Cakes

Soil physics affecting the liquid limit and plastic limit is a complex subject and is impacted by multiple factors such as grain size distribution, specific surface area,

adsorbed water layer thickness of clay minerals and the pore size distribution. The LL is strongly if not directly related to the specific surface of the soil [68]. The greater the total amount of water required to reduce the shear strength to that associated with the liquid limit, the greater is the liquid limit value. The undrained shear strength at LL for treated oil sands has been determined to be between 2 kPa and 5 kPa [20]. A general approximation of the shear strength at LL is possible since the average adsorbed water film thickness at LL is expected to be the same on all particle surfaces [68]. This in turn implies that as the amount of adsorbed water per unit of surface area increases, so does the LL.

When lime is added to the oil sands clays, several chemical reactions take place simultaneously but with different kinetics. These include cation exchange of Ca^{++} for sodium and other monovalent cations in the soil-water system and the pozzolanic reaction between silica and alumina released from the clay particles in the high pH environment. Both these reactions dramatically alter the surface chemistry of the clay and impact the Atterberg limits with an overall effect lowering the plasticity index (PI). The change in PL reflects the amount of water required to alter a dry soil into a state of consistency where the clay soil can be molded into a consistent cylindrical strip. The undrained shear strength at PL for oil sands has been determined to be 80 to 100 times the strength at LL [20]. The effect of adding lime on the plastic limit is normally quite predicable as the plastic limit increases upon addition of lime. However, the change in the liquid limit is less obvious as it may reduce, stay the same or increase with the

addition of lime. This is because of the complex interactions that impact the change in shear strength upon the addition of lime.

Perhaps the primary factor that impacts the change in liquid limit upon the addition of lime is the development of pozzolanic product that alters the strength by changing the bonding characteristics among particles, changing the size and shape of particles and changing the manner in which moisture is absorbed within the soil-lime-water complex. All of these affect the PI and affect it as a function of time.

Since pozzolanic reactivity and kinetics are strongly related to soil chemistry and soil physics, the target or threshold PI values for soils to be stabilized is expected to vary and depend heavily on the mineralogical composition of the soils.

A comparison of the initial (Day 0) and Day 28 LL and PL data of the FFT cakes at approximately 70% solids content after various treatments is presented in Figure 4.6 and Figure 4.7. The changes in plasticity index (PI) for the same samples over the first 28 days is shown in Figure 4.8. PI was calculated as the numerical difference between the LL and PL.

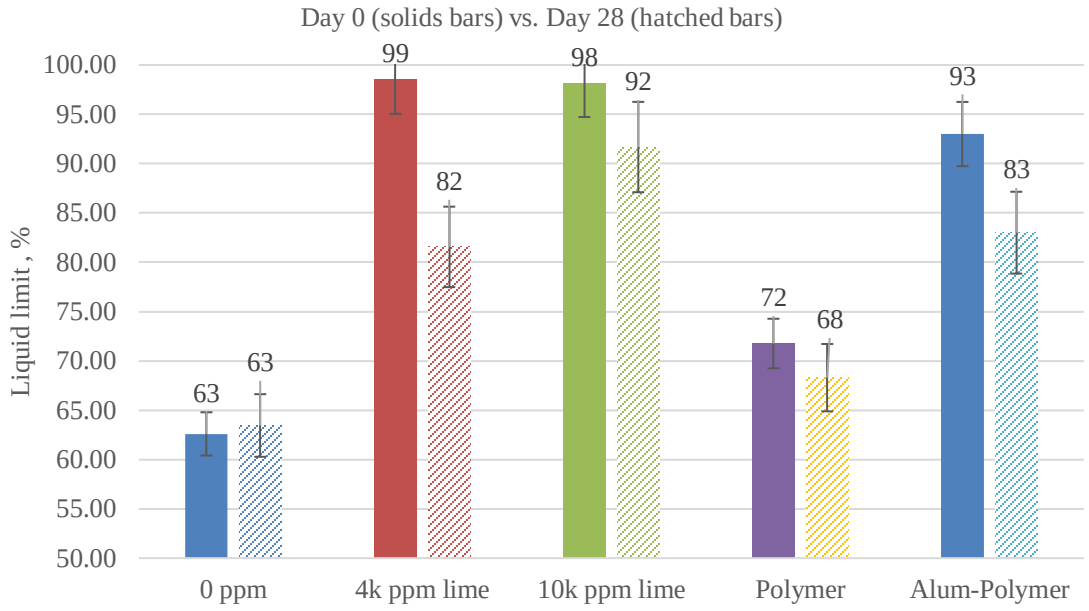

Figure 4.6 Comparison of Day 0 and Day 28 liquid limits of control and treated FFT cakes

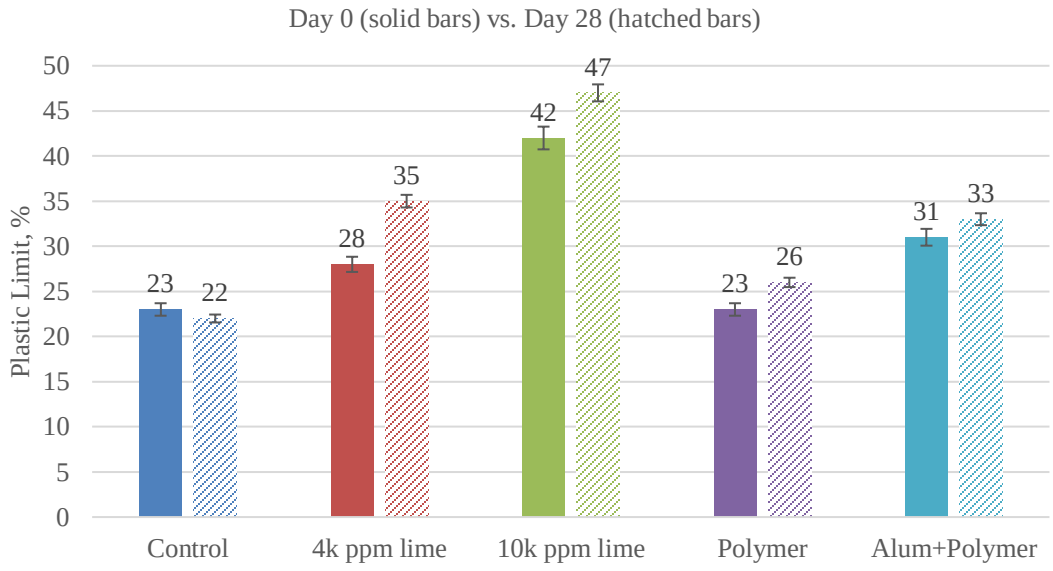

Figure 4.7 Comparison of Day 0 and Day 28 plastic limits of control and treated FFT cakes

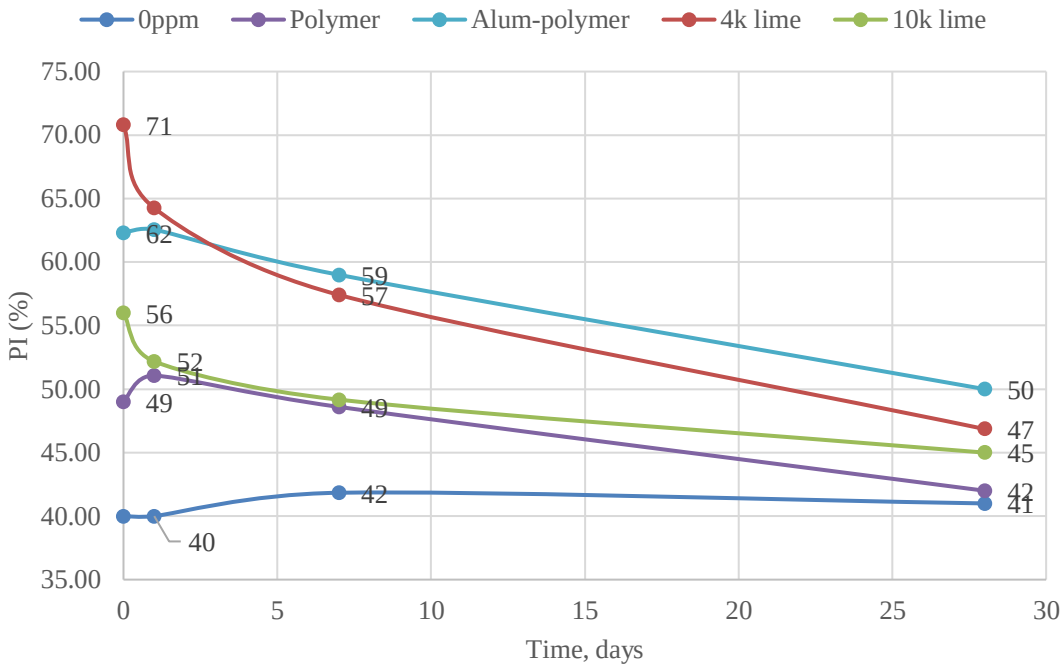

Figure 4.8 Comparison of plasticity index of the FFT cakes recorded from Day 0 to Day 28

The following conclusions can be drawn based on the Atterberg limits data presented in Figures 4.6-4.8:

1. The Atterberg limits of the untreated FFT cake (control sample) remain mostly unchanged over time as expected.
2. The LL and PL of all the treated cakes were higher compared to the control sample indicating that more clays were captured in the cake fractions during pressure filtration after coagulant and/or flocculant addition.
3. The initial (Day 0) water content to reach LL for both the 4000 ppm and 10000 ppm lime treated cakes were 15% to 26% higher compared to polymer and alum-

polymer cakes implying that the lime treated cakes were able to achieve a greater initial strength at lower solids concentrations.

4. The drop in LL over 28 days for the 4000 ppm lime cake was the highest at 17% compared to 6%, 5% and 2% drop in the lime overdose, polymer and alum-polymer cakes respectively indicating that an optimum lime dosage was more effective in coagulating the fine particles.
5. Lime outperforms the other treatment options when it comes to increasing both the initial PL of the FFT cakes and the continued increase in PL as a function of curing time. A higher PL is most critical for strength development with time since the rate of strength gain is an order of magnitude greater when the cakes transition from a plastic to a semisolid state compared to when they transition from a liquid to a plastic state.
6. The Day 0 PL of the 10000 ppm lime overdose cake sample was the highest among all samples and 50% greater than the 4000 ppm lime cake. This is likely due to the high clay content in the FFT indicated by an MBI of 12.2 thereby creating more exchange sites and increasing the calcium demand suggesting that the optimum lime dosage for strength development through pozzolanic reactions is more than 4000 ppm.
7. PI of all the treated samples dropped after 28 days. The maximum reduction in PI of 33% was observed with the 4000 ppm lime cake compared to 17% to 20% reduction through other treatments suggesting that 4000 ppm lime cake was most effective in modifying the texture of the clays present.

The incorporation of water as a structural component of the pozzolanic products such as calcium silicate hydrate and calcium aluminate hydrate is likely to be responsible for the increase in PL and lower PI of the lime treated cakes, as the water would be expected to report to mineral phase rather than the pores and voids in the filter cake. This excess water requirement is well known in soil stabilization applications and suggests that the ideal filtration of lime slurry treated FFT would provide specific wetness in the cake needed to provide the benefits to strength and Atterberg limits, unlike the non-treatment or flocculant treatments that require a thoroughly dried cake to develop significant strength.

In summary, a higher initial LL and a greater reduction in LL and increase in PL over time in the lime treated cakes compared to other treatments suggest that lime outperforms the other treatment options by capturing more clays in the cakes and subsequently modifying the clays over time due to chemical reactions at a high pH environment. The textural transformation of the high plasticity clays to medium compressibility silts in the lime treated cakes is illustrated through Figure 4.9.

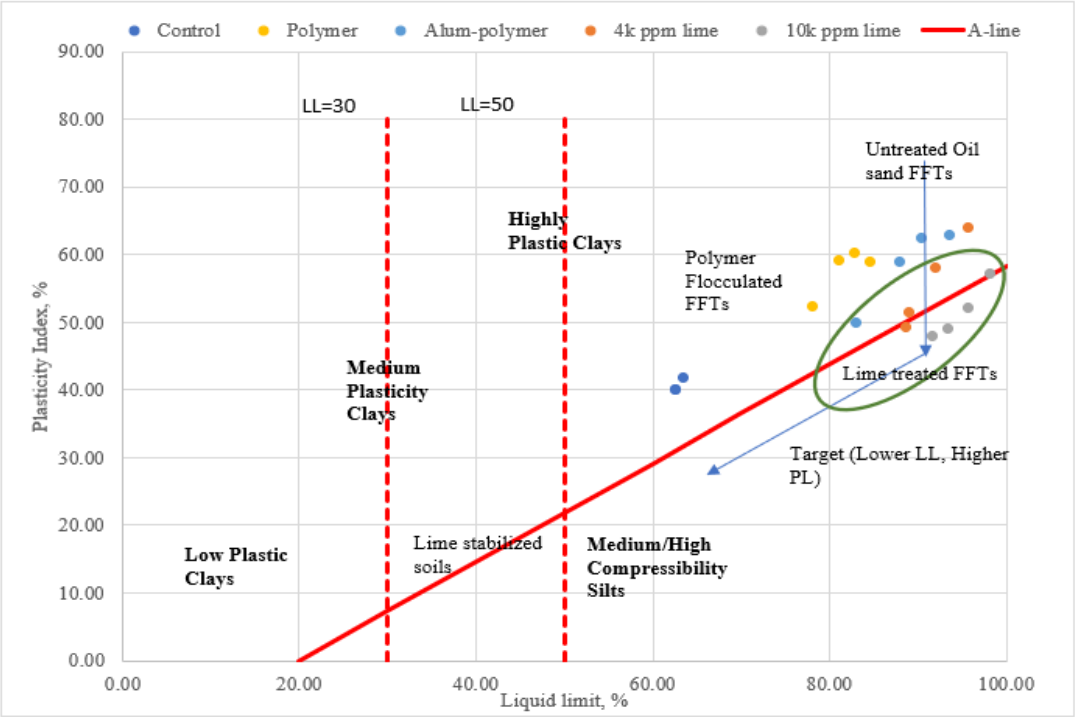

Figure 4.9 Comparison of the textural classification of FFT cakes

4.5.2. Clay Content in FFT Cakes

The main purpose of measuring the clay content i.e. particles finer than 2 micron, was to calculate the colloidal clay activity per equation 4.1.

$$Clay\ Activity = \frac{PI}{Clay\ content(<2\ micron)} \tag{4.1}$$

The colloidal clay activity is a useful parameter which is often used to classify if the clays are inactive, normal or active clays. Skempton classified clays having a colloidal activity of greater than 1.25 as active clays, those having activity between 0.75 and 1.25 as normal clays and those having an activity less an 0.75 as inactive clays [69]. The object of measuring the clay activity over time for the various treatment methods

was to have a tangible metric to compare their impact on modifying the clays through chemical reactions and to also normalize the liquidity index (LI) based on this effect. The discussion on LI will be presented in the next section.

Table 4.2 presents the initial (Day 0) clay activity of the various FFT cakes along with the percent reduction over 28 days.

Table 4.2 Impact of Treatment Options on Colloidal Clay Activity over 28 Days

Sample Description	**Initial Clay Activity (Day 0)**	**% Change in Clay Activity from Day 0 to Day 28**
Untreated cake	3.62	+4.3%
4000 ppm lime cake	7.73	-24.6%
10000 ppm lime cake	6.35	-17.7%
Polymer treated cake	5.11	-3.1%
Alum-polymer treated cake	6.14	-7.9%

The data presented in Table 4.2 shows that the clays present in FFT I are highly active with the clay activities well above the 1.25 threshold for active clays. The initial colloidal clay activity of the untreated cake was least due to poor clay capture in the cake fraction after pressure filtration. The initial clay activity of lime treated cakes are higher compared to other treatment due to higher quantities of clays in the cake. The data

supports the Atterberg limit discussion that the 4000 ppm lime treatment was most effective in modifying the clays.

4.5.3. Impact of Treatments on Liquidity Index of FFT Cakes

Liquidity index (LI) is a commonly used parameter for describing the consistency of soils. LI is defined by equation 4.2 and can be thought of as an index representing the water content of soils normalized over the range of water contents during which the soils are in a plastic state.

$$LI = \frac{water\ content\ (\%) - PL}{PI} \tag{4.2}$$

Soils having a LI greater than 1 are considered to exist in a liquid state, those having a LI between 0 and 1 exist in a plastic state and soils having a LI less than 0 are considered to be brittle solids. LI is also often correlated with other geotechnical properties of soils such as compressibility and shear strength.

Due to the predominance of clays in the FFT cakes, the LI was normalized for the clay content using equation 4.3 proposed by Carrier [70] to correlate LI with the remolded shear strength of clays. The normalized liquidity index is expressed as LI'.

$$LI' = \frac{LI}{0.75 + 0.181(Clay\ Activity)^{-1}} \tag{4.3}$$

The plot of LI' of the FFT cakes for a range of solids content between 50% and 70% after various treatment options is shown in Figure 4.10.

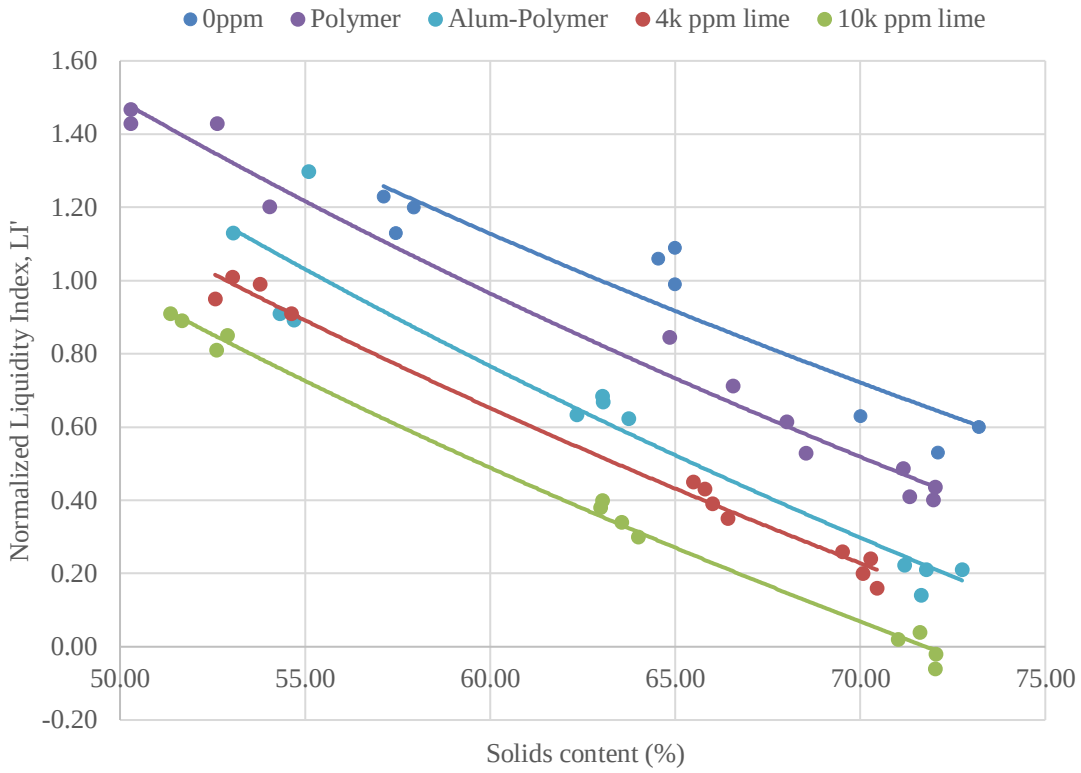

Figure 4.10 Plot of normalized LI of FFT cakes as a function of solids content after various treatment methods

The solids content required to transition from a liquid state to a plastic state (i.e. 0<LI'<1) is approximately 64%, 58% and 56% for the untreated cakes, polymer treated cakes and alum-polymer treated cakes respectively whereas the same threshold is attained at 53% for the 4000 ppm lime cake and at 50% for the 10000 ppm lime cake. This trend highlights the impact of lime treatment on transitioning the FFT cakes having initial moisture contents below their liquid limit to a plastic state thereby providing greater shear strengths at a lower solids content. This fact is more remarkable when analyzing the solids content at which the FFT cakes transition from a plastic to a solid

state (i.e. LI'<0) by extrapolating the data presented in Figure 4.10. The solids content required for this transition to take place is expected to be in excess of 80% for the no treatment and polymer treatment options while the alum-polymer cakes are expected to behave as solids above a solids content of 75%. The 4000 ppm and 10000 ppm lime treated cakes on the other hand attain sufficient grain-grain interaction through chemical modification of the clays to gain strength and lower the LI' below 0 at solids concentrations of approximately 73% and 71% respectively. It is pertinent to realize that the rates of strength gain contributed by every% increase in solids concentrations above 70% is exponentially higher compared to the increase in strength at lower solids concentrations. The impact of lime on strength gain at various concentrations is discussed in the next section.

The LI' trend discussed is also critical to the economics of the pressure filtration technique which is driven by cycle times. The rate of water release from the cakes tends to be much slower at solids concentrations above 65% as shown in the example in Figure 4.11 comparing the pressure filtration performance of lime and polymer treatments.

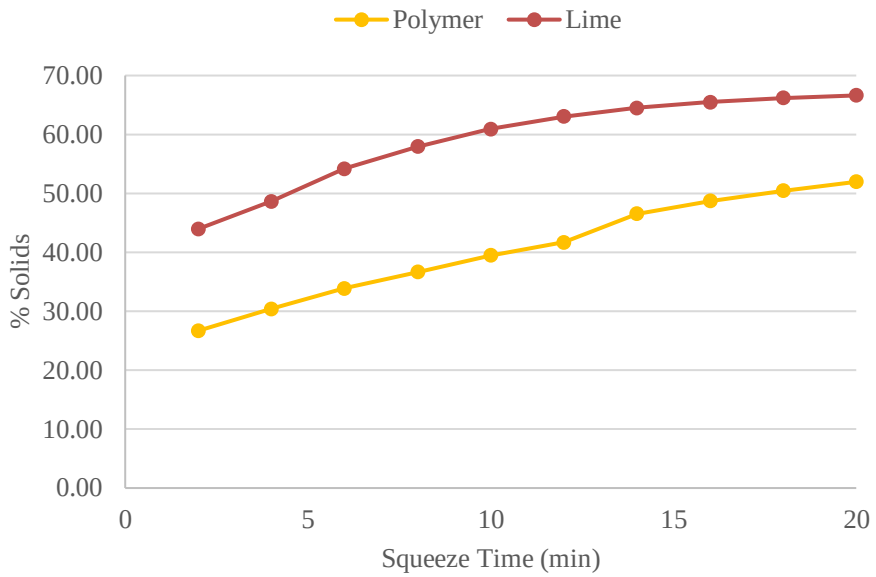

Figure 4.11 Comparison of pressure filter squeeze time as a function of solids concentration

Aside from the fact that lime is able to dewater the FFTs at a faster rate through the pressure filter, the data in Figure 4.11 illustrates the difficulties in dewatering at solids concentrations above 65%. The LI' discussion presented earlier is hence vital in terms of overall economics of the pressure filtration process as producing stronger cakes at lower solids content is critical to lowering the cycles times. Lime comfortably outperforms the other treatment options on this aspect. Moreover, the solids concentrations in the lime treated samples is expected to increase over time due to the formation of new solid phases during pozzolanic reactions which are not possible with acidic coagulants and polymers. The fact that the incorporation of structural water is important for pozzolanic reactions adds to list of benefits offered uniquely by lime in influencing the economics of the pressure filtration process.

4.5.4. Impact of Treatments on Undrained Shear Strengths of FFT Cakes

The peak undrained shear strength results are discussed first followed by a discussion about the residual shear strengths and sensitivity of the FFT cakes.

4.5.4.1. Peak Undrained Shear Strength

A family of peak undrained shear strength curves of the FFT cakes after various treatments recorded over the first 180 days is presented in Figure 4.12.

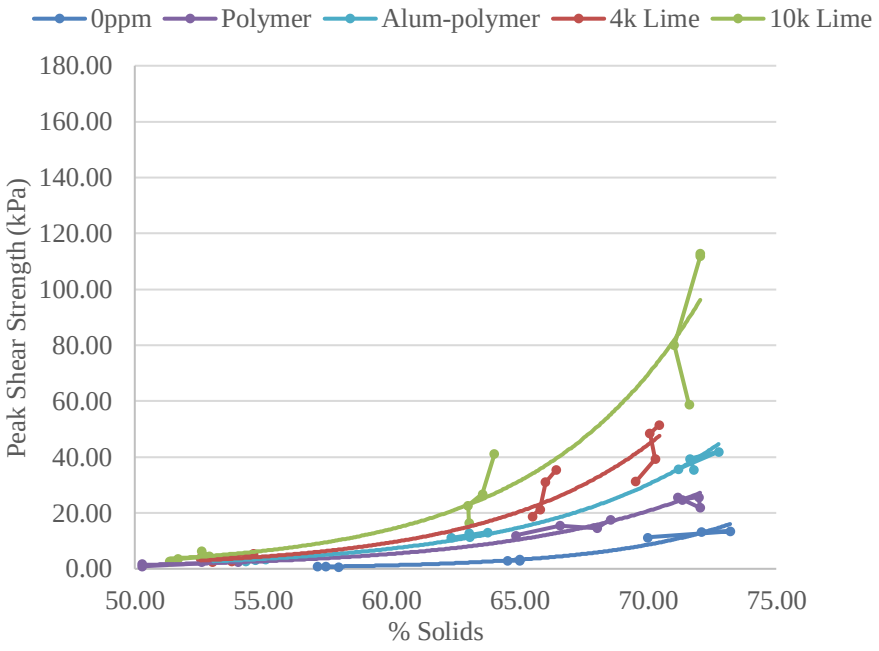

Figure 4.12 Peak undrained shear strength of various FFT cakes as a function of solids content

It is evident from Figure 4.12 that the treatment of FFT with both the 4000 ppm and 10000 ppm lime slurries demonstrated significant benefits to strength that continues

to increase with curing time, compared to the no treatment cake and cakes treated with polymer alone and a combination of alum and polymer. Most of the strength development in all samples occurred within the first 28 days after treatment but with varying magnitudes depending on the additive. The rate of strength gain between days 28 and 180 were less appreciable except for the 10000 ppm lime treated cake as shown in Figure 4.13 wherein the peak strength of all samples over the 180 days are presented for a solids concentration of approximately 70%.

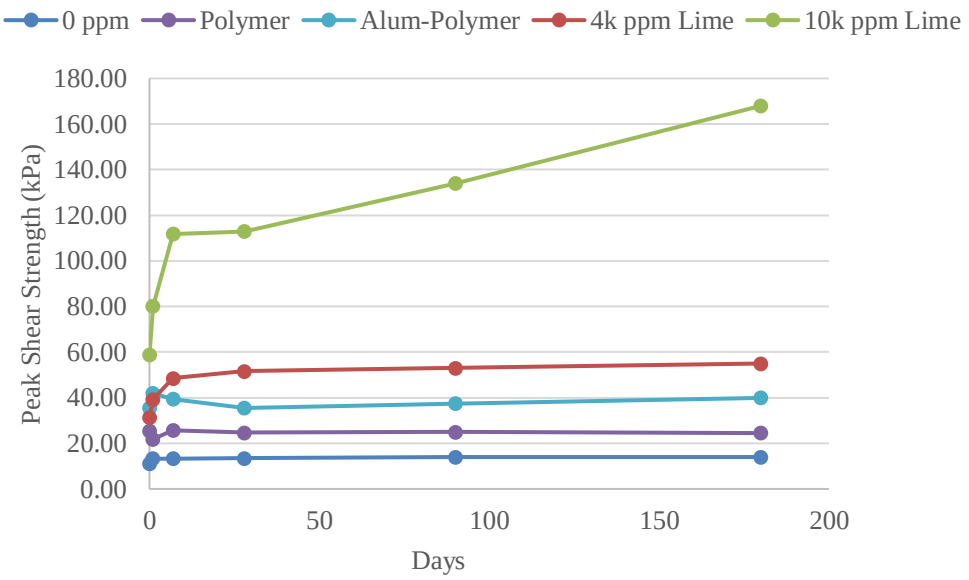

Figure 4.13 Rate of peak strength development in FFT cakes over 180 days

The initial (Day 0) peak shear strength measured at 70% solids for 4000 ppm lime slurry and alum-polymer were similar, 38 kPa versus 36 kPa respectively, both

outperforming no treatment at 14 kPa; however, the 4000 ppm lime slurry treated cake continued to gain strength reaching 49 kPa at 1 day and 55 kPa after 1 week, whereas the peak shear strengths for both the polymer, alum-polymer treated cakes and no treatment maintained the same strength over the same time period. The 10000 ppm lime slurry treated cake demonstrated significantly higher initial peak strength of nearly 60 kPa on Day 0 and continued to gain strength with time even beyond 28 days. This suggests that the optimum dosage of lime required for strength development was a lot higher than 4000 ppm which could be due to the very high clay content reflected by the FFT MBI of 12.2.

The peak strength results demonstrate that treatment using lime slurry to a pH above 12.0 allows for pozzolanic reactions to occur between calcium hydroxide and the aluminates and silicates in the clay minerals and develop durable, increasing strength, unlike the anionic flocculant that appear to develop a weak, shear-sensitive structure. Further, the data in Figure 4.13 also indicates that the onset of pozzolanic reactions takes place within 28 days after lime treatment and continues to occur with time in the presence of sufficient high levels of soluble calcium concentrations and pH above 12.0. The fact that the strength gain in the lime treated cake is sustained over a period of 180 days also suggests that the pozzolanic products formed are not labile and that the chemistry of the clays are permanently modified after lime addition.

4.5.4.2. Residual Undrained Shear Strength

Residual shear strength is an important parameter when it comes to determining the suitability of a material for use towards landform development and other forms of

reclamation. This is because the reclaimed material is often subjected to external loads and stresses such as those imposed by the placement of large machinery. Residual shear strength provides an idea of the sensitivity of the materials to external loads and their ability to retain their shear strengths post shear failure. Sensitivity of clays is defined by the ratio of their peak and residual undrained shear strengths. In the oil sands, materials suitable for reclamation are expected to have a sensitivity below 4.0 [20]. A high residual shear strength and a sensitivity of below 4.0 is hence critical for the long-term stability of reclaimed tailing materials.

The residual shear strengths of the FFT cakes measured on Day 0 and Day 180 after various treatments is shown in Figure 4.14. The sensitivity of the various FFT cakes after 180 days is shown in Figure 4.15 along with the change in sensitivity over the same time period.

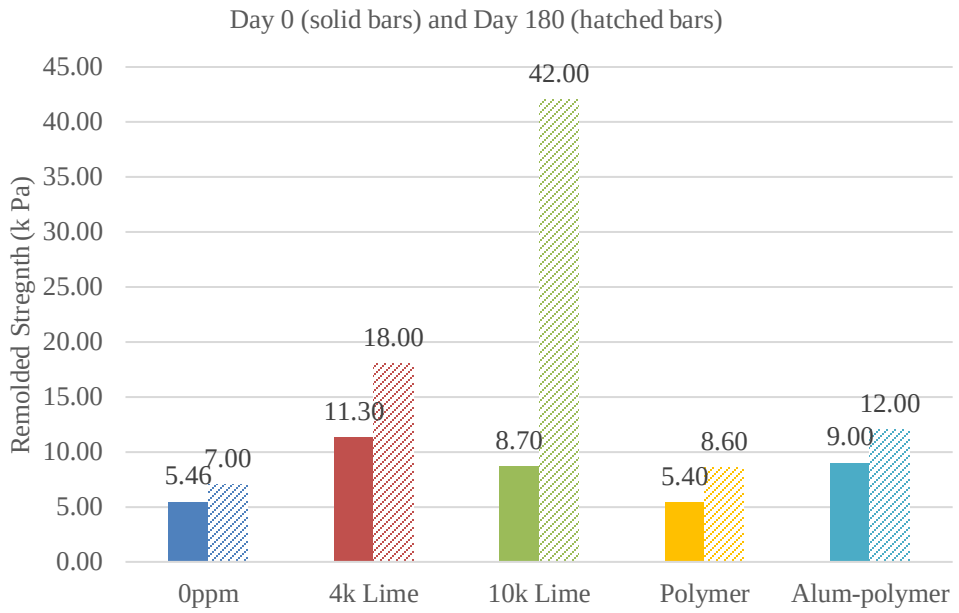

Figure 4.14 Comparison of Day 0 and Day 180 residual shear strengths of the FFT cake after various treatments

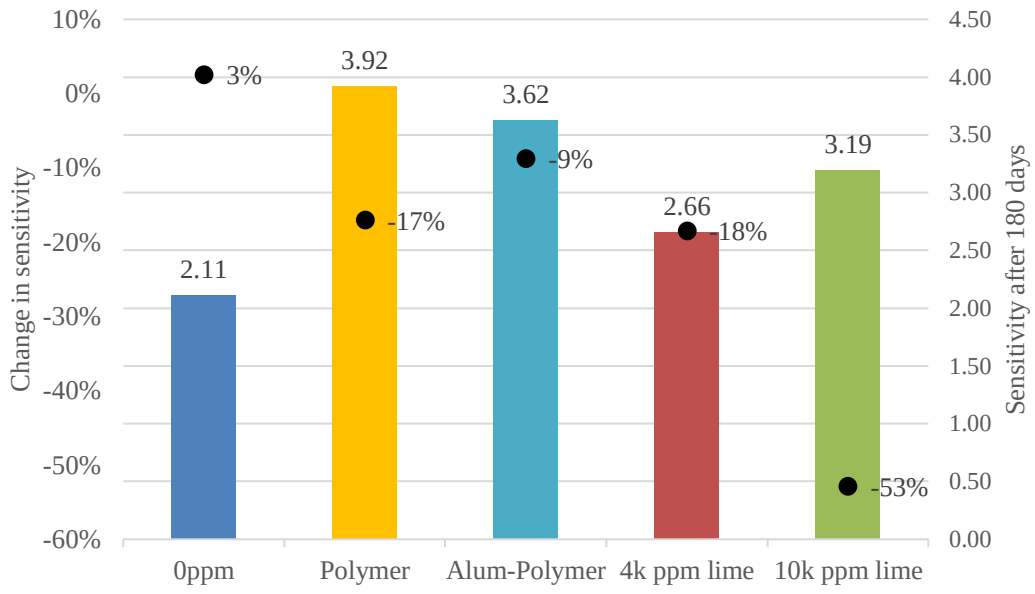

Figure 4.15 Impact of various treatments on sensitivity of FFT cakes after 180 days

In addition to increasing the peak strength of the FFT cakes with time, lime slurry treatment additionally demonstrated a higher residual shear strength compared to other treatments that also increased over the 180 days as shown in Figure 4.14. Most interestingly, the anionic polymer treatment showed little to no benefit to residual shear strength compared to no additive, reporting values between 5 kPa to 8 kPa that were insensitive to curing time. Similar to the peak strength trends, the 10000 ppm lime cake comfortably outperformed the other treatments by increasing the residual strength from 8.7 kPa on Day 0 to 42 kPa after Day 180.

Perhaps more relevant than the magnitudes of the residual shear strength of the FFT cakes are the changes in sensitivity of the FFT cakes over time. Pertinent to this, the following remarks can be made based on Figure 4.15:

1. The low sensitivity of the untreated cakes compared to the treated cakes should be disregarded since they are predominantly composed of sand fractions which result in low magnitudes of peak and residual shear strengths and unlike clays are not sensitive to shear.
2. The sensitivity of both the lime treated samples is lower compared to the polymer and alum-polymer cakes with the 4000 ppm lime cake displaying a sensitivity of less than 3.0.
3. The initial (Day 0) sensitivity of the 10000 ppm lime cake was 6.52 but the sensitivity dropped to 3.19 after Day 180 indicating that the clays initially present have been modified through chemical reactions with lime.

4.6. Numerical Model to Predict Long-Term Properties of Lime Treated FFTs

This section presents a numerical model to predict the changes in LI in lime treated FFTs over time. An empirical relationship is also presented to correlate LI to the residual strength of lime treated FFTs. The model was developed using the data collected from the experimental test program and using other relevant data provided by Graymont.

4.6.1. Model to Predict the Normalized Liquidity Index of Lime Treated FFTs

The objective of the model developed to predict LI' of the lime treated FFTs is to gain an insight about the changes in Atterberg limits expected during the first 6 months after lime treatment. The model was not developed to replace laboratory experiments entirely but to help design an efficient testing program which could be coupled with the model to predict the long-term performance of lime. The model was developed by comparing the experimental data of LI' of the untreated FFTs against the LI' data collected as a function of time and lime dosage and performing a regression analysis in Microsoft Excel to obtain the best fit parameters. The fitting parameters obtained were then individually analyzed as a function of other important properties impacting LI' namely the pH and solids concentration to develop sub-models to incorporate these parameters in lieu of the fitting parameters.

4.6.1.1. Model Inputs

The inputs required for the model are listed in Table 4.3 Inputs Required for the Lime LI' Prediction Model along with the symbols used in the model.

Table 4.3 Inputs Required for the Lime LI' Prediction Model

Input Description	Symbol
Initial Atterberg limits (LL, PL) of the FFT	$LL_{control\ FFT}$, $PL_{control\ FFT}$
Initial solids content of the FFT	$SC_{control\ FFT}$
%age of particles <2 micron in FFT	$\%\ Clays_{control\ FFT}$
Target solids content of the dewatered FFT cake	SC_{target}
Target pH of FFT after lime treatment	pH_{lime}
% of lime added to the FFT	$\%\ lime$

4.6.1.2. Step-Wise Procedure to Predict LI' of Lime Treated FFTs

The following steps should be followed in order to estimate the impact of lime slurry treatment on the LI' of the FFTs.

Step 1: Calculate the gravimetric water content of the FFT using equation 4.4.

$$Water\ content\ (WC_{control\ FFT}) = \left(-2.29 \times SC_{target}\right) + 203.8 \quad (4.4)$$

Step 2: Calculate the LI' of the FFT using equation 4.5.

$$LI'_{control\ FFT} = \frac{WC_{control\ FFT} - PL_{control\ FFT}}{0.75(LL-PL)+(0.181\times\%Clay_{control\ FFT})} \quad (4.5)$$

Step 3: Determine coefficient A based on SC_{target} using Figure 4.16 Chart to determine coefficient 'A' used in the LI' lime model.

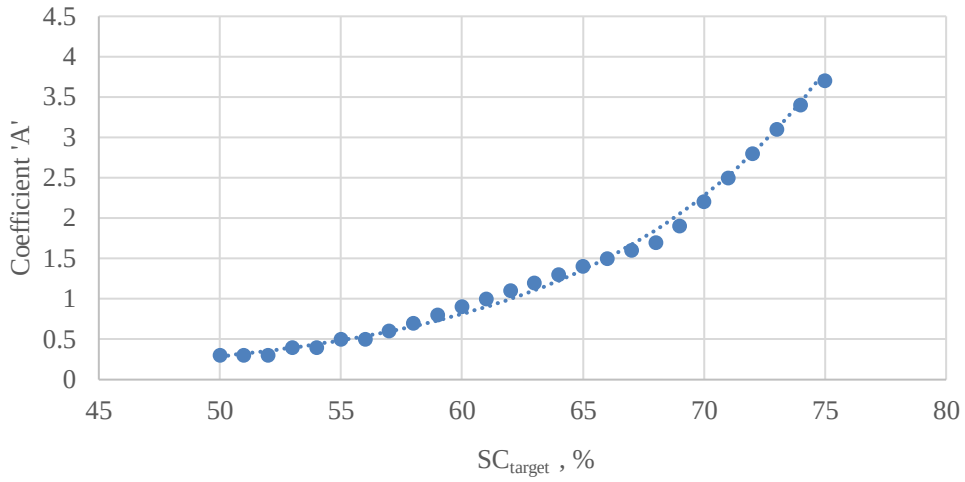

Figure 4.16 Chart to determine coefficient 'A' used in the LI' lime model

Step 4: Calculate LI' of the Day 0 of the lime treated cake, $LI'_{lime,Day\ 0}$ using equation 4.6.

$$LI'_{lime,Day\ 0} = LI'_{control\ FFT} \times \exp(-A \times \%\ lime) \quad (4.6)$$

Step 5: Calculate the approximate pH of the lime treated cake after Day n , $pH_{lime,Day\ n}$ using equation 4.7 which considers the impact of pH reduction with time only due to pozzolanic reactions and not due to carbonation or leaching.

$$pH_{lime,Day\ n} = pH_{lime} \times (n)^{-0.012} \quad (4.7)$$

Step 6: Determine coefficient B based on $pH_{lime,Day\ n}$ using Table 4.4.

Table 4.4 Table to Determine Coefficient 'B' used in the LI' Lime Model

$pH_{lime,Day\ n}$	B
<10.5	0.015
10.5 to 12	0.025
>12.0	0.035

Step 7: Calculate LI' of the lime treated FFT cake on Day n, $LI'_{lime,Day\ n}$ using equation 4.8.

$$LI'_{lime,Day\ n} = LI'_{lime,Day\ 0} - B \times \ln(n) \quad (4.8)$$

where $1 \leq n \leq 180$

4.6.1.3. Example Calculation and Model Validation

The inputs assumed for the example calculation are listed in Table 4.5. The example calculation was performed using the experimental data obtained for FFT I cakes after dewatering through the pressure filtration system.

Table 4.5 Inputs Assumed for Example Calculation using LI' Lime Model

Symbol	Value
$LL_{control\ FFT}$	62.6%
$PL_{control\ FFT}$	22.6%
SC_{target}	65%
$\%\ Clays_{control\ FFT}$	35%
pH_{lime}	12.4
$\%\ lime$	0.4%

Step 1: The $WC_{control\ FFT}$ was found to be 54.91% using equation 4.4.

Step 2: $LI'_{control\ FFT}$ was determined to be 0.89 using equation 4.5.

Step 3: Coefficient A was found to 1.4 using Figure 4.16.

Step 4: $LI'_{lime,Day\ 0}$ was to be 0.50 using equation 4.6.

Step 5 and Step 6: Coefficient B was found to 0.035 up to Day 17, 0.025 between Day 18 and Day 180 using equation 4.7 and Table 4.4.

Step 7: $LI'_{lime,Day\ n}$ predicted using equation 4.8 was plotted for 180 days as shown in Figure 4.17.

The experimental LI'data obtained for the 4000 ppm treated lime cake on Days 0, 1, 7, 28, 90 and 180 are also shown in Figure 4.17.

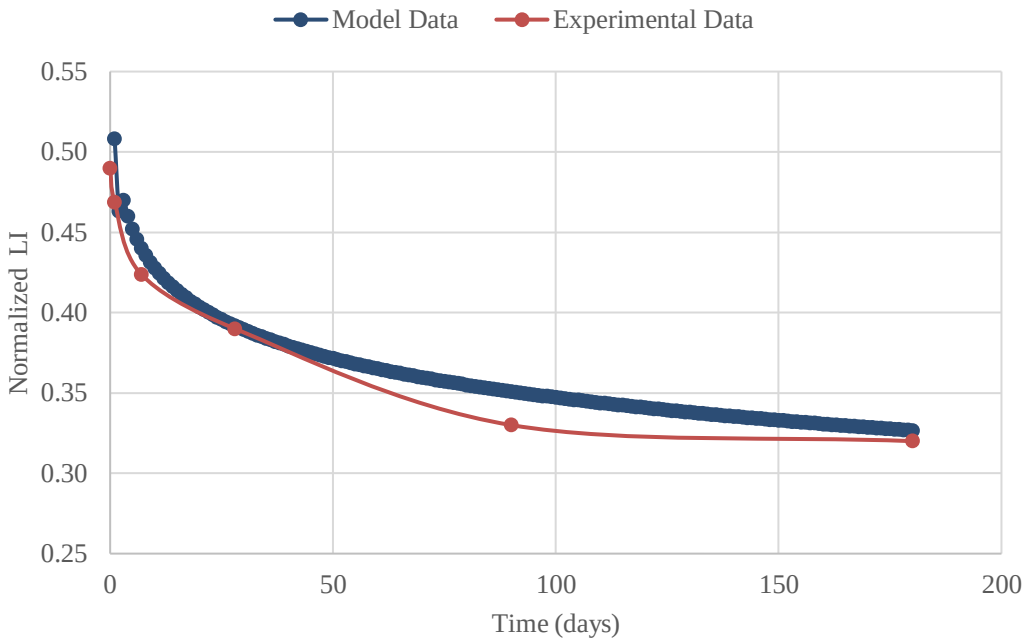

Figure 4.17 Comparison of LI' calculated using the model and experimentally

Figure 4.17 tends to point that the model predictions are more conservative compared to the experimental data. The results obtained using the model were similarly verified against all the LI' experimental data obtained through the pressure filtration study as shown in Figure 4.18 and resulted in a good R^2 value of 0.92.

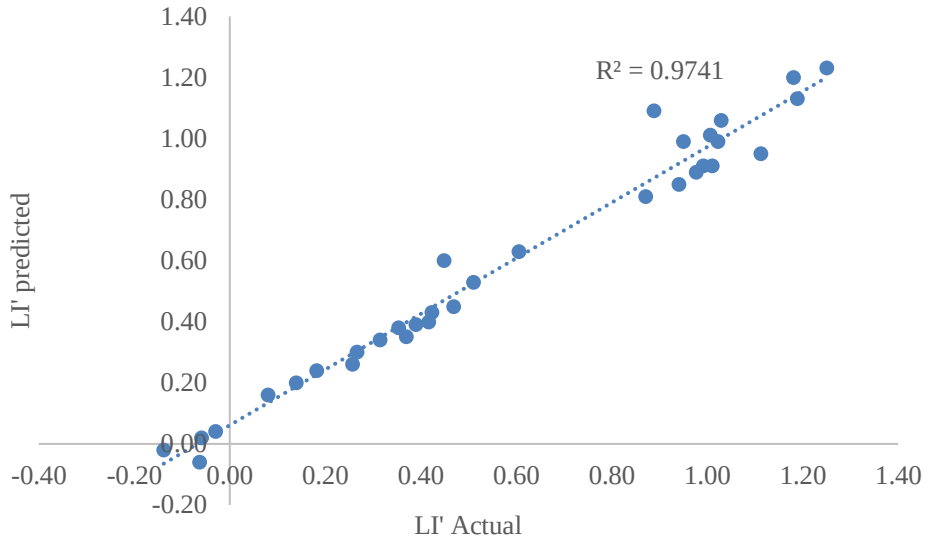

Figure 4.18 Validation of LI' lime numerical model using experimental data

4.6.1.4. Relationship to Predict the Residual Shear Strength of Lime Treated FFTs

An empirical relationship was developed to approximate the residual shear strength of the lime treated FFT cakes ($\Gamma_{residual,lime}$) for use as a companion tool together with the LI' model. The relationship is very similar to the one proposed by Carrier to predict the remolded strength of clays using a normalized liquidity index [70] except that it was exclusively developed to predict the remolded strength of oil sands FFT cakes treated with lime. The relationship was developed by fitting nearly 100 experimentally obtained $\Gamma_{residual,lime}$ and the corresponding LI' data points and is shown in Figure 4.19.

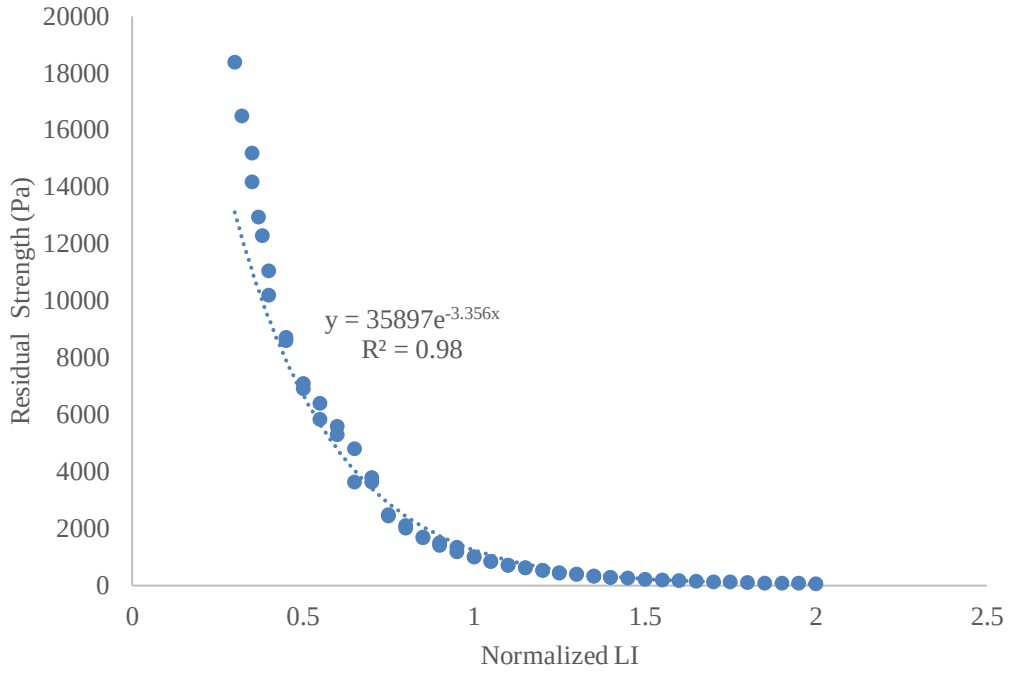

Figure 4.19 Correlation between LI' and residual strength for lime treated FFTs

$\Gamma_{residual,lime}$ may hence be approximated based on $LI'_{lime,Day\ n}$ using equation 4.9.

$$\Gamma_{residual,lime,Day\ n}(kPa) = 35.9 \times \exp\left(-3.35 \times LI'_{lime,Day\ n}\right) \quad (4.9)$$

4.6.1.5. Example Application Using the LI' Lime Model

The numerical model proposed for predicting the LI' of lime treated cakes can be used to illustrate the impact of lime on reducing LI' over time and for defining the pH targets required for various chemical reactions to occur in lime treated FFTs. In this example, LI' predicted is plotted as a function of time and initial pH of the lime treated FFT at a solids concentration of 55% as shown in Figure 4.20.

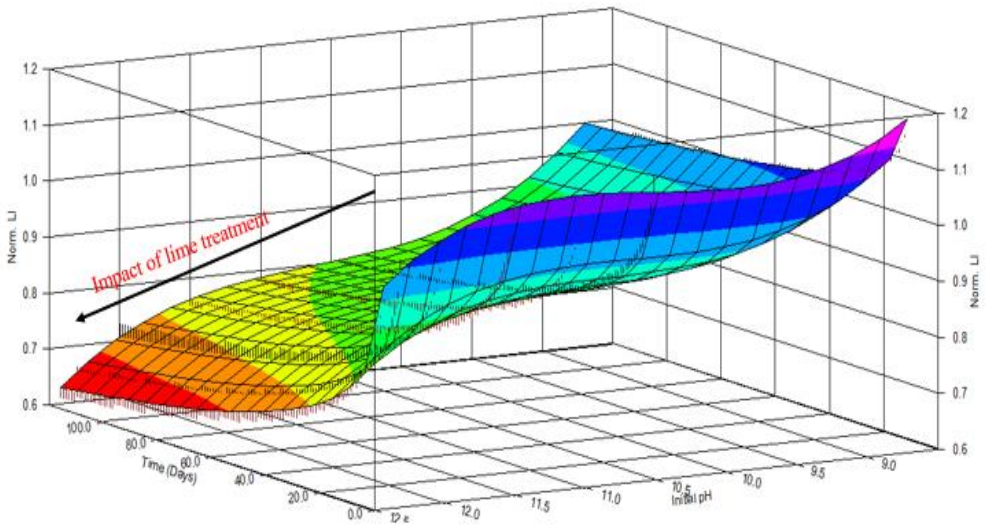

Figure 4.20 Impact of lime treatment and pH on changes in LI' over time

Figure 4.20 demonstrates the influence of pH on LI'. As the initial pH of the FFT increases from below 9.0 (untreated FFT) towards a pH of 12.5 with increasing dosages of lime, there is a greater reduction observed in LI' over time. Based on the plot above and the correlation established between shear strength and LI' through equation 4.8, a general understanding about the fate of lime at various pH levels. It can be said that up to a pH of 11.5, lime is consumed mainly on cation exchange reactions with the clays and for overall surface charge neutralization by consumption of the carbonate phases since there is minimal drop in LI' over time. Between a pH of 10.5 and 12.0, lime is also expected to modify the texture of the clays by lowering the PI and increasing the particle size. The strength building pozzolanic reactions are expected to occur above a pH of 12.0 wherein the rate of LI' reduction over time is maximum.

4.7. Summary and Conclusions

The impact of lime addition on influencing the geotechnical properties of the FFTs were investigated in this chapter. The experiments were designed to focus on understanding the immediate and long-term influence of lime on modifying the texture of the FFT solids and on development of shear strength. The solids or cake fraction analyzed was obtained after dewatering the FFT to solids concentration ranging between 55% and 70%. The performance of lime was compared with that of a polymeric flocculant and a combination of alum and polymer. Engineering tests were performed at various intervals over the first 180 days after treatment and included measurement of Atterberg limits, clay content and peak and residual undrained shear strengths. The results obtained were used to develop a numerical model to predict the liquidity index of lime treated FFT cakes over time as a function of the pH, clay content and initial Atterberg limits of the source FFT. An accompanying equation was also proposed to relate the liquidity index of the lime treated FFTs to their residual shear strength. The following conclusions can be drawn regarding the impact of lime on the geotechnical properties of the FFT cakes:

1. The initial (Day 0) LL of the lime treated cakes were higher compared to the other cakes due to improved capture of clays within the cake fraction. A higher Day 0 LL also suggests that the FFTs transition from liquids to a plastic solid at a lower initial solids concentration after adding lime.
2. The Day 0 PL of the 10000 ppm lime cake was noticeably higher compared to the other cakes and continued to increase with time at a higher rate suggesting

that the perceived optimum lime dosage of 4000 ppm corresponding to a pH of 12.4 was inadequate due to the high concentration of clays present in the FFT reflected by an initial MBI of 12.2.

3. The combined impact of lime on lowering LL, increasing PL and thereby reducing the PI and clay content of the FFT cakes over the initial 28 days after treatment results in modifying the overall texture of the FFT solids from highly plastic clays to lean silts. Polymer and alum-polymer treatments failed to modify the physical properties of the FFT clays relative to the performance of lime.
4. Lime clearly outperformed polymers and alum-polymers with respect to achieving a higher initial peak and residual shear strengths and a higher rate of strength development with time due to formation of new solid phases thereby offering the potential to reduce pressure filtration cycle times and benefit the overall economics of the process.
5. The lime treated cakes meet the criteria of 20 kPa shear strength requirement with a sensitivity of less than 4.0 proposed by McKenna [20] for use towards development of uplands supporting steep slopes in excess of 1 in 6. In fact, lime meets the proposed criteria at than 65% solids content within 1 day after treatment with a 4000 ppm dosage. Lime treated cakes were also able to meet strength targets of above 100 kPa required for hard-ground reclamation techniques [20] at approximately 70% solids content at a higher lime dosage of 10000 ppm.

6. The numerical model developed to predict changes in liquidity index of lime treated FFT cakes over time is in good correlation with the experimental results and serves as a tool for defining the FFT specific pH and lime dosage requirements in field applications to meet targeted strength requirements.

In summary, the engineering results discussed in this chapter support the findings discussed in the previous chapter regarding the physicochemical effects of lime and provide strong evidence regarding the unique ability of lime to chemically modify the clays present in the FFTs and result in strength development over time.

5. EVALUATING THE LONG-TERM DURABILITY OF LIME TREATMENT IN HYDRAULIC STRUCTURES: A CASE STUDY*

5.1. Objectives of the Case Study

The primary objective of this study was to investigate the changes in engineering and mineralogical properties of lime treated sections of the FKC and to substantiate the durability of lime treatment in hydraulic structures. The performance of lime treated soils at the FKC was evaluated through the following specific actions:

1. Procure native and 40-year-old lime treated samples from the FKC embankment slopes and perform basic engineering characterization including determining the Atterberg limits, particle size distribution and optimum moisture content (OMC) along with basic chemical characterization including determining soil pH, lime fixation point and CEC.
2. Compare the current engineering properties namely compressive strength, expansion index and erosion resistance of the native and lime treated FKC soils.
3. Evaluate the transformation in mineralogy of the native soils 40 plus years after lime treatment using XRD, X-ray fluorescence (XRF) and thermogravimetric analysis (TGA).

* Parts of sections 5.1, 5.2, 5.3, 5.4 and 5.6 of this chapter have been accepted for publication in the Journal of Transportation Research Record.

4. Compare the moisture distribution patterns of the native and lime treated FKC soils across a cross-section of the embankment during a wetting cycle using Hydrus-2D.

5.2. Soil Sampling and Characterization

Soil samples were collected from the lime treated sections of the FKC slopes using a rotary drill (Figure 5.1). The gradient of the slope and the built-up strength of the lime treated soils made it challenging to recover undisturbed cores that could be used for compressive strength and erosion resistance tests. The lime treated soil samples were extracted from above 3 feet of the existing water line following an extended drought at depths of 1-2 feet below the surface of the canal slope. The chosen sampling location was regarded by FWA as the average water line level and falls well within the water line when the canal operates at full capacity. The presence of lime in the treated sections was confirmed on-site by testing for reaction resulting in increased pH using a phenolphthalein indicator. The brittle nature of the lime treated soils combined with the mechanical disturbance caused during the coring process meant that approximately 20% of the material recovered was collected as a fine fraction and the rest were collected as odd-shaped chunks as shown in Figure 5.1. The fine fraction was used for basic engineering and chemical characterization tests performed on the lime treated soils.

Native soil samples were extracted from the same depth as the lime treated samples using a hand auger at sections of the canal that were left untreated at the time of construction. The native soil samples were visually identified as moderately plastic clays.

Figure 5.1 Soil sampling operation at a lime treated section of the FKC

Basic engineering characterization of the samples included determining the Atterberg limits by ASTM D4318 [67], soil classification after particle size distribution analysis by ASTM D7928-17 [71] and moisture-density relationship testing to determine the optimum moisture content (OMC) following ASTM D1557 [72]. A summary of the average soil properties of the native and lime treated soils recovered is presented in Table 5.1. All the tests were replicated to ensure consistency in results.

Table 5.1 Basic Engineering Characterization of FKC Soils

Sample Description	**Liquid Limit (%)**	**Plastic Limit (%)**	**Plasticity Index (%)**	**% Passing 74 µm**	**USCS Class**	**OMC (%)**
Untreated Soils	41	18	23	69.2	CL	21.4
Lime Treated Soils	34	28	6	48.5	ML	18.1

The USBR reported the FKC soils had an average plasticity index (PI) of 36 before lime treatment and that the PI of the soils dropped to 9, 72 hours after mixing with 4% quick lime [14].The considerably lower current PI of the lime treated soils sampled during the current study in comparison to the untreated soils is testimony to the permanent textural modification of the treated FKC soils from lean and fat clays to inorganic low plasticity silts as identified at the time of construction and in Table 5.1.The cumulative particle size distribution of the FKC soils is shown in Figure 5.2 to highlight the textural changes to the soils as a result of lime treatment.

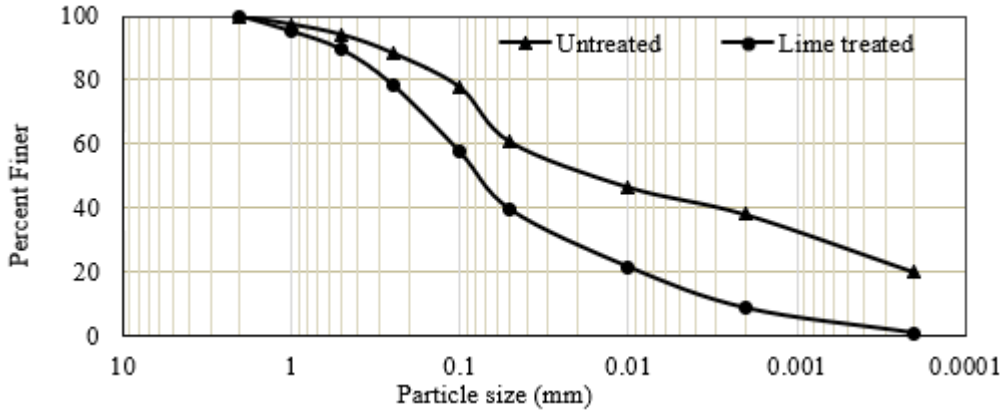

Figure 5.2 Particle size distribution of the FKC soils

The untreated samples are composed of nearly 33% sands (0.05 mm to 2 mm), 37% silts (0.002 mm to 0.05 mm) and 30% clays (< 0.002 mm). The silt and clay fractions in the lime treated samples drops to 31% and 9%, respectively, while the sand fraction increases to nearly 60%. The particle size distribution trends confirm the sustained impact of lime on coagulating the clays.

Soil pH and CEC are two of the most basic and indicative measurements of soil chemical properties [73]. The pH of the FKC soils were measured in accordance with ASTM D4972 [74] while the CEC of the native soil was determined using the same procedure described in Chapter 3.

The pH of the native FKC soils was found to 6.30. The lime treated soils had a pH of 8.90 indicating considerable presence of hydroxyl ions released from lime. The quick lime demand required to raise the pH of the native soils to 12.40 [75] was found to be 3.4% indicating that the lime dosage used in the 1970s during initial repair operations was targeted to promote long-term strength building pozzolanic reactions [1]. The

relatively high current pH of the treated FKC soils indicates that lime treatment continues to be effective and has assisted in the formation of new mineral phases which are investigated at depth in this study.

The USBR had reported the presence of highly expansive clays across the FKC canal linings [14]. The CEC of the native soils was measured to confirm the presence of expansive clay minerals such as montmorillonites at the location where the soils were sampled. The CEC of the untreated FKC soils was found to 27.5 meq/100g indicating that the native soils extracted for the current study contained significant enough amounts of expansive clay minerals and were representative of the soils treated with lime in the 1970s.

5.3. Experimental Methods

The durability assessment of lime treated soils at the FKC included laboratory methods to evaluate engineering properties of the soils as well as methods to understand the mineralogical transformation of the treated FKC soils. A brief description of the choice of method, sample preparation procedures and key test specifications for all test methods used in this study is presented in this section.

5.3.1. Methods Used to Evaluate Engineering Properties of FKC Soils

Three engineering properties of soils critical in the assessment of soils in constant contact with water were investigated in this study namely unconfined compressive strength (UCS), expansion index and erosion resistance. The challenges described during soil sampling did not allow us to follow standard testing protocols for determining the strength and erosion properties of the FKC soils. We intend to extract

intact cores for these tests from the bottom of the canal during the winter of 2020 when the FKC is scheduled to be emptied for routine maintenance.

5.3.1.1. Unconfined Compressive Strength (UCS)

The UCS test was performed in accordance with ASTM D2166 [76]. The soil specimens recovered from our sampling exploration at the FKC were not suitable to be trimmed and used for UCS test. The lime treated FKC soils were remolded at OMC (Table 5.1) and compacted using a Harvard miniature compaction apparatus to obtain 1.3 in. diameter by 3.9 in. height samples. The moisture contents of the untreated and lime treated samples before remolding at OMC were recorded to be 13.8% and 8.7% respectively which were within ±1% of the moisture contents as recovered from the site. The samples were then cured at 40 °C for 7 days at a relative humidity of 70% before running the UCS test. In this study, we report the current remolded strength of the native and lime treated FKC soils and interpret the results with reference to the actual strengths of the soils reported within a year after initial repair.

5.3.1.2. Expansion Index (EI)

The EI of the untreated and treated FKC soils was determined in accordance with ASTM D4829 [77] using 4 in. diameter by 2 in. height samples cured to reach an initial degree of saturation of 50%.

5.3.1.3. Erosion Resistance

The susceptibility of the FKC soils to erosion was tested indirectly by measuring the turbidity of a 1% suspension of the fine clay fraction (< 2μm) prepared with distilled water using a UV-vis spectrometer. Turbidity of the samples were compared as a

function of absorbance of the fine clay suspension to light near the visible wavelength range (380 nm to 800 nm). Standard procedures to measure the erodibility of soils such as the jet erosion test and the erosion function apparatus test could not be executed due to the unavailability of intact undisturbed samples.

5.3.2. Methods Used for Mineralogical Investigation of FKC Soils

The mineralogical evolution of the FKC soils after lime treatment was investigated by three analytical methods namely XRD to determine the mineralogical composition of the soils, XRF to quantify the total oxide composition in the soils and TGA to identify pozzolanic products and to complement the XRD analysis. Powdered samples were used for XRD, XRF and TGA analysis by grinding the FKC soils using a mortar and pestle followed by sieving to pass 45 μm sieve.

5.3.2.1. XRD Analysis

The soil minerals present in the powdered native and lime treated FKC samples were determined using a Bruker D-8 X-ray diffractometer using CuKα radiation powered to 40 kV at 40 mA. Phase identification was done by matching against the mineral collection data from the International Center for Diffraction Data (ICDD).

Exactly 4.50 g of the samples tested were mixed with 0.5 g of ZnO (internal standard) and 15 mL of ethanol followed by milling for 5 minutes in a micronizer to eliminate preferential orientation of the particles. The suspension was then spray-dried [78] in a heated chamber to generate spherical aggregates. The spray-dried samples were then side loaded prior to XRD analysis. In addition, the clay fraction of the samples (passing 2 μm) was extracted and analyzed to identify the cations saturating the

interlayer of swelling clay minerals. The samples were scanned from 3 to 80 degrees (2θ) for 60 min at 0.02 degrees/sec.

5.3.2.2. XRF Analysis

The powdered samples were pressed into a pellet applying a force of 30 tons for 45 seconds in a XRF pellet press to minimize errors in data measurement. The pelletized samples were tested for the elemental total oxide composition using a high-power (200 W) sequential Rigaku Supermini 200 wavelength dispersive XRF spectrometer instrument operated at a tube voltage of 50 KV and energy resolution of 140 eV.

5.3.2.3. TGA Analysis

The thermal analysis system 'SDT Q-600' manufactured by TA Instruments was used to record the weight change of the samples from 100^{o}C temperature to 1000^{o}C with a ramp rate of 10^{o}C/minute. A precise quantity of 50 mg of powdered sample was used for all measurements. To minimize any errors due to hygroscopic effects on the moisture sensitive of expansive clay minerals present in the FKC soils, the samples were preheated to 100^{o}C for 48 hours prior to taking TGA measurements.

5.4. Experimental Methods

This section discusses the experimental results pertinent to demonstrating the long-term durability of lime treatment at the FKC. The effect of lime on the engineering properties of the soils is discussed first and is followed by a discussion of the results substantiating the mineralogical transformation of the lime treated soils.

5.4.1. Effect of Lime on Engineering Properties of FKC Soils

A concurrent increase in long-term strength, reduction in expansion index and erodibility of the FKC soils 40 years after lime treatment were used as the criteria to establish the geo-mechanical stability of the lime treated soils from an engineering standpoint. The results obtained in support of this assertion are summarized in Table 5.2 and discussed in this section. The UCS and EI measurements were recorded on 3 samples each and the average values and standard error (Error) are reported.

Table 5.2 Summary of the Effect of Lime on Engineering Properties of FKC Soils

Sample Description	**Compressive Strength**		**Expansion Potential**			**Relative Erosion Resistance**	
	UCS (psi)	**Error (psi)**	**EI**	**Error**	**Category**	**Absorbance Intensity**	**Category**
Untreated Soils	15	2.8	54.9	3.5	Moderate	0.23	High
Lime Treated Soils	140	8.7	12.5	2.2	Very Low	0.14	Low

5.4.1.1. Impact of Lime Treatment on UCS of FKC Soils

The UCS of the native soils was reported to be around 12 psi at the time of construction [14]. The UCS of intact lime treated soils recorded a strength of 250 psi immediately after construction and nearly 500 psi one year after treatment [54]. The

average current remolded strength of the lime treated samples was found to be 140 psi and there was no difference in strength of the native soils over time (Table 5.2). The measured remolded strength of the lime treated soils is within the 80 psi to 200 psi range reported after a 7-day curing period for stabilized clay soils having similar PI [79]. As indicated earlier, we were unable to recover intact soil cores that could be either used as is or trimmed to report a more accurate representation of the actual strength of the lime treated sections 40 plus years after treatment. It is important to note that the remolding lime treated soils significantly disturbed the chemical bonds between calcium ions from lime and the soil minerals thereby negatively impacting the strength measurements. Hence the present compressive strength of intact lime treated cores is expected to be higher than the strength reported in this study. In fact, it is remarkable that sufficient residual lime was apparently present to produce this substantial strength gain in the remolded samples. In any case, a ten-fold increase in compressive strength of the remolded lime treated soils compared to the native soils five decades after treatment sufficiently demonstrates the impact of lime in contributing to long-term strength of the FKC soils.

5.4.1.2. Impact of Lime Treatment on EI of FKC Soils

The impact of lime in reducing the expansion index of the FKC soils is evident from the results presented in Table 5.2. An improvement in volumetric stability of high plasticity soils after lime treatment serves as a critical performance measure of long-term durability especially in hydraulic structures which are subjected to constant contact with water. A ‘very high’ potential degree of expansion for the native FKC soils and a ‘low’

expansion index for the lime treated soils was reported after initial repair [14]. The textural modification of the FKC soils from lean clays to low plasticity silts after lime treatment lowers the colloidal clay activity in the soils thereby minimizing volume change when subjected to climatic cycles. The 'very low' risk of expansion in the lime treated sections after 40 years of lime treatment provides strong, additional support for the long-term durability of lime treated soils.

5.4.1.3. Impact of Lime on Erosion Resistance of FKC Soils

The absorbance patterns of the fine clay particles (< 2μm) subjected to light in the wavelength range between 380 nm to 800 nm is presented in Figure 5.3.

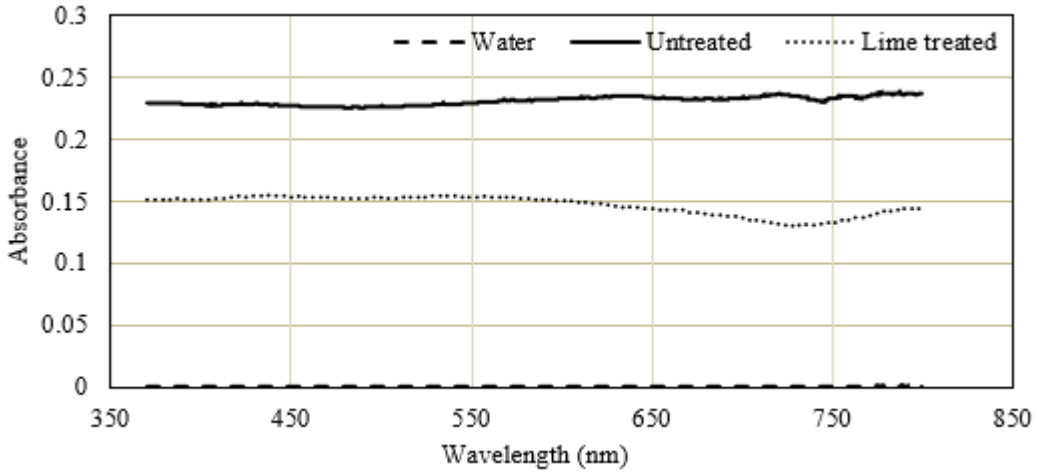

Figure 5.3 Absorbance patterns of FKC soils subjected to light in visible wavelength range

A higher absorbance intensity is a direct function of the turbidity of the suspensions as reflected by the zero-absorbance observed in distilled water [80]. A clear

drop in turbidity of the fine clay suspensions was observed in the lime treated soils (Figure 5.3). The data obtained herein provides valuable insight into the effectiveness of lime treatment in controlling the dispersive nature of the native FKC soils thereby making them less prone to erosion [81]. A more rigorous analysis of the erodibility of the FKC soils must involve the use of in-situ erosion tests using the erosion function apparatus (EFA) to track the scour rate as a function of key parameters such as shear stresses and velocity of water flow which could not be performed in this study due to the challenges faced in recovering undisturbed samples. Nevertheless, when comparing the absorbance intensities of the native FKC soils with the lime treated soils at the same suspension concentration, lower absorbance intensities observed in the treated samples would imply a lower scour rate of the soils due to reduced dispersion. This indirect measure of the erosion resistance of lime treated soils is supported by the fact that no erosion related failure has been reported since initial repair in the 1970's.

5.4.2. Effect of Lime on Mineralogical Transformation of FKC Soils

The findings pertaining to the changes in mineralogy of the lime treated FKC soils over time are presented in this section. Special emphasis is placed on identification and quantification of the new mineral phases formed due to the long-term geochemical reactions occurring in the soil-lime system using three analytical techniques namely XRD, XRF and TGA.

5.4.2.1. Quantitative XRD Analysis of FKC Soils

The XRD pattern of the untreated FKC soils along with the quantification of soil minerals is presented in Figure 5.4.

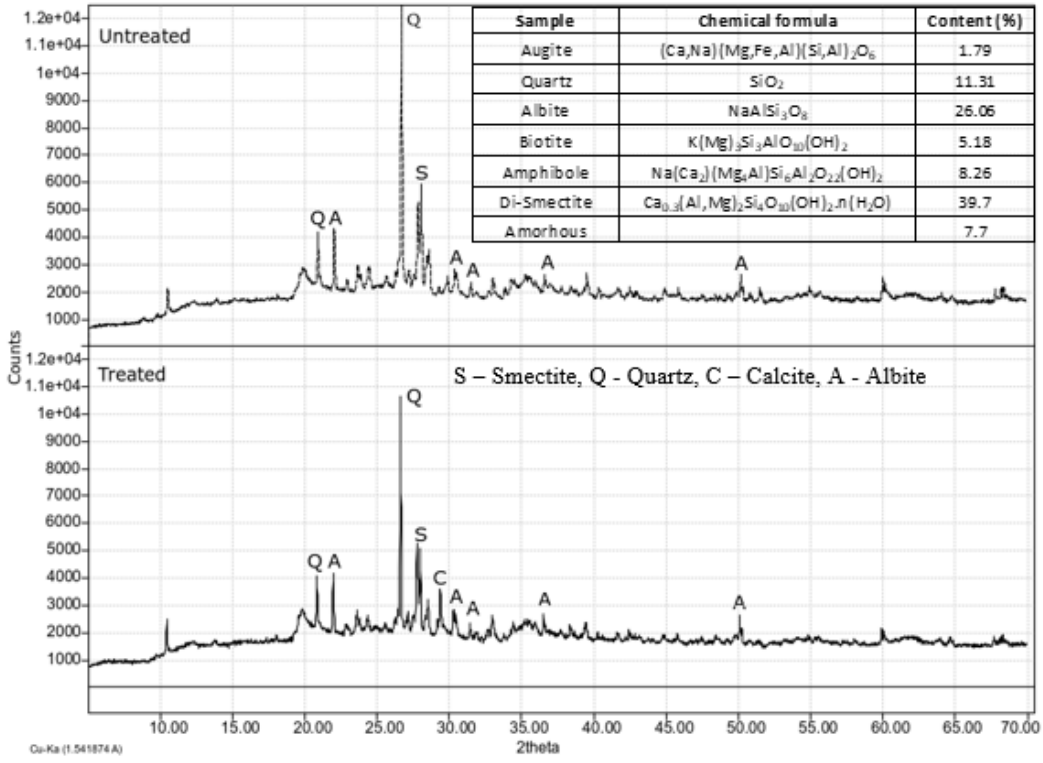

Sample	Chemical formula	Content (%)
Augite	$(Ca,Na)(Mg,Fe,Al)(Si,Al)_2O_6$	1.79
Quartz	SiO_2	11.31
Albite	$NaAlSi_3O_8$	26.06
Biotite	$K(Mg)_3Si_3AlO_{10}(OH)_2$	5.18
Amphibole	$Na(Ca_2)(Mg_4Al)Si_6Al_2O_{22}(OH)_2$	8.26
Di-Smectite	$Ca_{0.3}(Al,Mg)_2Si_4O_{10}(OH)_2.n(H_2O)$	39.7
Amorhous		7.7

Figure 5.4 XRD pattern of the untreated and treated FKC soils

The fitting criteria of R_{wp} <10% and goodness of fit (GOF) <3 validates the accuracy of the quantification. The presence of 39% smectite in the soils explains the moderate expansion index of the native soils and correlates well with the CEC (27.5 meq/100g) obtained. In addition, 7.7% of the amorphous phases present in the soil was composed of 4% amorphous SiO_2 and other minor phases. This was calculated by subtracting out the total equivalent crystalline SiO_2 fraction from the total SiO_2 obtained from XRF [82]. The amorphous SiO_2 serves as a critical source of silica to assist in the formation of C-S-H due to its high reactivity.

5.4.2.2. XRF Analysis

The XRF data provides the total elemental composition in equivalent oxide form for both the native and lime treated FKC soils. As anticipated, the lime treated soils had 3.9% more CaO compared to the untreated soils (Table 5.3). There were no major differences in the oxide composition of the other elements. The increase in CaO content 40 years after lime treatment proves that there was no significant leaching of lime or its associated pozzolanic products over time which substantiates the long-term durability of lime treatment.

Table 5.3 XRF Analysis of FKC Soils

Element/ Composition	**Untreated Soils (%)**	**Lime Treated Soils (%)**
CaO	4.6	8.5
SiO_2	55.6	53.9
Al_2O_3	20.6	20.1
Fe_2O_3	12.1	11.2
SO_3	0.0	0.0
MgO	2.9	3.0
K_2O	1.8	1.1
Na_2O	0.6	0.6
Total Organic Carbon	1.8	1.7

5.4.2.3. TGA Analysis

The peaks observed in the differential thermogram (DTG) of the untreated and lime treated samples were used to confirm the presence of different minerals as seen in Figure 5.5. Minerals with water in the interlayer such as C-S-H and smectite and others with hydroxyl functional groups such as amphiboles and biotite lose weight at different temperatures due to water loss and dihydroxylation, respectively. The C-S-H phase shows water loss from 50°C to 600°C [83] with a peak at 150°C as seen in Figure 5.5. Dehydroxylation of amphibole and biotite was validated by the peak at 450°C [84] in both the treated and untreated sample. In addition, the calcite formed due to lime treatment decarbonates above 600°C to CaO and CO_2 and was identified by the peak at 700°C

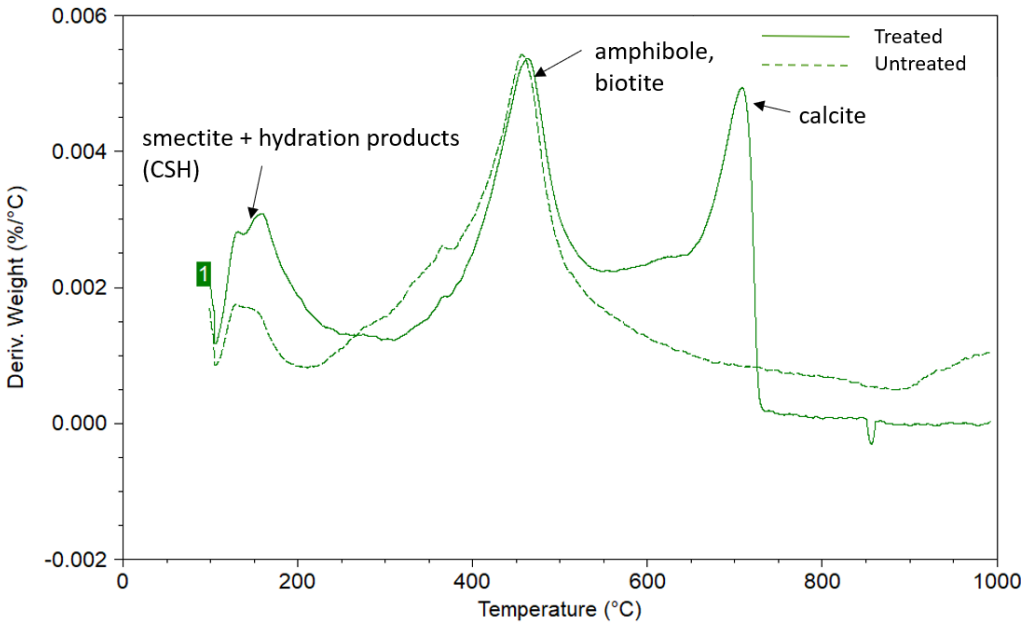

Figure 5.5 Differential TGA analysis of the untreated and treated soil specimen

5.4.3. Discussion of Soil-Lime Reactions in FKC Soils

In the presence of water, hydrated lime, $Ca(OH)_2$ dissolves releasing Ca^{2+} and OH^- ions.

$$Ca(OH)_2 \rightarrow Ca^{2+} + 2OH^- \quad (5.1)$$

The OH^- ions released increases the soil pH of the lime treated soils to as high as 12.45. Smectite, which is the primary expansive clay mineral in the FKC soils is unstable above pH 12.0 and partially dissolves [85] releasing amorphous silica and alumina in the process.

$$\text{Smectite} + 6H^+ + 2H_2O \rightarrow 1.4Al^{3+} + 0.6Mg^{2+} + 0.6Na^+ + SiO_2(am) \quad (5.2)$$

C-S-H precipitates in an alkaline environment (pH 10-12) when sufficient quantities of the highly reactive SiO_2 (am) released from smectite dissolution and Ca^{2+} ions released from lime react in the presence of water. The formation of a representative C-S-H [86] can be written as equation 5.3.

$$1.5Ca^{2+} + 4H_2O + SiO_2(am) \rightarrow (CaO)1.5.(SiO_2)(H_2O)2.5 + 3H^+ \quad (5.3)$$

C-S-H has a chemical formula of $(CaO)X.(SiO_2)Y.(4H_2O)Z$ [17]. The values of X, Y and Z can range from 0.8-3.5, 0.6-2.5 and 1.5-2.5, respectively [86]. The varying stoichiometry of CaO, SiO_2 and H_2O can be attributed to the solid solution and disorderly nature of C-S-H. The H_2O in C-S-H is also comprised of equivalent H^+ and OH^- ions ($H_2O \rightarrow H^+ + OH^-$) . The OH^- ions from lime dissolution (Equation 5.1) is consumed in the formation of C-S-H which reduces the pH. Furthermore, the pH buffering capacity of expansive clay minerals like smectite can also reduce the pH as observed in the FKC soils [87, 88]. The gel-like C-S-H structure holds the soil matrix

together and contributes to the strength and durability of the soil. Hence, the stability of C-S-H at equilibrium is used as the main criterion to substantiate the long-term durability of the lime treated FKC soils.

Calcite formation is expected in lime treated soils due to the reaction of hydrated lime with atmospheric CO_2. Calcite contributes to the durability of soil-lime system by acting as an inert filler material by occupying the pore space within the soil matrix [89]. In addition, calcite also assists in strength development by cementing some of the undissolved smectites. The TGA data that confirm the presence of C-S-H and calcite in the lime treated samples collected for this study.

In conclusion, the calcium from lime ends up in either calcite or C-S-H or remains in calcium hydroxide. In the case of the FKC soils, the fate of calcium was consumed in a 1:3.5 proportion between calcite and C-S-H with a negligible fraction remaining unreacted. This distribution is similar to what was observed on a 30-year-old lime-treated embankment by Haas and Ritter [90].

5.5. Evaluating the Impact of Lime Treatment on Moisture Distribution in FKC Soils Using Hydrus-2D

Hydrus-2D is a software tool that uses finite element modelling (FEM) to investigate engineering issues associated with water flow [91]. Hydrus-2D has the ability to analyze irregular geometries and has the capability to analyze the impact of real climate data on water flow [92].

As part of the case study on the FKC canal, Hydrus-2D was used to simulate the moisture distribution of the soils beneath the pavement surface adjacent to the

embankment slopes when subjected to wetting and drying climatic cycles. The primary objective of the analysis was to emphasize the impact of lime treatment on mitigating of vertical movement caused due to swelling of the soils when exposed to differential moisture fluctuations during a flood.

5.5.1. Hydrus-2D Model Geometry and Boundary Conditions

The geometry of the design and boundary conditions used for the simulations are shown in Figure 5.6.

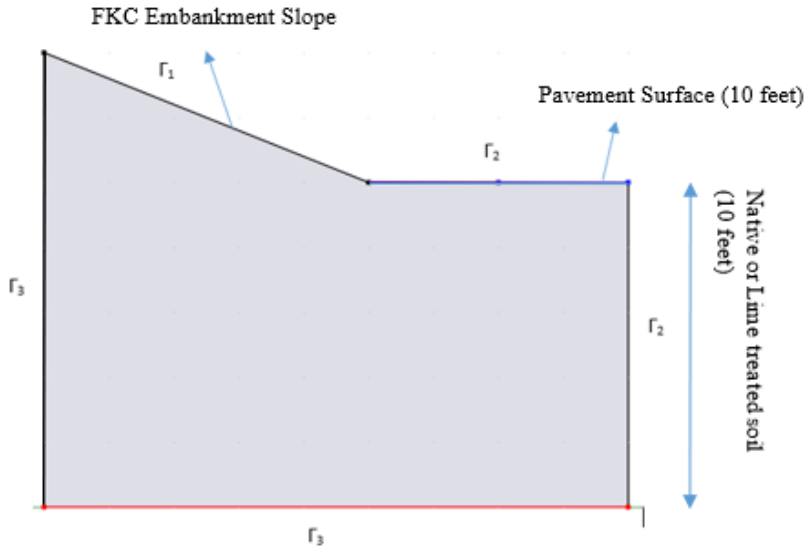

Figure 5.6 Design and boundary conditions used for Hydrus-2D simulations

The boundary condition Γ_1 represents boundaries with a variable suction head influenced by rainfall, Γ_2 represents boundaries through which there is no moisture influx and Γ_3 represents the boundaries having a constant suction head. The pavement surface is assumed to be sealed and hence was assigned a boundary condition Γ_2. The

matric suction at the bottom of the 10 feet moisture active zone was assigned a constant suction head value corresponding to equilibrium suction (U_e). U_e for the FKC location was found to be a pF of 3.4 corresponding to a Thornthwaite moisture index of 10 according to the equation proposed by Lytton [19]. The suction head at locations in constant contact with water (U_{min}) was assumed to correspond to a pF of 2.5 (i.e. vertical surface adjacent to the embankment slope with boundary condition Γ_3), the maximum level of matric suction after a normal drying cycle (U_{max}) was assumed to be equal to a pF of 6.0 which corresponds to the suction at air dry state.

The soil water characteristic curves (SWCC) of the native and lime treated FKC soils were generated using the artificial neural network (ANN) model developed by Saha [93] using the engineering properties in Table 5.1. The SWCC curves of the native and lime treated FKC generated using the ANN approach are shown in Figure 5.7.

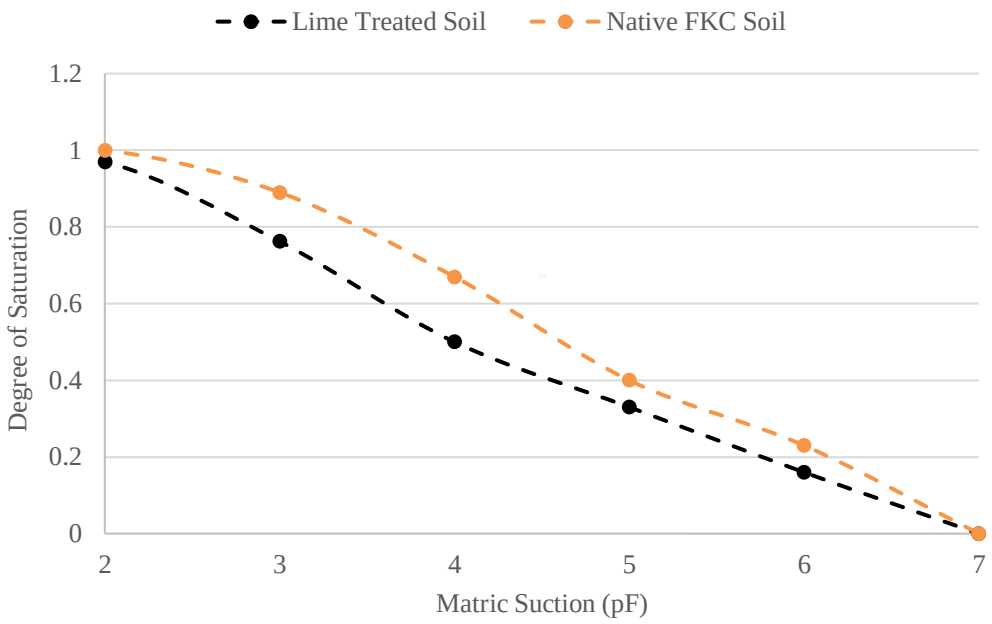

Figure 5.7 SWCC curves of the native and lime treated FKC soils

The general constitutive equations governing water flow in Hydrus-2D were explained in detail by Zhang [94]. The van Genuchten model parameters of the soils were obtained by fitting the van Genuchten model constitutive equations [95] to the SWCC curves in Figure 5.7. The material properties and the hydraulic conductivity (K_s) of the soils used for simulating water flow are provided in Table 5.4.

Table 5.4 Material Properties Used in Hydrus-2D for Simulating Water Flow

Soil Description	**Saturation Water Content**	**Residual Water Content**	**K_s, cm/day**	**Reverse of Air Entry Value, α**	**Pore Size Distribution Index, n**
Untreated Soils	0.38	0.071	4.8	0.008	1.09
Lime Treated Soils	0.33	0.134	6.9	0.013	1.32

5.5.2. Moisture Distribution Simulation Results and Discussion

The moisture distribution patterns across the entire geometry of the embankment was analyzed after assigning a pF of 3.4 as the initial value of Γ_1 which corresponds to an equilibrium state. The soils were allowed to wet to a pF of 2.5 corresponding to U_{min} during a 6-day rainfall period with a total precipitation of 5.2 inches. The moisture distribution response of the native FKC soils and lime treated FKC soils during the simulated wetting cycle are shown in Figure 5.8 and Figure 5.9 respectively.

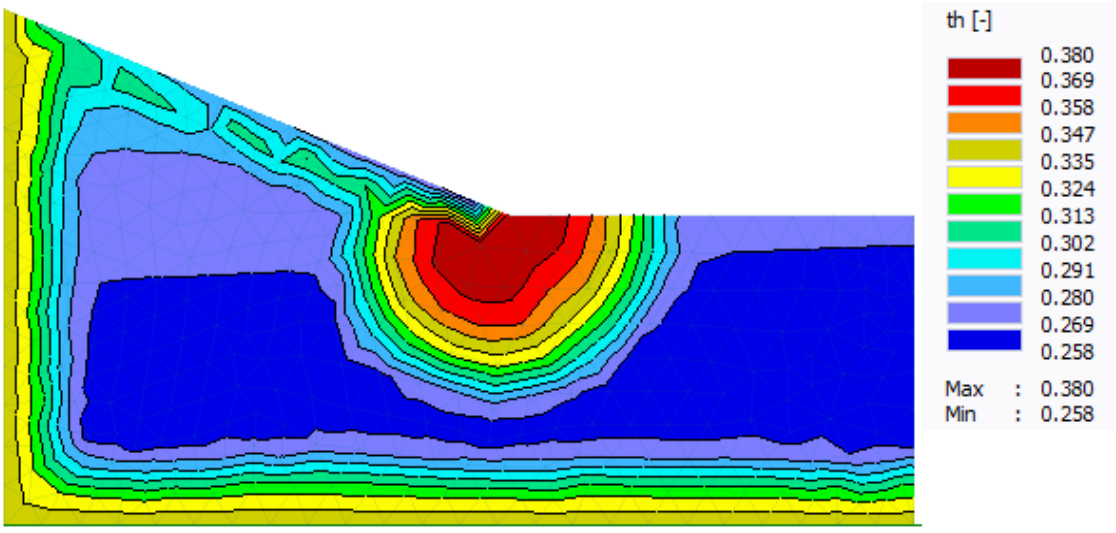

Figure 5.8 Moisture distribution patterns of native FKC soils during a wetting cycle

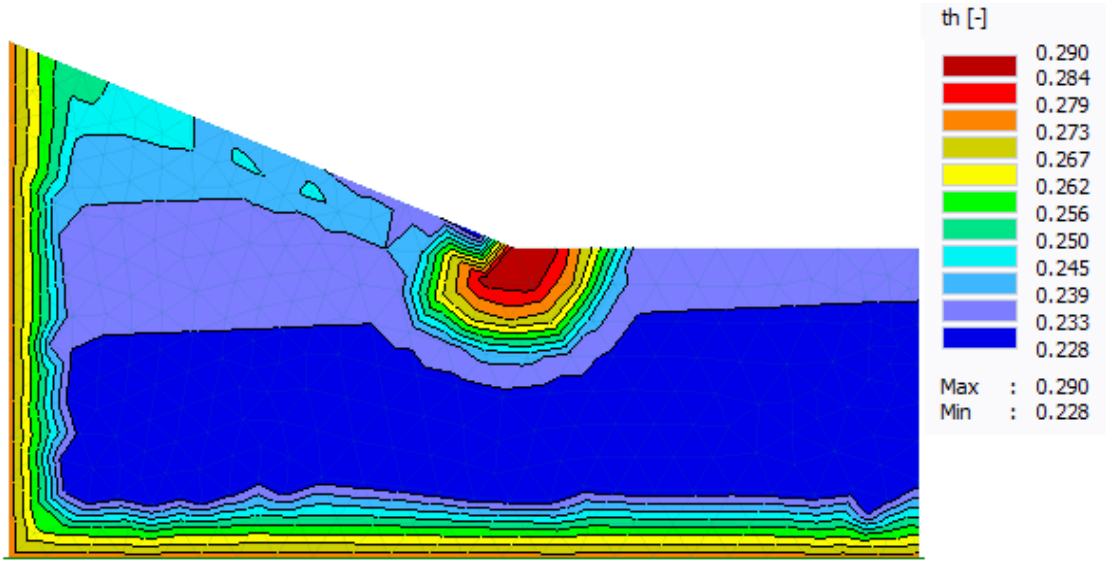

Figure 5.9 Moisture distribution patterns of lime treated FKC soils during a wetting cycle

As expected the moisture distribution patterns reveal that the moisture contents are maximum directly below the downward embankment slope which was the only source of moisture influx during the rainfall period simulated.

The following remarks can be made regarding the impact of lime treatment based on the moisture distribution patterns shown in Figure 5.8 and Figure 5.9:

1. The area of concentration of the accumulated moisture from the rainfall in the region below the embankment slope is significantly reduced after lime treatment indicating that the moisture was more evenly distributed across the geometry of the embankment. This is a result of the improved drainage characterisitcs of the soils after lime treatment due to their textural modification from lean clays to lean silts. The reduction in PI from 23 to 9 accompanied by a reduction in expansion index discussed earlier are the two engineering properties in support of the improved moisture distribution patterns observed.
2. The magnitude of water contents post the wetting cycle in native FKC clays is higher compared to the lime treated soils which is directly influenced by the ability of the native clays to swell by absorbing and retaining greater quantities of moisture.

In summary, the Hydrus-2D analysis shows the impact of lime on improving the durability of the FKC sections during climatic cycles and prevent issues related to expansion and development of shrinkage cracking in the embankment slopes. The Hydrus-2D analysis also emphasizes the need to consider the changing material properties of the soils after stabilization with lime in order to accurately characterize

their volumetric stability. The method improvements proposed towards this end are discussed in the next Chapter.

5.6. Summary and Conclusions

The long-term durability of lime treatment at the FKC was evaluated from an engineering and mineralogical standpoint after 40 plus years of performance. Hydrus-2D analysis was performed to evaluate the impact of lime on influencing the moisture distribution across the FKC embankments and adjacent pavement sections. The following conclusion were drawn from this study:

1. The drop in PI of the lime treated soils in comparison to the native soils was a testimony to the durable textural modification of the treated FKC soils from lean clays to inorganic low plasticity silts. The particle size distribution trends confirmed the sustained impact of lime in coagulating the clay colloids. The native soil comprised of 39.7% smectite.
2. The pH of the native FKC soils was found to 6.30. The lime treated soils had a pH of 8.90 indicating considerable presence of hydroxyl ions released from hydrated lime. The pH of the lime treated soils dropped from 12.40 to 8.90 during the 40 plus year performance period due to carbonation and mineralogical transformations.
3. A difference of nearly 4% Ca^{2+} ions in the XRF analysis and the concomitant high pH of the lime treated soils proved that there was negligible leaching of lime and/or calcium compounds since initial treatment.

4. A concurrent increase in long-term strength, reduction in expansion potential and erodibility of the FKC soils was used as the criteria to establish the geo-mechanical stability of the lime treated soils from an engineering standpoint. Lime treatment increased the mean UCS strength of remolded soils from 15 psi to 140 psi, decreased the risk of expansion from moderate to very low and lowered the turbidity of the fine clay suspensions leading to improved erosion resistance.
5. The formation of C-S-H was confirmed by the peak at 150 °C and the formation of calcite was confirmed by the peak at 700 °C in the DTG of the lime treated soil.
6. The Hydrus-2D analysis support the improvements in physical properties of the lime treated soils and confirm the improvements in drainage characteristics of the FKC soils.

The results obtained shows that the lime content used at the FKC was appropriate to ensure a lasting impact even after 40 plus years of service life in constant contact with water. While more similar case studies are required before generalizing this important finding, preliminary indications are that leaching of lime remains limited in hydraulic structures and therefore need not be assessed at the formulation stages of similar projects. The findings of this study together with the on-site feedback regarding the remarkable performance history of lime at the FKC affirm the long-term durability of lime treatment for soils in permanent or intermittent contact with water for long periods and strengthens the case for the use of lime in the repair of hydraulic structures.

6. METHOD IMPROVEMENTS TO CHARACTERIZE THE VOLUMETRIC STABILITY OF LIME STABILIZED EXPANSIVE SUBGRADE SOILS

6.1. Objectives

This chapter presents the modifications proposed to two existing methods that are used to predict the vertical movement and volumetric stability of expansive soils. Both the methods investigated are discussed in terms of their application for the design of pavements. The first such method is the Tex-124-E procedure developed by the Texas Department of Transportation [18] to determine the potential vertical rise (PVR) in pavements constructed on expansive subgrade soils. The second method is a matric suction-based approach that uses the constitutive equations initially proposed by Mitchell [57] and subsequently modified by Lytton [19] to predict the total vertical movement in pavements due to swelling and shrinking of expansive subgrade soils.

The motivation behind proposing modifications to the two existing methods are to improve the accuracy of predictions by correctly accounting for field conditions at the design location in question including the effects of changes in material properties due to chemical stabilization of soils using lime.

6.2. Modifications Proposed to the Tex-124-E Method

6.2.1. Background

The Tex-124-E method uses three major design inputs namely the plasticity index (PI) of the soils and the initial moisture state (θ_i) of the soils to predict the PVR due to expansive soils in 1-foot increments over a preset depth of calculation. The

method then limits the total PVR to an allowable value ranging between 1.0 and 1.75 inches to calculate the depth of non-swelling or inert material required from the top of the pavement surface to the existing native subgrade layer. The depth of non-swelling material determined using this method ultimately influences the thickness of the chemically stabilized (lime or cement) subgrade layer underneath the pavement surface and base layers. To put the above discussion in perspective, the Tex-124-E design inputs namely, PI and θ_i, directly influence the thickness of the lime stabilized subgrade (LSS) layer.

6.2.2. Limitations in the Tex-124-E Method to Define the Initial Moisture State of Soils

The modifications proposed to the Tex-124-E method involves addressing the limitations in the existing practice to define θ_i. The current method assigns θ_i of the soils as either 'dry', 'average' or 'wet' by comparing the in-situ moisture state of the soils (w) against an approximation of the moisture content limit at dry condition (θ_{dry}) and the moisture content limit at wet condition (θ_{wet}) using the liquid limit (LL) of the soils according to equation 6.1 and equation 6.2 [18].

$$\theta_{dry}, \% = (0.2 \times LL) + 9 \quad (6.1)$$

$$\theta_{wet}, \% = (0.45 \times LL) + 2 \quad (6.2)$$

The Tex-124-E method then uses the charts in Figure 6.1 corresponding to the assigned initial moisture state and the PI of the soils to calculate the percentage of volumetric change.

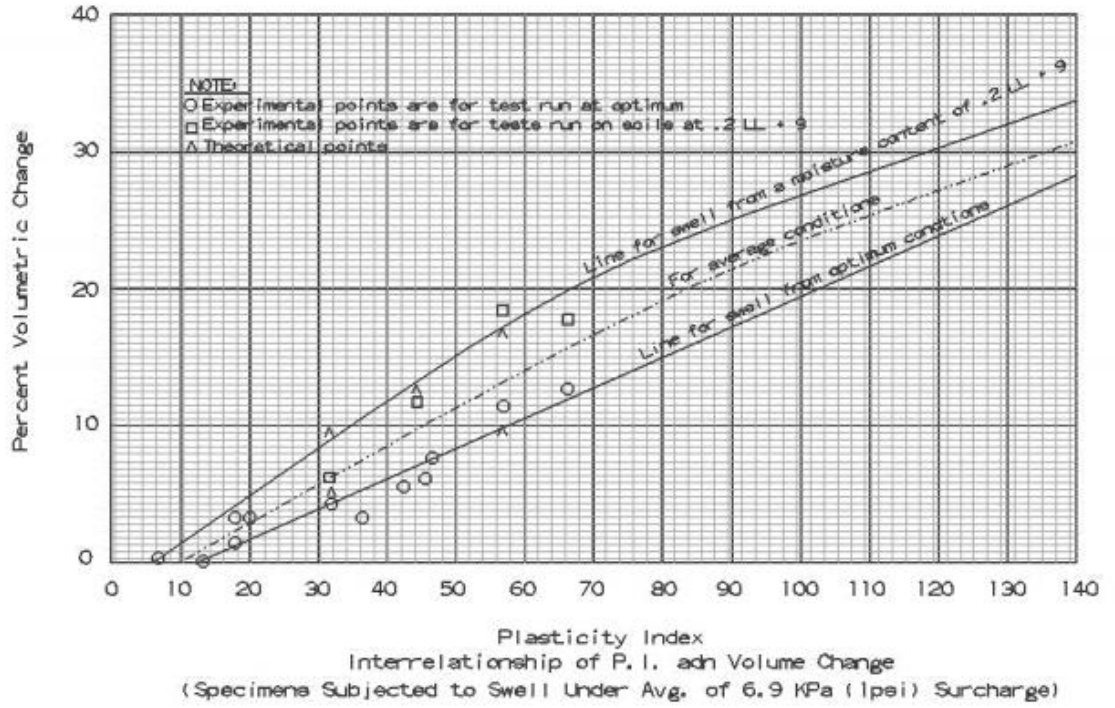

Figure 6.1 Relationship between PI and volume change used in Tex-124-E method (reprinted from [18])

There are several limitations in the existing Tex-124-E method which were discussed briefly in Chapter 1 and have been extensively summarized by Lytton [19]. The two major limitations of the method are that the PVR predictions are over conservative due to the fact that vertical movement due to heaving alone is considered and the effects of movement due to shrinking of soils is ignored. It is evident from Figure 6.1 that a 'dry' initial moisture state assumption yields the highest volume change followed by the 'average' moisture condition while a 'wet' initial moisture state results in the least volume change. This trend is agreeable in principle to determine the volume change resulting due to swell since the amplitude of matric suction or the net moisture

energy the soils are subjected to while transitioning from a dry to a wet state is significantly greater compared to when the soils are initially in a wet state. However, two important limitations exist in the method currently used to define θ_i:

1. The equations used to define the dry and wet moisture limits are purely empirical and rely solely on the LL rather than accounting for the actual pore size distribution and hydraulic properties of the soil such as through the SWCC curve.
2. The prediction of volume change in Figure 6.1 does not involve a gradual transition between the three initially assigned moisture states thereby resulting in significantly underpredicting or overpredicting volume change in cases where θ_i is within 2% of the wet or dry boundary defined by equation 6.1 and equation 6.2.

6.2.3. Modified Approach to Define the Initial Moisture State of Soils in Tex-124-E

The focus of the modified approach is to address the first limitation by proposing a more fundamental method to define θ_i. The second limitation is an inherent flaw in the Tex-124-E method, which cannot be corrected since it is connected with the other assumptions used to develop Figure 6.1. Nevertheless, the lack of a gradual transition to calculate volume change between the three moisture states necessitates a more rational approach to define θ_i.

The following steps are proposed to define θ_i using the SWCC for use in the current Tex-124-E method and to logically consider the impact of chemical stabilization:

Step 1: Obtain the equilibrium suction (U_e) of the location either as function of climate alone using equation 6.3 proposed by Lytton [19] or as a function of both soil type and climate by the equations proposed by Saha [96] .

$$U_e\,(pF) = 3.563 \times \exp\,(-0.0051 \times TMI) \tag{6.3}$$

Where TMI is the Thornthwaite moisture index of the location in question which can be defined using the maps developed by Saha [96] .

Step 2: Generate the SWCC of the native or the LSS soils using the ANN approach developed by Saha [93] or as a function of the product of PI and % passing 74 micron (P200) using the SWCC plots in Figure 6.2 obtained from a report on the mechanistic-empirical pavement design guide (MEPDG) [97].

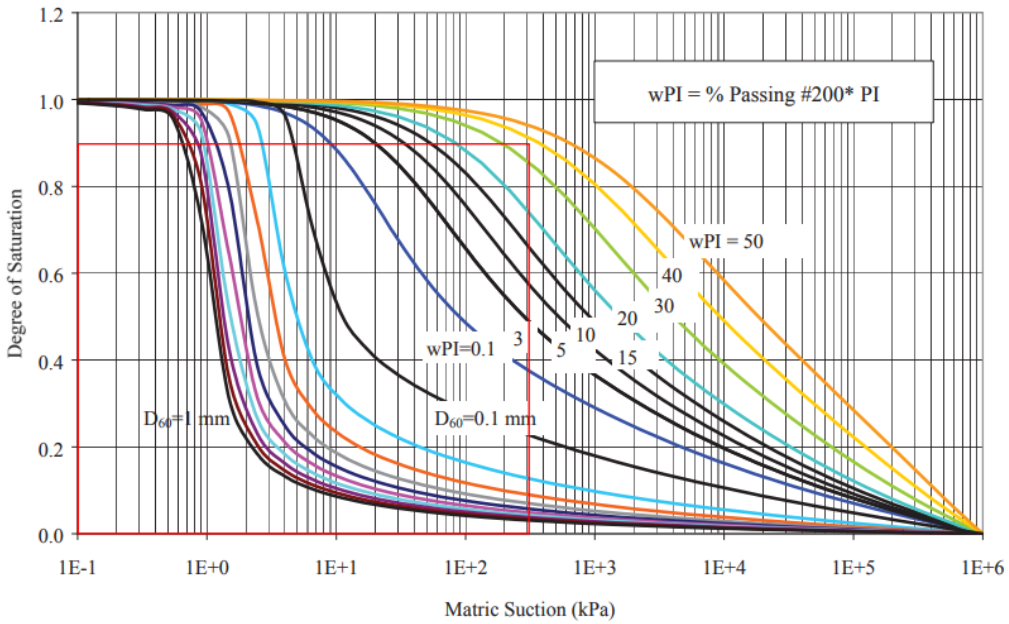

Figure 6.2 SWCC plots based on product of PI and P200 (reprinted from [97])

Step 3: Obtain the degree of saturation of the soils at U_e, S_{eq} directly from the SWCC plots.

Step 4: Calculate in-situ degree of saturation, S_i using equation 6.4 based on the maximum dry density (γ_d) of the soils assuming a nominal value from 2.65 to 2.70 for specific gravity, G_s.

$$S_i(\%) = \frac{w.G_s.\gamma_d}{G_s\gamma_w - \gamma_d} \tag{6.4}$$

Step 5: Assign θ_i for the soils by compare S_i against S_{eq} using Table 6.1 for $0 \leq PI.P200 \leq 50$ and Table 6.2 for $PI.P200 > 50$.

Table 6.1 Proposed Criterion for Defining θ_i for PI.P200 up to 50

Criteria	$\boldsymbol{\theta_i}$
$S_i \leq S_{eq} - 2\%$	Dry
$S_{eq} - 2\% < S_i < S_{eq} + 2\%$	Average
$S_i \geq S_{eq} + 2\%$	Wet

When $PI.P200 > 50$, a revised criterion is recommended in Table 6.2 considering the high swell-shrink propensity of such soils.

Table 6.2 Proposed Criterion for Defining θ_i for PI.P200>50

Criteria	$\boldsymbol{\theta_i}$
$S_i \leq S_{eq}$	Dry
$S_i > S_{eq}$	Average

Engineering judgement was used to develop the criteria for defining θ_i based on the standard deviation of the difference between S_i and S_{eq} for nearly 450 soil borings obtained from Texas.

6.2.4. Comparison of Initial Moisture States Obtained Using Existing and Modified Methods

The θ_i condition obtained following the existing Tex-124-E guidelines were compared against those obtained used the modified approach and the results are presented in Table 6.3. The soil properties for the comparison were obtained from native and lime treated soil borings taken from four locations along the SH 130 project in Texas. The average U_e for this location was calculated to be 3.56 pF corresponding to a TMI of 0 and G_s of the soils was assumed to be 2.65.

Table 6.3 Comparison of θ_i Obtained Using the Proposed and Existing Approaches

Soil Type	Location	LL (%)	PI (%)	PI. P200	w (%)	γ_d (lb./ft^3)	S_i (%)	S_{eq} (%)	θ_i- Proposed	θ_i- Tex-124-E
Native Soils	B1	56.6	36	30	22.6	96	82.9	83.4	AVG	AVG
	B2	60.2	40	35	22.2	98	85.5	86.6	AVG	DRY
	B3	84.1	59	56	27.1	95	96.9	95.2	AVG	DRY
	B4	91.1	69	66	20.1	98	77.5	96.7	DRY	DRY
Lime Treated Soils	B1	48.2	22	17	19.6	93	66.8	68.1	AVG	DRY
	B2	48.4	25	22	19.8	94	69.2	71.0	AVG	DRY
	B3	65.8	36	32	23.8	92	79.1	84.5	DRY	DRY
	B4	74.6	43	39	17.6	94	61.5	88.1	DRY	DRY

The θ_i condition obtained using both the existing and modified approach were either ‘average’ or ‘dry’ and never ‘wet’ for all the cases compared in Table 6.3. This is likely because the soil borings were obtained either during the summer months or following a dry period during the year.

However, it is obvious from Table 6.3 that the current Tex-124-E method is more conservative compared to the modified approach proposed for both native soils and soils chemically stabilized using lime. The θ_i condition for four of the eight cases moved from a ‘dry’ state to an ‘average’ state. The ‘average’ initial moisture state in lime treated soils is a result of the decreased maximum dry density (γ_d) after lime treatment

accompanied by an increase in the optimum moisture content [98]. Little stated that a 3 to 5 lb./ft^3 drop in γ_d was typical after lime treatment of clays [2] due to the immediate physicochemical interactions between lime and the soil minerals. The general transition from a 'dry' to 'average' initial moisture state in the native soils illustrate the impacts of using the SWCC based approach to predict θ_i compared to using the LL only. The current Tex-124-E method both neglects the impact of chemical stabilization and fundamental concepts describing soil behavior such as γ_d and SWCC on θ_i and ultimately overestimates volume change contributing to PVR caused by expansive soils.

6.3. Modifications Proposed to the Suction Method

6.3.1. Background

A suction-based approach to calculate vertical movement due to both swelling and shrinking of soils was proposed by Lytton [19] to address the limitations in the Tex-124-E method. The suction-based approach is based on fundamental soil properties influencing vertical movement such as the matric suction (U), diffusivity coefficient of the soils (α), annual frequency of climatic cycles (n) and mechanical stresses induced as a result of soil expansion and overburden effects. The first step in this approach uses equation 6.5 proposed by Mitchell [57] to generate a suction profile as a function of depth (z).

$$U(z) = U_e \pm U_0 \exp\left[-\left(\frac{n\pi}{\alpha}\right)^{0.5} z\right] \quad (6.5)$$

U_e represents the equilibrium suction and U_0 is the double amplitude of the suction variation between either the minimum suction limit (U_{min}) and the maximum suction limit (U_{max}) with respect to U_e. U_{min} represents soils in their saturated state (pF

2.5). U_{max} represents soils either in an air-dry state (pF 6.0) in the absence of vegetation or soils at the suction limit corresponding to the wilting point of trees (pF 4.7). A typical suction profile generated using this approach is shown in Figure 6.3.

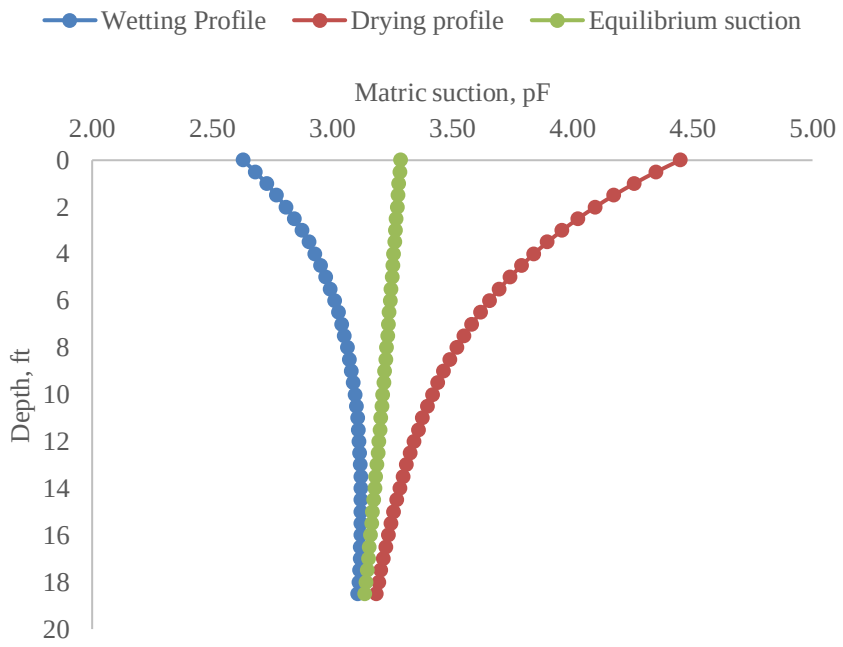

Figure 6.3 Typical suction profile with depth for Houston soils generated using the Mitchell constitutive equation.

The volume change of the soils ($\frac{\Delta V}{V}$) is then calculated over the suction amplitude influencing soil swell during a wetting cycle (ΔpF_{wet}) or the suction amplitude driving soil shrinkage during a drying cycle (ΔpF_{dry}) using the suction compressibility index (γ_h) according to equation 6.6.

$$\gamma_h = \frac{\frac{\Delta V}{V}}{\Delta pF} \tag{6.6}$$

In addition to considering the impact of stresses due to soil expansion or shrinkage using γ_h, the suction method also considers the impact of mechanical stresses surrounding the soil, which are not presented herein to focus on the scope of the modified approach. γ_h is either determined through pressure plate experiments [58] or more commonly by using charts based on experimental results obtained on reconstituted soil samples [99]. In summary, the suction-based approach is technically sound and yields reliable estimates of vertical movement, but it does not consider a shift factor to relate the experimentally obtained values of γ_h to those corresponding to intact soils.

6.3.2. Experimentally Obtained Values of Suction Compressibility Index for Texas Subgrade Soils

The pressure plate experiment was conducted in accordance with the ASTM D6836 procedure [100] on the same four soils compared in Table 6.3 both in their intact state and after reconstituting them at their optimum moisture contents. The experimental results obtained are summarized in Table 6.4.

Table 6.4 Impact of Chemical Stabilization and Soil Fabric on γ_h

Location	γ_h , native soils			γ_h, lime stabilized soils		
	Intact	**Reconstituted**	**% Change**	**Intact**	**Reconstituted**	**% Change**
B1	0.023	0.033	30.3	0.009	0.014	35.1
B2	0.034	0.048	29.1	0.006	0.009	36.7
B3	0.051	0.067	23.8	0.015	0.025	40.0
B4	0.063	0.095	33.6	0.031	0.041	24.4
Mean	0.042	0.060	29.25	0.015	0.022	34.0

The results in Table 6.4 indicate that the γ_h values of reconstituted soils is anywhere between 23.8% to 40% higher compared to the intact samples regardless of whether or not the soils where chemically stabilized with lime. The mean γ_h values for the both intact and reconstituted native soils are approximately 2.7 times higher compared to the lime stabilized soils proving the benefits of lime treatment on controlling volume change in expansive soils. The key fact however is that the true impact of lime on reducing vertical movement is not captured using data obtained after reconstituted the field samples during experimental measurements of γ_h. In summary, altering the soil fabric including tree roots and cracks during remolding of samples plays a critical role in changing the matric suction levels driving soil expansion and shrinkage and must be accounted for during the design of pavements on expansive soils.

6.3.3. Proposed Shift Factor to Relate Suction Compressibility Index of Reconstituted and Intact Soils

The pressure plate test is the closest way of simulating actual volume change occurring in soils during a drying cycle. However, the test is very labor intensive and hence impractical to conduct on large design projects. Designers are forced to rely on empirical charts to determine γ_h as a function of soil classification and cation exchange capacity [99] thereby completely ignoring the impact of soil fabric modification due to not just vegetation, wormholes, cracks and roots but also due to chemical stabilization using lime.

Modification of the soil fabric during the remolding process essentially alters the packing arrangement of the fine soil and in turn the porosity of the soil. The soil samples transition anywhere from the loosest packing state represented by a simple cubic arrangement towards the tightest packing state represented by a rhombohedral arrangement. The porosity of the soils hence ranges from 47.64% in the loosest packing state possible to 25.95% in the densest packing state possible [101]. The individual soil grains in in-situ soils with an intact soil fabric are obviously in contact with lesser number of particles compared to soils compacted in the lab. The difference in porosity between an intact and remolded sample is illustrated by Figure 6.4 which is a modified representation of a typical SWCC for soils before and after modification of soil fabric.

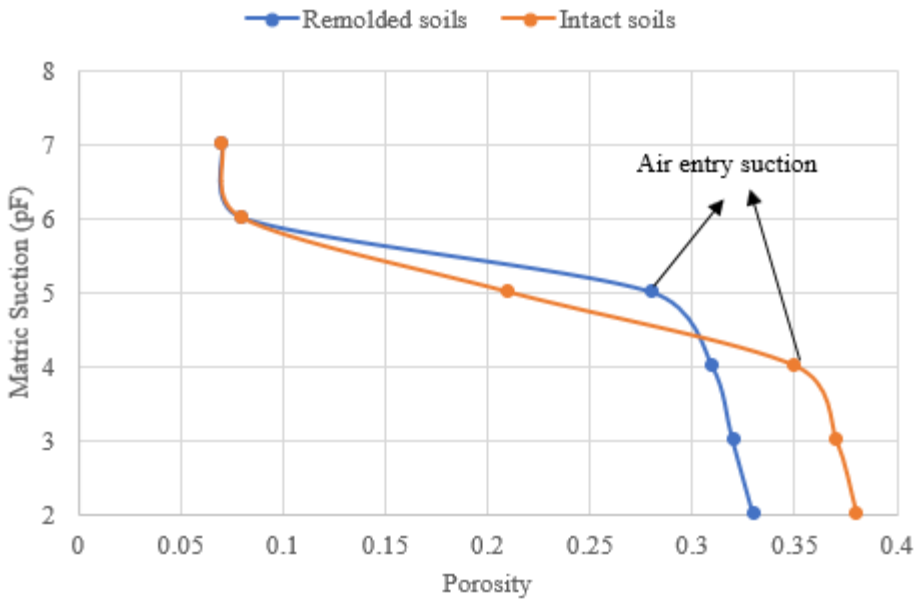

Figure 6.4 Changes in soil porosity as a function of matric suction due to alteration of soil fabric during remolding.

Figure 6.4 reaffirms the fact that the porosity in remolded soils is lower compared to intact soils due to higher matric suction requirements for air entry into the pores. The changes in porosity of the soils due to the changes in their packing arrangement serves as the premise for the proposed shift factor for relating the γ_h values of reconstituted and intact soils. The various packing types, the corresponding soil porosity (n) and the packing factors are summarized in Table 6.5, adapted from [101].

Table 6.5 Packing Characteristics of Soil Particles (Adapted from [101])

Packing Type	***n*,%**	**Packing Factor**
Simple cubic	47.64	1
Orthorhombic	39.54	0.866
Tetrahedral	30.19	0.75
Rhombohedral	25.95	0.70

Given that there exists an inverse relationship between packing factor and air entry suction explained through Figure 6.4 and Table 6.5, a shift factor or suction multiplier (X) is proposed to convert between packing arrangements based on the relationship between n and the inverse of the packing factor as plotted in Figure 6.5.

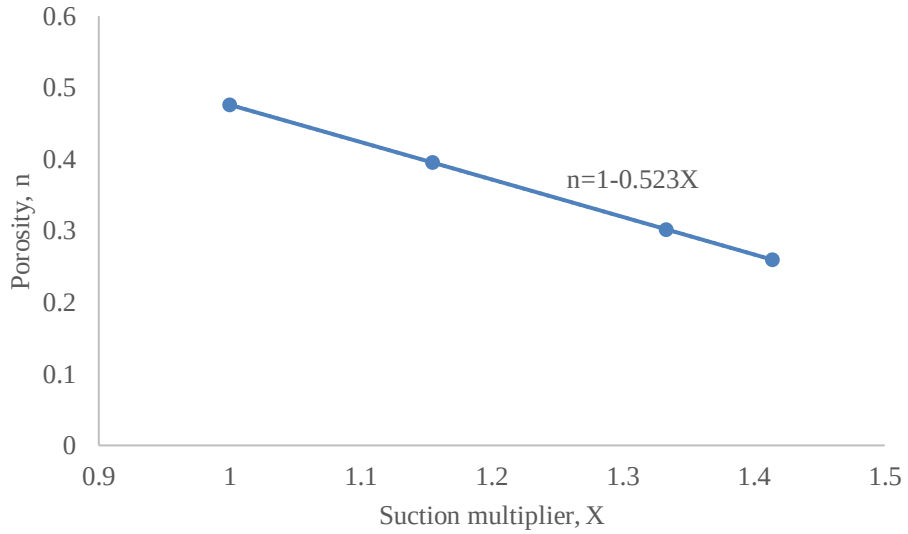

Figure 6.5 Porosity values plotted as a function of the proposed suction multiplier

Based on the regression plot in Figure 6.5, X may be written in terms of n according to equation 6.7.

$$X = 1.91 \times (1 - n) \tag{6.7}$$

Equation 6.8 is proposed to shift the γ_h values for reconstituted soils, $\gamma_h(reconstituted)$ such as those obtained through the charts proposed by Mckeen [99] to the γ_h value expected in the in-situ soils, $\gamma_h(intact)$ using the soil porosity after remolding, $n_{reconstituted}$.

$$\gamma_h(intact) = \frac{\gamma_h(reconstituted)}{1.91 \times (1 - n_{reconstituted})} \tag{6.8}$$

The shift factor in the denominator of equation 6.8 ranges from 1.0 when the soil fabric is fully intact to 1.4 when the soil fabric is fully disturbed implying that the γ_h values of reconstituted soils are theoretically between 0% and 40% greater compared to the γ_h values of in-situ soils. The experimental data in Table 6.4 is also in agreement with the proposed shift factor.

6.3.4. Summary and Conclusions

Two method improvements were proposed in this Chapter to improve existing methods to predict vertical movement caused by expansive subgrade soils.

The existing method to define the initial moisture state of soils in the Tex-124-E method compares the in-situ moisture content of the soils against a ‘dry’ and ‘wet’ state based entirely on an empirical relationship using the liquid limit of the soils. A more fundamental approach is proposed based on the soil water retention curve and equilibrium suction of the location to assign the initial moisture of the soils for use with the existing Tex-124-E method. The modified approach considers the impact of

maximum dry density of the soils and thereby improves the accuracy of volume change and vertical movement calculations for soil chemically stabilized using lime.

The suction-based method to predict vertical movement relies heavily on the suction compressibility index to calculate the volume change of soils subjected to changes in matric suction during climatic cycles. The existing methods to estimate the suction compressibility index rely on guidelines based on experimental results obtained on reconstituted soils thereby ignoring the impact of modifications to the soil fabric. A shift factor is proposed based on the packing theory and changes in porosity of the soils during remolding to relate the suction compressibility index values of reconstituted and intact soils.

The method improvements proposed significantly improve the accuracy of vertical movement predictions and reduce the degree of conservatism in both the Tex-124-E method and the suction-based method. The modifications also help understand the true impact of lime stabilization on minimizing vertical improvement and improving the overall volumetric stability of expansive soils thereby facilitating cost savings on the design and maintenance of pavements built on expansive soils.

7. EXECUTIVE SUMMARY AND RECOMMENDATIONS FOR FUTURE WORK

7.1. Executive Summary

A physicochemical and geotechnical evaluation was conducted to evaluate the uses of lime and lime products for the treatment of soil minerals in new and existing industrial applications.

The first area of focus was to investigate the role of a hydrated lime slurry as a coagulant in the treatment of fluid fine tailings (FFTs) generated during the bitumen extraction process from the oil sands deposits in Alberta, Canada. Two oil sands FFTs, FFT G and FFT I, having a solids concentration by mass of approximately 30% were dewatered using a decanter centrifuge and pressure filtration process respectively after various treatment options to achieve solid cake fractions with solids concentrations ranging between 55% to 70%. First, the impact of lime slurry on the chemical and mineralogical (physicochemical) properties of the FFT G cakes were evaluated using analytical methods including pH, cation exchange capacity (CEC), X-ray diffraction (XRD) and scanning electron microscopy (SEM). The mineralogical composition of FFT G predominantly comprised kaolinite, illite and quartz. There were three major findings from the physicochemical evaluation. First, lime slurry was shown to enhance the capture of clays within the cake fraction and clarify the release water. Second, addition of lime formed calcite in the cake by depleting the carbonates and bicarbonates and coagulated the clays through cation exchange reactions up to a pH of 11.5. Finally, above a pH of 12.0, lime slurry modified the activity of the clays within 28 days after

treatment by either cementing the kaolinites through calcite or by forming pozzolanic products after solubilizing the clay minerals.

Next, the impact of lime slurry on the immediate and long-term (first 6 months) geotechnical properties of FFT I were evaluated by measuring the changes in Atterberg limits, clay content and undrained shear strength of the pressure filter cakes. Three major findings were established from the geotechnical evaluation of FFT I. First, lime was shown to effectively increase the plastic limit (PL) of the cakes. Second, the lime treated cakes achieved peak shear strengths in excess of 20 kPa at a below optimum dosage at less than 65% solids content within 1 day and over 100 kPa at a near optimum dosage at 70% solids content within 28 days after treatment. Third, lime treatment reduced the filtration cycle times and thereby improved the overall economics of the pressure filtration process due to the rapid strength development and formation of new solid minerals through pozzolanic reactions. Lime was also found to outperform a polymeric flocculant and other calcium-based coagulants including gypsum and alum in terms of improving clay chemistry and cake strength at various stages during the physicochemical and geotechnical evaluations. The final phase of research conducted on the use of lime in oil sands tailings management was to develop a numerical model using experimental results to predict the changes in liquidity index and residual shear strength of lime treated FFT cakes with time. The model predictions showed excellent correlation with the experimental results indicated by an R^2 value of 0.97.

The second area of focus of this dissertation was to evaluate the long-term durability of lime treatment in hydraulic structures in constant contact with water. This

focus area is linked to the use of lime in the oil sands application as the reclaimed solids ultimately have a final destination as part of a structure where long-term durability is a key factor. The field case study was performed on native and 4% lime treated soils obtained from the slopes of the Friant-Kern canal (FKC) nearly 50 years after initial treatment with lime. The focus of the case study was to evaluate durability from both a physicochemical and engineering standpoint considering the effects of lime leaching and carbonation. There were major findings from the case study. First, the pH of the lime treated sections dropped from 12.4 at the time of construction to 8.9 due to carbonation and consumption of hydroxyl ions during pozzolanic reactions. Second, there was minimal to no leaching of lime as indicated by a 4% difference in calcium concentrations between the native and lime treated soils. Finally, the overall geomechanical stability of the lime treated sections were established based on a concurrent increase in compressive strength accompanied by a reduction in expansion and erosion potential of the FKC soils. The final phase of research in the case study included analyzing the moisture distribution patterns in the native and lime treated soils beneath the pavement adjacent to the FKC embankment slopes using Hydrus-2D. The Hydrus-2D analysis reaffirmed the benefits of lime treatment on improving the drainage characteristics of the soils as a result of textural modification of the FKC soils from lean clays to lean silts.

The third area of focus of this dissertation was to propose improvements to predict the volumetric stability of expansive soils and understand the true impact of lime stabilization on mitigating vertical movement caused by expansive subgrade soils. This

focus area is also linked to the use of lime to stabilize the oil sands clays as accurate assessment of volumetric stability of the reclaimed fine clays will play an important role when determining their utility as a pavement sublayer material. Towards this end, two method improvements were proposed to existing vertical movement prediction methods. First, a modified approach was proposed to define the initial moisture state of soils for use with the Tex-124-E method by considering the soil-water characteristic curve (SWCC), equilibrium suction of the location and dry density of the soils in lieu of the existing empirical approach which relies solely on the liquid limit (LL) of the soils. Second, a shift factor was proposed based on the packing theory of soil particles and consequent changes in soil porosity to relate the suction compressibility index of reconstituted soils to those of intact soils. The benefits of the proposed method improvements were demonstrated using example calculations performed on experimental data obtained from soil borings in Texas. The modified methods yielded more accurate results considering the changes to material properties as a result of chemical stabilization with lime.

In summary, the results and contributions of this dissertation will serve as a platform for future field trials and experimental work in efforts to commercialize the use of lime and lime products for the management of oil sands tailings and construction and repair of soils in hydraulic structures. The method improvements proposed to characterize the volumetric stability of expansive subgrade soils, if implemented correctly are expected to assist with improving the accuracy in determining the thickness

of the lime stabilized subgrade layer and result in overall cost savings in the design of pavements on expansive subgrade soils.

7.2. Recommendations for Future Work

Since a majority of the work presented in this dissertation involves the application of lime in relatively new applications, this research reveals the many fruitful avenues through which this work can be used to address environmental and geotechnical challenges related to the effective dewatering and reclamation of mine waste tailings using lime products.

Some of the potential topics pertinent to the management of oil sands tailings include evaluating the impact of lime addition on other geotechnical properties including but not limited to hydraulic conductivity and permeability, pore size distribution and water retention characteristics, unconfined compressive strength and compressibility as a function of void ratio and effective stresses using the large-scale consolidation test. There is also potential for a more extensive and advanced mineralogical evaluation of lime treated tailings after separating the clays using size fractionation. Another interesting and relevant future research topic would be to explore the use of geochemical modelling to predict the long-term mineral phases that are likely to develop after lime addition.

The next steps in research to strengthen the case for using lime for the construction of hydraulic structures would be to conduct compressive strength on intact cores recovered from lime treated sections of hydraulic structures. Another important topic of research should involve a more advanced characterization of the impact of lime

on mitigating erosion of the soils. This would involve analysis of the scour rate as a function of shear stresses and velocity using experiments such as erosion function apparatus (EFA) and jet erosion test (JET) on intact lime treated soils.

REFERENCES

[1] D. N. Little, *Stabilization of pavement subgrades and base courses with lime*, Kendal/Hunt Publishing Company, Iowa, 1995.

[2] D. N. Little, M. R. Thompson, R. L. Terrell, J. A. Epps, and E. J. Barenberg, "Soil stabilization for roadways and airfields", *A Report by Little (Dallas N) and Associates*, Bryan, Texas, 1987.

[3] D.N. Little and T.Scullion, "Guidelines for modification and stabilization of soils and base for the use in pavement structure", *A Report Prepared for Texas Department of Transportation*, 2005. https://ftp.txdot.gov/pub/txdot-info/cmd/tech/stabilization.pdf

[4] S. Diamond and E. B. Kinter, "Mechanisms of soil-lime stabilization", *Highway Research Record*, vol. 92, pp. 83-102, 1965.

[5] D. N. Little, *Evaluation of structural properties of lime stabilized soils and aggregates*, National Lime Association, 1998. https://www.lime.org/documents/other/SOIL.PDF

[6] M. Fustic et al., "Bitumen and heavy oil geochemistry: a tool for distinguishing barriers from baffles in oil sands reservoirs", *Bulletin of Canadian Petroleum Geology*, vol. 59, no. 4, pp. 295-316, 2011.

[7] B.Ozum and J.D. Scott, "Coupling of oil sands mature fine tailings and bitumen extraction", in *Proceedings of the Tailings and Mine Waste Conference*, Keystone, Colorado, 2012.

[8] Alberta Energy Regulator (AER), *State of fluid tailings management for mineable oil sands, 2018*, Alberta Energy Regulator, Alberta, Canada, 2018. https://www.aer.ca/documents/oilsands/2018-State-Fluid-Tailings-Management-Mineable-OilSands.pdf

[9] R. Donahue, S. Jeeravipoolvarn, J. Scott and B. Ozum, "Properties of nonsegregating tailings produced from the Auora oil sands mine tailings", in *First International Oil Sands Tailings Conference, Oil Sands Tailings Research Facility*, pp. 143-152, Alberta, Canada, 2008.

[10] J. Boswell and P. Cavanagh, "Stewarding dam safety in Alberta: The Dam Integrity Advisory Committee (DIAC)" in *Sixth International Oil Sands Tailings Conference*, pp. 246-251, University of Alberta Geotechnical Center, Alberta, 2018.

[11] M. Armstrong, R. Petter, and C. Petter, "Why have so many tailings dams failed in recent years?", *Resources Policy*, vol. 63, article 101412, 2019. https://doi.org/10.1016/j.resourpol.2019.101412

[12] Z. Lyu, J. Chai, Z. Xu, Y. Qin and J. Cao, "A comprehensive review on reasons for tailings dam failures based on case history" *Advances in Civil Engineering*, vol. 19, article 4159306, 2019. https://doi.org/10.1155/2019/4159306

[13] L. L. Garver, "Canal repair techniques using lime-stabilized soil" in *Lime for Environmental Uses*: *ASTM International*, pp. 115-120, West Conshohocken, PA, 1987.

[14] A. K. Howard and J. P. Bara, "Lime stabilization on Friant-Kern canal", *Engineering and Research Center, Bureau of Reclamation, Report No. REC-ERC-76-20*, Denver, Colorado, 1976. https://www.usbr.gov/tsc/techreferences/rec/REC-ERC-76-20.pdf

[15] P.C. Knodel, "Lime in canal and dam stabilization", *U.S. Department of the Interior, Bureau of Reclamation, Report No. GR-87-10,* Denver, Colorado,1987. https://www.usbr.gov/tsc/techreferences/research/GR8710.pdf

[16] National Oceanic & Atmospheric Administration (NOAA), *In: Information, N.C.F.E. (ed.)*, Fresno, 2020. https://www.noaa.gov/climate

[17] H. F. Taylor, *Cement chemistry*, Thomas Telford, London, 1997.

[18] Texas Department of Transportation (TxDOT), "Tex-124-E: Test procedure for potential vertical rise of natural subgrade soils", Texas, 2017.

[19] R. Lytton, C. Aubeny, and R. Bulut, "Design procedure for pavements on expansive soils: volume 1", *A Report Prepared for the Federal Highway Administration*, No. 0-4518-1, Texas Transportation Institute, 2004.

[20] G. McKenna, B. Mooder, B. Burton and A. Jamieson, "Shear strength and density of oil sands fine tailings for reclamation to a boreal forest landscape," in *Fifth International Oil Sands Tailings Conference (IOSTC)(DC Sego, W. Wilson, and NA Beier, editors)*, pp. 130-153, 2016.

[21] D. Hockley, "Clay effects on tailings geotechnical properties", in *Clay Minerals Society*, NAIT, Alberta, Canada, 2017.

[22] F. Kaswalder, D. Cavalli, A. Hawkey and A. Paglianti, "Tailings dewatering by pressure filtration: process optimisation and design criteria" in *21st International Seminar on Paste and Thickened Tailings*, Australian Center for Geomechanics, pp. 427-438, Perth, Western Australia, 2018.

[23] J. Chaponnel and T. Wisdom, "FLSmidth colossal filter–demonstration plant" in *Proceedings of the 21st International Seminar on Paste and Thickened Tailings*, Australian Centre for Geomechanics, pp. 53-62, Perth, Western Australia, 2018.

[24] K. Kasperski, "A review of properties and treatment of oil sands tailings", *AOSTRA Journal of Research*, vol. 8, pp. 11-53, Canada, 1992.

[25] O.P. Sahu and P.K. Chaudhari, "Review of chemical treatment of industrial waste water", *Journal of Applied Sciences and Environmental Management*, vol. 17, no. 2, pp. 241-257, 2013.

[26] J. Matthews, W. Shaw, M. MacKinnon and R.G. Cuddy, "Development of composite tailings technology at Syncrude", *International Journal of Surface Mining, Reclamation and Environment*, vol. 16, no. 1, pp. 24-39, 2002.

[27] Q. Lu, B. Yan, L. Xie, J. Huang, Y. Liu, and H. Zeng, "A two-step flocculation process on oil sands tailings treatment using oppositely charged polymer flocculants", *Science of the Total Environment*, vol. 565, pp. 369-375, 2016.

[28] R. J. Mikula, K. L. Kasperski, R. D. Burns, and M. D. MacKinnon, "Nature and fate of oil sands fine tailings" *ACS Publications*, vol. 251, pp. 677-723,1996.

[29] P.H. Mercier, Y. Le Page, Y. Tu and L.S. Kotlyar, and technology, "Powder X-ray diffraction determination of phyllosilicate mass and area versus particle thickness distributions for clays from the Athabasca oil sands", *Petroleum Science and Technology*, vol. 26, no. 3, pp. 307-321, 2008.

[30] P. Bayliss and A.A. Levinson, "Mineralogical review of the Alberta oil sand deposits (lower cretaceous, Mannville group)", *Bulletin of Canadian Petroleum Geology*, vol. 24, no. 2, pp. 211-224, 1976.

[31] R. J. Chalaturnyk, J. Don Scott and B. Özüm, "Management of oil sands tailings", *Petroleum Science and Technology*, vol. 20, no. 9-10, pp. 1025-1046, 2002.

[32] S. Lane, "Lime coagulation and stabilization of total oilsands tailings" in *Annual Technical Meeting*: *Petroleum Society of Canada*, Banff, Canada, 1983.

[33] C. Rogers and S. Glendinning, "Modification of clay soils using lime", in *Lime Stabilisation: Proceedings of the Seminar held at Loughborough University Civil & Building Engineering Department*, pp. 99-114, 1996.

[34] M. J. Tate, J. Leikam, J. Fox and N. Romaniuk, "Use of calcium hydroxide as a coagulant to improve oil sands tailings treatment", in *22nd International Conference on Tailings and Mine Waste*, pp. 720-732, University of Alberta Geotechnical Centre, Denver, Colorado, 2017.

[35] N. Romaniunk, "Dewatering and altering of MFT characteristics using lime (CaO) additive", *A Report by Apex Engineering*, 2016.

[36] M. Choquette, M.A. Berube and J. Locat, "Mineralogical and microtextural changes associated with lime stabilization of marine clays from eastern Canada", *Applied Clay Science*, vol. 2, no. 3, pp. 215-232, 1987.

[37] J. Locat, H. Trembaly, and S. Leroueil, "Mechanical and hydraulic behaviour of a soft inorganic clay treated with lime", *Canadian Geotechnical Journal*, vol. 33, no. 4, pp. 654-669, 1996.

[38] T. D. Tran, Y.J. Cui, A.M. Tang, M. Audiguier and R.Cojean"Effects of lime treatment on the microstructure and hydraulic conductivity of Héricourt clay", *Journal of Rock Mechanics and Geotechnical Engineering*, vol. 6, no. 5, pp. 399-404, 2014.

[39] D. Hunter, "Lime-induced heave in sulfate-bearing clay soils", *Journal of Geotechnical Engineering*, vol. 114, no. 2, pp. 150-167, 1988.

[40] S. Wild, M. Abdi, and G. Leng-Ward, "Sulphate expansion of lime-stabilized kaolinite II: reaction products and expansion", *Clay Minerals*, vol. 28, no. 4, pp. 569-583, 1993.

[41] M. MacKinnon, J. Matthews, W. Shaw and R.G. Cuddy, "Water quality issues associated with composite tailings (CT) technology for managing oil sands tailings", *International Journal of Surface Mining, Reclamation and Environemnt*, vol. 15, no. 4, pp. 235-256, 2001.

[42] R. Loerke, X. Tan and Q. Liu, "Dewatering of oil sands mature fine tailings by dual polymer flocculation and pressure plate filtration", *Energy and Fuels*, vol. 31, no. 7, pp. 6986-6995, 2017.

[43] K. Cafferata, C. Cote, R. Heffel, W. Duttlinger and A. Chengara, "Dynamic inline flocculation and pressure filtration of oil sands MFT" presented at the *International Seminar on Paste and Thickened Tailings*, British Columbia, Canada, 2014.

[44] H. A. Kaminsky, T. H. Etsell, D. G. Ivey, and O. Omotoso, "Distribution of clay minerals in the process streams produced by the extraction of bitumen from

Athabasca oil sands", *Canadian Journal of Chemical Engineering*, vol. 87, no. 1, pp. 85-93, 2009.

[45] Y. Tu *et al.*, "Recovery of bitumen from oilsands: gelation of ultra-fine clay in the primary separation vessel", *Fuel*, vol. 84, no. 6, pp. 653-660, 2005.

[46] N. Beier, W. Wilson, A. Dunmola, and D. Sego, "Impact of flocculation-based dewatering on the shear strength of oil sands fine tailings", *Canadian Geotechnical Journal*, vol. 50, no. 9, pp. 1001-1007, 2013.

[47] BGC Engineering, "Review of reclamation options for oil sands tailings substrates" in *Oil Sands Research and Information Network*, University of Alberta, Alberta, Canada, 2010.

[48] Alberta Energy Regulator (AER). *Directive 074- Tailings Performance Criteria and Requirements for Oil Sands Mining Schemes*,Alberta, Canada, 2009. http://www.assembly.ab.ca/lao/library/egovdocs/2009/alog/171321.pdf

[49] Alberta Energy Regulator (AER). *Directive 085- Fluid tailings management for oil sand mining projects*, Alberta, Canada, 2017. https://www.aer.ca/documents/directives/Directive085.pdf

[50] J.P. Perry, "Lime treatment of dams constructed with dispersive clay soils", *Transactions of the ASAE*, vol. 20, no. 6, pp. 1093-1099, 1977.

[51] K. A. Gutschick, "Lime stabilization under hydraulic conditions," in *Zement-kalk-gips*, vol. 32, pp. 91-91, Walluf, Germany, 1979.

[52] T.N. McDaniel, R.S. Decker, "Dispersive soil problem at Los Esteros dam", *Journal of Geotechnical and Geoenvironmental Engineering*, vol. 105, ASCE 14804 Proceeding, New York, 1979.

[53] R. L. Torres, "Internal erosion and dispersive soils on a well-built dam using lime" in *European Club of ICOLD- WG Internal Erosion*, Brno, Czech Republic, 2011.

[54] G. Herrier, R. Berger, and S. Bonelli, "The Friant-Kern canal: a forgotten example of lime-treated structure in hydraulic conditions", *6th International Conference on Scour and Erosion*, Paris, 2012.

[55] Friant Water Authority (FWA), "Map of the Friant Kern canal, California", *Personal Communication*, 2020.

[56] R. Fleming, G. Sills, and E. Steward, "Lime stabilization of levee slopes" in *Proceedings Second Interagency Symposium On Stabilization Of Soils And Other Materials*, Metairie, LA, 1992.

[57] P. W. Mitchell, "The structural analysis of footings on expansive soil" in *Expansive Soils*, pp. 438-447, 1980.

[58] N. Hariharan, "Effect of ionic stabilization on vertical movement in expansive subgrade soils in Texas", *Thesis*, Texas A&M University, College Station, Texas, 2013.

[59] M. J. Tate, J. Leikam, J.D. Scott, M.Mehranfar, N.Romaniuk and B.Ozum, "Impacts of calcium compounds on oil sands water chemistry" in *Tailings and Mine Waste*, Keystone, Colorado, 2016.

[60] L. Boxill, "Potential for use of methylene blue index testing to enhance geotechnical characterization of oil sands ores and tailings," in *Proceedings of Tailings and Mine Waste*, British Columbia, Canada, 2011.

[61] H. Kaminsky, "Demystifying the methylene blue index" in *Proceedings of the 4th International Oil Sands Tailings Conference*, Alberta, Canada, 2014.

[62] W.D. Keller, "Processes of origin and alteration of clay minerals", *Soil Clay Mineralogy*, vol. 3, 1964.

[63] S. Gunasekaran, G. Anbalagan, S. Pandi, "Raman and infrared spectra of carbonates of calcite structure", *Journal of Raman Spectroscopy: An International Journal for Original Work in all Aspects of Raman Spectroscopy,*

Including Higher Order Processes, and also Brillouin and Rayleigh Scattering, vol. 37, no. 9, pp. 892-899, 2006.

[64] Y. Deng, N. White and J.B. Dixon, *Soil mineralogy laboratory manual*, 15th ed., Texas A&M University, College Station, Texas, 2014.

[65] R. T. Chancey, P. Stutzman, M. C. Juenger and D.W. Fowler, "Comprehensive phase characterization of crystalline and amorphous phases of a Class F fly ash", *Cement and Concrete Research*, vol. 40, no. 1, pp. 146-156, 2010.

[66] ISO/TS 17892-12, "Geotechnical investigation and testing–laboratory testing of soil–Part 12: Determination of Atterberg limits", *International Organization for Standardization*, United Kingdom, 2005.

[67] ASTM D4318-17, "Standard test methods for liquid limit, plastic limit, and plasticity index of soils", *ASTM International*, West Conshohocken, PA, 2017.

[68] J. K. Mitchell and K. Soga, *Fundamentals of soil behavior*. John Wiley & Sons, New York, 2005.

[69] A. J. Skempton, "The colloidal activity of clays", *Selected Papers on Soil Mechanics*, pp. 106-118, 1953.

[70] W. Carrier and J.F. Beckman, "Correlations between index tests and the properties of remoulded clays", *Geotechnique*, vol. 34, no. 2, pp. 211-228, 1984.

[71] ASTM D7928-17, "Standard test method for particle-size distribution (gradation) of fine-grained soils using the sedimentation (hydrometer) analysis", *ASTM International*, West Conshohocken, PA, 2017.

[72] ASTM D1557, "Standard test methods for laboratory compaction characteristics of soil using standard effort (12 400 ft-lbf/ft^3 (600 KN-m/m^3)) ", *ASTM International*, West Conshohocken, PA, 2007.

[73] E. McLean, "Soil pH and lime requirement. Methods of soil analysis: Part 2 Chemical and Microbiological Properties", *American Society of Agronomy*, vol. 9, pp. 199-224, 1983.

[74] ASTM D4972, "Standard test methods for pH of soils", *ASTM International*, West Conshohocken, PA, 2019.

[75] ASTM D6276, "Standard test method for using ph to estimate the soil-lime proportion requirement for soil stabilization", *ASTM International*, West Conshohocken, PA, 2019.

[76] ASTM D2166, "Standard test method for unconfined compressive strength of cohesive soil", *ASTM International*, West Conshohocken, PA, 2016.

[77] ASTM D4829, "Standard Test Method for Expansion Index of Soils", *ASTM International*, West Conshohocken, PA, 2011.

[78] S. Hillier, "Use of an air brush to spray dry samples for X-ray powder diffraction", *Clay Minerals*, vol. 34, no. 1, pp. 127-135, 1999.

[79] M. Mahedi, B. Cetin, and D. J. White, "Performance evaluation of cement and slag stabilized expansive soils", *Transportation Research Record*, vol. 2672, no. 52, pp. 164-173, 2018.

[80] K. L. Goodner, "Estimating turbidity (NTU) from absorption data", *Sensus Technical Note (SEN-TN-0010)*, pp. 1-4, 2009.

[81] S. San Lim, "Experimental investigation of erosion in variably saturated clay soils", *Thesis*, University of New South Wales, Sydney, Australia, 2006.

[82] G. B. Singh and K. V. J. C. Subramaniam, "Quantitative XRD study of amorphous phase in alkali activated low calcium siliceous fly ash", *Construction and Building Materials*, vol. 124, pp. 139-147, 2016.

[83] K. Scrivener, R. Snellings, and B. Lothenbach, *A practical guide to microstructural analysis of cementitious materials*, CRC Press, Boca Raton, Florida, 2016.

[84] D. G.Schulze, "An introduction to soil mineralogy", *Soil Mineralogy with Environmental Applications*, vol. 7, pp. 1-35, 2002

[85] F. Claret, A. Bauer, T. Schäfer, L. Griffault and B.Lanson, "Experimental investigation of the interaction of clays with high-pH solutions: A case study from the Callovo-Oxfordian formation, Meuse-Haute Marne underground laboratory (France)", *Clays and Clay Minerals*, vol. 50, no. 5, pp. 633-646, 2002.

[86] B. Lothenbach *et al.*, "Cemdata18: A chemical thermodynamic database for hydrated Portland cements and alkali-activated materials", *Cement and Concrete Research*, vol. 115, pp. 472-506, 2019.

[87] Y. Liu, Y. Zhao, J. Dong, P. Liu, Z. Zhu, and Y.Sun, "pH buffering capacity of geological media on landfill leachate", *Huan jing ke xue= Huanjing kexue*, vol. 29, no. 7, pp. 1948-1954, 2008.

[88] R. N. Yong, B. P. Warkentin, Y. Phadungchewit, R.Galvez, "Buffer capacity and lead retention in some clay materials", *Water, Air, and Soil Pollution*, vol. 53, no. 1-2, pp. 53-67, 1990.

[89] M. Cao, X. Ming, K. He, L. Li, and S.Shen, "Effect of macro-, micro-and nano-calcium carbonate on properties of cementitious composites—A review", *Materials*, vol. 12, no. 5, p. 781, 2019.

[90] S. Haas and H.J. Ritter, "Soil improvement with quicklime–long-time behaviour and carbonation", *Road Materials and Pavement Design*, vol. 20, no. 8, pp. 1941-1951, 2019.

[91] J. Norambuena-Contreras, G. Arbat, P. G. Nieto, D. Castro-Fresno, "Nonlinear numerical simulation of rainwater infiltration through road embankments by FEM", *Applied Mathematics and Computation*, vol. 219, no. 4, pp. 1843-1852, 2012.

[92] J. Šimůnek, M. T. Van Genuchten, and M. Šejna, "The HYDRUS software package for simulating the two-and three-dimensional movement of water, heat, and multiple solutes in variably-saturated porous media", *Technical Manual*, version 2.0, 2012.

[93] S. Saha, F. Gu, X. Luo, and R.L.Lytton, "Prediction of soil-water Characteristic Curve for unbound material using Fredlund–xing Equation-based ANN approach", *Journal of Materials in Civil Engineering*, vol. 30, no. 5, p. 06018002, 2018.

[94] J. Zhang, D. N. Little, N. Hariharan and Y.R. Kim, "Prediction of climate specific vertical movement of pavements with expansive soils based on long-term 2D numerical simulation of rainwater infiltration", *Geotechnics*, vol. 115,p. 103172, 2019.

[95] M. T. Van Genuchten, "A closed-form equation for predicting the hydraulic conductivity of unsaturated soils 1", *Soil Science Society of America Journal*, vol. 44, no. 5, pp. 892-898, 1980.

[96] S. Saha, N. Hariharan, F. Gu, X. Luo, D. N. Little, and R. L. Lytton, "Development of a mechanistic-empirical model to predict equilibrium suction for subgrade soil", *Journal of Hydrology*, vol. 575, pp. 221-233, 2019.

[97] Applied Research Associates, "Guide for mechanistic-empirical design of new and rehabilitated pavement structures", *A Report Prepared for National Cooperative Highway Research Program (NCHRP)*, No. 1-37A, 2004.

[98] R. L. Terrel, J. A. Epps, E. J. Barenberg, J. Mitchell, and M. R. Thompson, "Soil Stabilization in Pavement Structures-A User's Manual Volume 2: Mixture Design Considerations", *A Report by Terrel, Epps and Associates*, Seattle, WA, 1979.

[99] R. G. McKeen, "Design of Airport Pavements for Expansive Soils", *Final Report, New Mexico Engineering Research Institute*, Albuquerque, New Mexico,1981. https://apps.dtic.mil/dtic/tr/fulltext/u2/a104660.pdf

[100] ASTM D6836-16, "Standard test methods for determination of the soil water characteristic curve for desorption using hanging column, pressure extractor, chilled mirror hygrometer, or centrifuge", *ASTM International*, West Conshohocken, PA, 2016.

[101] T. F. Yideti, B. Birgisson, D. Jelagin, and A.Guarin, "Packing theory-based framework for evaluating resilient modulus of unbound granular materials", *International Journal of Pavement Engineering*, vol. 15, no. 8, pp. 689-697, 2014.

APPENDIX A

PROCEDURE TO DETERMINE PLASTIC LIMIT OF OIL SAND FFT CAKES USING THE DROP CONE PENETROMETER

A.1. Summary of Test Method

The drop or falling cone penetrometer is used commonly to determine the liquid limit (LL) of soils but not the plastic limit (PL) of soils. A new method is proposed for specifically determining the plastic limit of filtered or centrifuged oil sands tailing cakes based on the correlation between peak undrained shear strength at LL and PL. In this method the water content of the oil sands tailings cake is adjusted from its initial state by either drying in a convection oven at 43°C (110°F) in most cases or by wetting using water to achieve a penetration depth of approximately 5.45 mm using a 30° apex angle cone with a mass of 400-gram that is allowed to free fall for 5 sec. The test is repeated to obtain a minimum of three penetration depths between 4 mm and 7 mm including a minimum of one penetration depth above and below 5.45 mm. The plastic limit is then reported as the gravimetric water content at which the 30°/400-gram cone penetrates the cake to a depth of 5.45 mm.

A.2. Theory

The LL is defined as the gravimetric water content when a 60°cone with a mass of 60-gram, penetrates the cake to depth of 10 mm when allowed to free fall for 5 seconds. The average undrained shear strength at the LL for the oil sand tailing cakes was found to be approximately 1.5 kPa while the undrained shear strength at the plastic

limit for the same materials was found to be about 70 times the strength at LL based on experimental verification. Per the ISO 17892-6 standard, the peak undrained shear strength (Γ_{max}) can be estimated using the drop cone method according to equation A.1.

$$\Gamma_{max} = \frac{c \times g \times m}{i^2} \quad \text{(A.1)}$$

where c is the tip angle of the cone, m is the mass of the cone in grams, i is the penetration depth in millimeters and g is the acceleration due to gravity.

Hence, by assuming the Γ_{max} at PL to be equal to 105 kPa, the average penetration depth required was found to be 1.2 mm using a 60°/60-gram cone set up and 5.45 mm using a 30°/400-gram cone set up. Since the penetration depths when using the drop cone penetrometer for shear strength measurements must range between 4 mm and 20 mm, the PL of oil sand cakes was proposed as the water content corresponding to a penetration depth of 5.45 mm using a 30°/400-gram cone set up.

A.3. Equipment and Reagents

The equipment and reagents required to perform this test are listed below:

1. Humboldt H-5237 semi-automatic digital drop cone penetrometer
2. Timer device
3. 70 grams of oil sand cake fraction finer than 0.4 mm
4. Demineralized water in a plastic spray bottle
5. Flat glass plate
6. Spatula and other mixing tools
7. Water content cup
8. Aluminum container

9. Paper Towels
10. Calibrated weighing balance
11. Convection Oven for drying

A.4. Sample Preparation

1. Take about 70 g of the same cake sample used for determining the liquid limit and transfer it into a separate container. Make sure to label the container with the composition of the sample, date of sampling and the solids content%age.
2. Thoroughly homogenize the cake by either using a spatula for by hand depending on the consistency by setting the sample on a flat glass plate.
3. Fill the aluminum container with the cake sample. Try not to allow any voids for air pockets while also not over working the sample.
4. Use a flat spatula to create a smooth surface that is level with the edge of the cup.
5. Proceed to take an initial penetration depth measurement using the Humboldt H-5237 cone penetrometer.
6. If the initial penetration depth is ≤4 mm
    a) Transfer the sample to the glass plate, spread the sample in a thin layer and add demineralized water anticipating 1 mm increase in penetration depth for every 3 ml of water added.
    b) Add enough water to attain a penetration depth between 4 mm and 5.45 mm and remold the sample by thoroughly dispersing the water within the cake and ensuring no flakes are present. This step should take no more

than 2 min as excessive mixing will dry out the sample and take it back to its original state.

c) Repeat steps 3 through 5.

d) Record the penetration depth and immediately transfer a minimum of 6 g of sample into a water content cup to record the water content of the samples according to ASTM D2216 (ASTM D2216, 2010).

e) Repeat step 6.a by adding enough water in 3 ml increments to attain two additional penetration depths between 4 mm and 7 mm with a minimum of one measurement above and below 5.45 mm. Ensure good dispersion of water every time the sample is remolded and transferred back to the aluminum container for measurements. When adding water greater than 10 ml in a single step, the sample must be allowed to equilibrate for a minimum of 15 min before taking measurements.

7. If initial penetration depth is ≥7 mm (most cases)

a) Transfer the sample back to a watch glass and place it in a convection oven at 40°C (110°F) for 30 min to 1 hour until the sample appears to be nearing its plastic limit.

b) Remold the sample in a flat glass plate by thoroughly mixing with the help of a spatula to avoid dry or wet pockets within the soil matrix.

c) Repeat steps 3 through 5.

d) Record the penetration depth and immediately transfer a minimum of 6 g of cake into a water content cup to record the water content of the samples.

e) Repeat step 7.a by further air drying the sample to attain two additional penetration depths between 4 mm and 7 mm with a minimum of one measurement above and below 5.45 mm.

8. If initial penetration depth is between 4 mm and 7 mm,

a) Record the penetration depth and immediately transfer a minimum of 6 g of sample into a water content cup to record the water content of the sample.

b) Transfer the sample back to the glass plate and either add water following the steps outlined in step 6 or air dry the sample sufficiently to record two additional penetration depths between 4 mm and 7 mm with a minimum of one measurement above and below 5.45 mm.

A.5. Calculation of Plastic Limit

Make a plot of penetration depth (mm) versus gravimetric water content (%) using data gathered from the three measurement points similar to Figure A.1. PL is calculated using the regression equation as the gravimetric water content corresponding to a penetration depth of 5.45 mm.

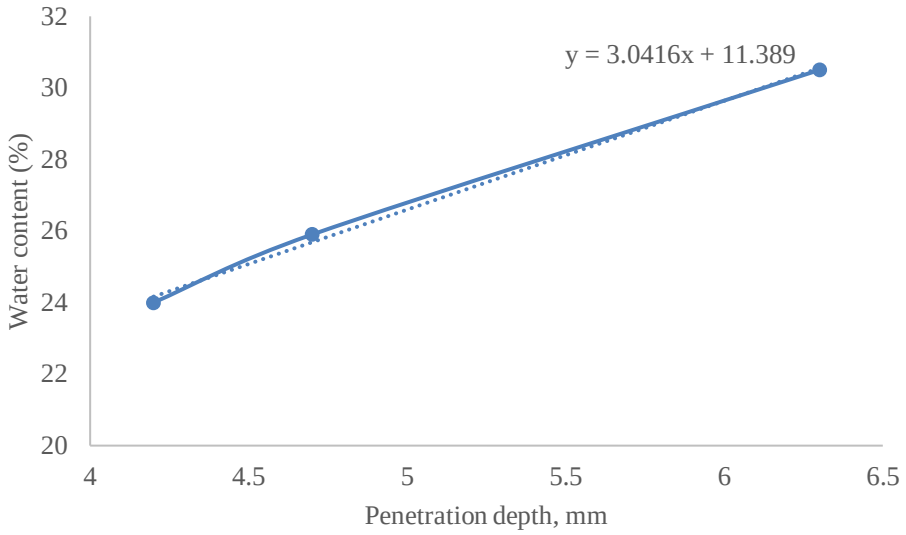

Figure A. 1 Example plot of penetration depth against the water content obtained for an oil sands cake sample